1-1-2011

Environmental monitoring of landfill sites using multi-temporal remote sensing images

Kamil Said Faisal
Ryerson University

ENVIRONMENTAL MONITORING OF LANDFILL SITES USING MULTI-TEMPORAL REMOTE SENSING IMAGES

By
Kamil Said Faisal
Bachelor of planning
From the faculty of Environmental Design
King Abdul Aziz University, Jeddah, Saudi Arabia, 2006

A Thesis
Presented to Ryerson University
In Partial Fulfillment of the
Requirements for the Degree of
Master of Applied Science
In the Program of
Civil Engineering

Toronto, Ontario, Canada, 2011

AUTHOR'S DECLARATION

I hereby declare that I am the sole author of this thesis or dissertation.

I authorize Ryerson University to lend this thesis or dissertation to other institutions or individuals for the purpose of scholarly research.

Author's Signature: _____ Date: _____

I further authorize Ryerson University to reproduce this thesis or dissertation by photocopying or other means, in total or in part, at the request of other institutions or individuals for the purpose of scholarly research.

Author's Signature: _____ Date: _____

ENVIRONMENTAL MONITORING OF LANDFILL SITES USING MULTI-TEMPORAL REMOTE SENSING IMAGES

By

Kamil Said Faisal

Master of Applied Science

Program of Civil Engineering

Ryerson University

2011

ABSTRACT

In this study, multi-temporal Landsat images obtained from the U.S. Geological Survey are used to monitor two landfill sites, the Trail Road landfill (Ottawa, Canada) and the Al-Jleeb landfill (Al-Farwanyah, Kuwait). The objectives are: 1) to study the land surface temperature (LST) of the two landfill sites; 2) investigate the relationship between the LST and landfill gas in the Trail Road landfill; and 3) detect suspicious dumping areas within the Al-Jleeb landfill. It was found that the LST of the landfill sites are always higher than the air temperature and the immediate surroundings. The correlation between the LST and the methane recorded in the Trail Road landfill is not obviously strong, and five suspicious locations were identified within the Al-Jleeb landfill by overlaying the highest LST contours. The study demonstrates the usefulness of remote sensing techniques that can provide supplementary information for landfill monitoring.

ACKNOWLEDGEMENT

I owe immense thanks to many people whose assistance was indispensable in completing this research endeavor. First among these is Dr. Ahmed Shaker, my supervisor, who was always there for me no matter what or when even with his extremely busy schedule. Also, special thanks and appreciation go to Mr. Wai Yeung Yan, a PhD student at Ryerson University. My thesis wouldn't have been achievable without the knowledge and effort that I received from him regarding geographic information systems and remote sensing.

Special thanks go to the Environment Public Authority of Kuwait Government for the data and the information they have provided about the Al-Jleeb landfill. Special thanks also are extended to the City of Ottawa, Town of Nepean, and Dillon Consulting, Limited, for the data and information that they provided on the Trail Road landfill. Moreover, I would like to thank Mr. Peter Filipowich from the Government of the City of Ottawa, who provided the annual monitoring program reports on the Nepean and Trail Road Landfills.

Special thanks also are given to the King Abdul-Aziz University and the Saudi Culture Bureau. They both gave me the opportunity to study abroad at Ryerson University with full support and assistance. Finally, I would like to thank the people who contribute the most to my life-- my parents, my wife and my daughter, Toleen. Without them, none of this work would have been possible.

TABLE OF CONTENTS

LIST OF TABLES

LIST OF FIGURES

LIST OF APPENDIX

LIST OF ACRONYMS

ATCOR:	Atmospheric Correction
DEM:	Digital Elevation Model
DN:	Digital Number
ETM^+:	Enhanced Thematic Mapper Plus
GIS:	Geographic Information System
GMT:	Greenwich Mean Time
IRS:	Indian Remote Sensing
LST:	Land Surface Temperature
MOE:	Ontario Ministry of the Environment
MIR:	Middle Infrared
NDVI:	Normalized Difference Vegetation Index
NIR:	Near Infrared
PAN:	Panchromatic
SAR:	Synthetic Aperture Radar
SAVI:	Soil Adjusted Vegetation Index
SPOT:	Système Probatoire d'Observation de la Terre
SWIR:	Short Wave Infrared
TIR:	Thermal Infrared
TM:	Thematic Mapper
USGS:	United States Geological Survey
UTM:	Universal Transverse Mercator

1. INTRODUCTION

1.1. Background

Globally, million of tons of municipal solid waste are disposed in landfills sites every day. Landfill gas is a natural by-product of decayed organic material compiled from household waste, yard waste, food waste, etc., disposed in these landfills. This landfill gas is mainly a combination of methane (CH_4), carbon dioxide (CO_2) plus a certain amount of non-methane organic compounds (benzene C_6H_6, toluene CH_3, and chloroform $CHCl_3$). Landfill is considered to be the third largest emission source in the world after rice cultivation and biomass burning from manmade activities. Previously, open dumps and unmanaged landfills represented a significant issue in many of the developing countries. Over the last few decades, however, many of these countries have attempted to transfer their waste disposal activities from uncontrolled systems to landfills (Plasynski et al, 2008).

The North American countries generate about 120,000 tons of waste per day (Bonger et al., 2007). Some of this waste gets recycled, but the majority is dumped into landfills. The problem of dumping waste is that it may cause potential risks in the long term for both human health and the environment. Therefore, in Canada, landfill disposal is controlled by different specific regulations, such as Ontario Regulation 232/98. Such regulations apply to new or expanding landfill sites and includes specific requirements for site design, operation, closure, and financial assurance.

The process of monitoring these landfills is to assess the chemical decomposition of landfill gas,

soil samples, ground water, and surface water within the site. One of the goals of this monitoring is to determine the impacts of the landfill site on the environment and the surrounding area. Currently, most of the landfill sites are designed with leachate collection systems to convert the landfill gas into green power. Traditional monitoring programs, such as field sampling and laboratory testing, consume both time and effort. In cases of their large spatial extent, such monitoring schemes can cost millions of dollars, and it is difficult to investigate the impacts of landfill sites on the surroundings. In this study, the use of multi-temporal remote sensing images are analyzed to monitor the Trail Road landfill site in the City of Ottawa, Canada, and detect suspicious dumping areas within the Al-Jleeb landfill site in the City of Al-Farwanyah, Kuwait. The purpose of this study is to provide useful supplementary information for landfill site monitoring and management, instead of simply replacing the current, more traditional monitoring schemes.

1.2. Problem Definition

1.2.1. The Trail Road Landfill, Ottawa, Canada

The Trail Road landfill was constructed in December of 1978 and started operation in 1980. The Trail Road landfill includes four development stages with a total area of around 2.02 km². A comprehensive monitoring system was established including landfill gas monitoring wells, surface water monitoring stations, and groundwater monitoring stations. There are more than 20 landfill gases monitoring wells established on the landfill site and surrounding areas of the landfill. To monitor surface water and groundwater, 13 and 83 monitoring stations were set up in the landfill site and the surrounding areas, respectively. However, the drawbacks of a traditional monitoring program are: 1) it needs special equipment and testing which are costly; 2) field sampling and laboratory testing are time consuming; and 3) it is difficult to identify the effects of the landfill on

the surrounding areas. In this case study, multi-temporal remote sensing images (year 2001 to year 2009) were introduced to determine the spatial distribution of the land surface temperature (LST) due to the emissions of landfill gas. Analysis of LST provides additional information for the authorities to study the bio-degradation process of the disposed wastes within the landfill site. A preliminary analysis was also conducted to investigate the relationship between the amount of methane (CH_4) recorded from the ground monitoring wells and the LST derived from the remote sensing images.

1.2.2. The Al-Jleeb Landfill, Al-Farwanyah, Kuwait

The Al-Jleeb landfill is located in Al-Farwanyah which is southwest of the City of Kuwait. Unauthorized dumping of household and industrial wastes was found in the landfill site in the early 1980s. Recently, the expansion of residential areas in the City of Al-Farwanyah has come quite close to the landfill site. The odors emanating from the landfill sites have negative impacts on the urban areas and may result in health hazards for the public residents. Although the Government of Kuwait has spent vast monies and effort to detect the location of the unrecorded dumping areas within Al-Jleeb landfill site, some of the records were found missing due to the Gulf War in 1991. In this case study, we investigate the use of multi-temporal Landsat satellite images (year 1985 to year 2001) to determine the location of suspicious dumping areas within the Al-Jleeb landfill site. The findings from this study can help the authority make appropriate decisions and set up a ground monitoring system within the landfill site and carry out better city planning for the future development of the nearby urban areas.

1.3. Research Objectives

In this study, the research objectives are:-

1. To investigate the use of multi-temporal, remote- sensing images and determine the spatial distribution of LST (*The Trail Road landfill, Ottawa, Canada*),
2. To study the relationship between the amount of methane (CH_4) measured from the ground monitoring wells and the LST derived from the remote sensing images (*The Trail Road landfill, Ottawa, Canada*), and
3. To determine the precise unauthorized dumping areas based on the LST derived from the multi-temporal remote sensing images (*The Al-Jleeb landfill, Al-Farwanyah, Kuwait*)

1.4. Structure of the Thesis

Based on the objectives of the study, this thesis is presented in six chapters. Chapter 1 introduces the background of the study, research problem, the objectives, and the structure of the thesis. Chapter 2 discusses the background of the landfill design, the existing landfill monitoring methods, applications of geographic information systems and the remote sensing in landfill monitoring, and a review of satellite remote sensing sensors. Chapter 3 presents the research methodology, including the details of the atmospheric correction model for the remote sensing images and the computation of LST from the thermal band of these remote sensing images. Chapter 4 describes the details of the experimental work. These include the study areas, details of the multi-temporal remote sensing data, and the procedures of data processing and the analysis, using remote sensing and GIS techniques. Chapter 5 analyzes the results of both case studies. Comparisons between the LST and the air temperature as well as the LST for the development stages are conducted on the Trail Road landfill. A correlation analysis is also performed to find the relationship between the LST and the amount of landfill gas. In the Al-Jleeb landfill, suspicious dumping areas are detected

using the multi-temporal LST images. Finally, Chapter 6 offers the conclusions for the two case studies and makes recommendations for future useful research undertakings.

2. LITERATURE REVIEW

2.1. Landfill Design

Municipal solid waste management is a critical issue for urban management and city planning (Schubeler, 1996). The main purpose of waste management is to provide sufficient protection to the environment and the general public from the risky effects of waste (Yahaya et al., 2011). Landfill (or dumping) is known as a site selected for the disposal of waste materials by interment, and it is the oldest category of waste treatment. Apart from recycling and burning, landfill is one of the methods of waste handling commonly adopted in many countries. The Code of Federal Regulations (CFR) defines a landfill as a separate area of land or a digging site that receives domestic waste or a waste mound (U.S. Federal Emergency Management Agency, 2002).

The bio-degradation process for solid waste leads to the formation of leachate which is a kind of harmful and toxic fluid containing dissolved and suspended materials. Without special treatment, leachate is not soluble. Therefore, a landfill must be designed correctly to protect the environment. By using a mixture of a composite liner and a leachate collection system (see Figure 2.1), the surrounding areas of the landfill can be isolated from the leachate contamination. The design standard of a composite liner system requires a high liner covering with a lower layer of soil of at least two feet of soil, together with hydraulic conductivity no greater than 1×10^{-7} centimeter per second (U.S. Environmental Protection Agency, 1998). The leachate collection system is defined as a network of pipes that collects the leachate from the landfill site and then pumps that collected leachate to the surface of the landfill (U.S. Environmental Protection Agency, 1998).

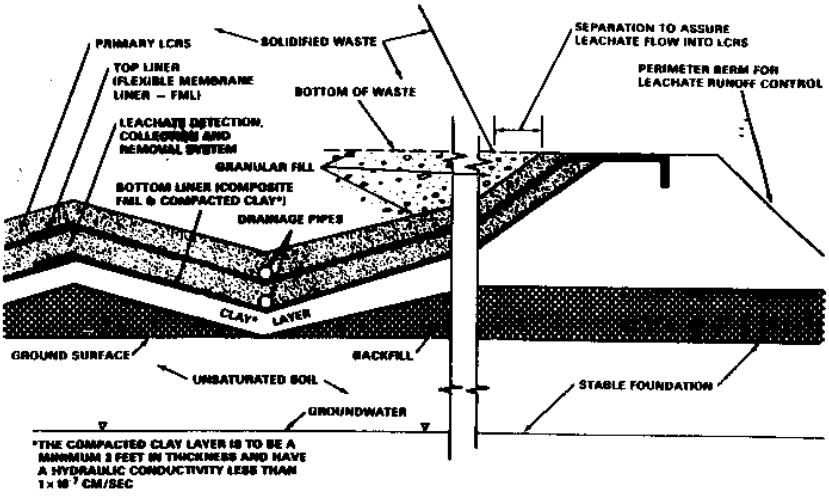

Figure 2.1. A composite liner and leachate collection system (U.S. Environmental Protection Agency, 1998)

There are different types of waste disposal sites that are categorized according to the wastes to be handled. The most common landfill site is designed for the disposal of domestic garbage, which includes a variety of manmade products or natural items, such as packaging, food waste, furniture, clothing, grass clippings, etc. Industrial waste and hazardous waste are not allowed to be disposed of in a landfill site designed for domestic waste. The design criteria for this different kind of waste, such as location, covering material, monitoring systems, and even recordkeeping requirements, are different for these types of landfills (U.S. Environmental Protection Agency, 1998).

If a landfill site is not properly sited, developed, operated, and closed, there can be a significant impact on the environment and the nearby communities. Therefore, landfills must be well situated and designed to prevent contamination to the soil, groundwater and surface water. For any landfill site selection, the main issue is to make sure that the site is designed environmentally and socially acceptable. Previously, the size and location of a landfill site were the critical criteria in the design

process to ensure that the facility met the designed disposal needs. However, optimal landfill site location can be based on such factors as the waste generation areas and transportation routes. It is also economical to build a landfill close to the generation areas (such as urban areas or industrial areas) and have shortest route to the site to reduce transportation costs (Ball, 2005). Regarding the site selection of a landfill, Babalola and Busu (2011) introduced several criteria to use to determine the appropriate locations for a landfill, such as 1) distance from urban areas, 2) distance from farms and agricultural areas, 3) distance from transportation routes, 4) distance from the railways, 5) nature of surface and underground water, 6) topography, and 7) wind orientation.

Currently, landfills are monitored by setting up monitoring systems within the site to acquire testing samples. The purpose is to determine the organic content in the testing samples and their bio-chemical properties. Table 2.1 summarizes the organic content to be determined in the waste management, including moisture content, volatile solids content (VS), total organic carbon content (TOC), cellulose (CEL)m hemicelluloses (HEM), lignin (LIG) with leaching tests (Cobo et al., 2008). Moreover, Biochemical Methane Potential (BMP) or respirometry measurements are now becoming more popular as one of the closest approaches to achieve landfill biological stability (Cobo et al., 2008). However, a monitoring scheme requires the set-up of expensive equipment and conducting of laboratory testing which are both time and cost consuming. Moreover, that system is limited to the landfill site, and somewhat costly and complicated to be able to extend the measurements out of the landfill site. Therefore, the issue has encouraged new research efforts for using remote sensing and geospatial information technology to assist in the ongoing monitoring of landfill sites.

Table 2.1. Summary of landfill site monitoring methods (Cobo et al., 2008)

Analyses	Fundamentals
Moisture Content	• Measure the weight of the loss of water when heating waste at 45ºC or at 105ºC until a constant weight is reached.
Volatile Solid Content	• Measure the weight of the loss of volatile material when the dry sample is heated at 550 ºC
Organic Carbon Content	• By using an infrared detection, CO_2 is produced when a sample interact with oxygen at 900 ºC - 1300 ºC (Francois et al., 2006)
Cellulose, Hemicelluloses and Lignin(CEL, HEM, LIG)	• *Cellulose* (CEL) is hydrolysed into glucose in two stages using sulphuric acid. • *Hemicellulose* (HEM) is determined by the measurement of galactose, manose, xylose, and garabinose after digestion. The glucose measured comes from broken cellulose. • *Lignin* (LIG) is the remaining suspended solids after hydrolysis and the combustion of the solid waste at 550ºC (Mehta et al, 2002).
Leaching Test	• Leaching measures the contaminants released from the solid part of the waste into the water part under the pressure of different reactions (Ham et al,.1993).
Biochemical Methane Potential (BMP) and Gas production (GP)	• Identifies the quantity of methane (CH_4) from anaerobically decomposing organic matter in laboratory tests. • The sample is incubated with a seed of appropriate bacteria under good conditions (Kelly et al., 2006).

Respirometry (RA, RI)	• Evaluates the activity of a sample through its oxygen consumption. • The sample is mixed with a seed and incubated under aerobic conditions. CO_2 production (converted to oxygen consumption) or direct O_2 consumption is measured (Environment Agency, 2005).

2.2. Geographic Information Systems and Remote Sensing for Landfill Monitoring

There are several research studies that use a geographic information system (GIS) and remote sensing for landfill site selection and monitoring. Mahamid and Thawaba (2010) investigated the appropriate landfill site location for the City of Ramallah, Palestine. In Ramallah, most of the landfill sites are not well organized. In addition, the solid wastes are dumped (without any prior treatment) which affects both nature and the public health. The main goal of the current research is to develop a suitable landfill site that offers fewer hazards to the environment and humans. The use of GIS can be used to identify potential sites for an appropriate landfill site in the Cty of Ramallah, using geospatial data acquired from different institutions and governmental agencies, such as land use, topography, road networks, ground and surface water, infrastructure data, and urban areas. Overlay analysis and buffer analysis around sensitive areas were both carried out to generate a final map which indicates the most suitable location for a landfill site.

Nas et al. (2010) demonstrated a case study in the City of Konya, Turkey, for appropriate site selection for the landfill, using the GIS and multi-criteria evaluation (MCE). The ArcGIS ArcMap 9.0 and its extensions can be customized to build MCE. Eight GIS layers were acquired for this site selection, including the urban areas, land use/land cover, land slope, archaeological sites, transportation routes, local wells, and irrigational canals. Each layer was ranked with different weights where 0 indicated an unsuitable area and 10 indicated the most suitable area. The final

map shows all the suitable locations for the landfill site for the different categories. The categories were classified as: 6.8% were the most appropriate, 15.7% were appropriate, 10.4% were moderately appropriate, 25.8% were poorly appropriate, and 41.3% were inappropriate. At the end of the analyses, three locations were identified as the most appropriate landfill site locations for the City of Konya.

In the study by Silvestri and Omri (2008), it was reported that the Veneto region in Italy has considerable problems with illegal landfills. These landfills were formed approximately 30–50 years ago and were then hidden or forgotten. Therefore, this study proposed a method based on the use of remote sensing and photogrammetry techniques to detect these illegal landfill sites. New aerial photographs were acquired in 2000, and historical aerial photograph data from 1955 to 1987 were also obtained. This aerial data were used to assess the study sites and identify the different types of surfaces and vegetation cover. Pan-sharpened IKONOS satellite images were also collected in June and July of 2001. The collected data were then radiometrically calibrated and atmospherically corrected. An atmospheric visibility index was considered, using secondary data collected at ground level, while the optical thickness of the atmosphere was measured using a sun-photometer. The experiential work included 1) recognition of possible contaminated sites using maximum likelihood (ML) classification on the IKONOS images; 2) manual digitization of the detected sites; and 3) site selection from all the digitized sites and their conversion into GIS. The classification was conducted for four classes: Very stressed brown–yellow vegetation (Class 1); non-uniformly stressed vegetation cover (Class 2); bare soil with very low vegetation (Class 3); and lightly stressed vegetation (Class 4). The results showed that all the illegal landfills had large areas of stressed vegetation cover.

Ottavianelli et al. (2007) introduced the Synthetic Aperture Radar (SAR) interferometric products and hypersepctral data to monitor the Brogborough landfill located midway between Milton Keynes and Bedford in the U.K. The study used the ground-based SAR (GB-SAR) system to measure the microwave signals for the landfill site. The measurements of capped area and the open cells were conducted in the landfill site for a comparative analysis of angular measurements of polarizations. Moreover, coherence (or decorrelation) and SAR backscatter signal method were used to identify the dumping areas. The study demonstrated that the decorrelation method is of particular use to detect the properties and characteristics of the surface of the landfill, i.e., surface roughness, soil moisture affected by topography, speckle, and wave polarization. The results showed that high decorrelation and backscatter values can be an indication of the suspicious location of waste deposits.

Another research was conducted in the City of Venice, Italy (Biotto et al., 2009). The main goal in this case study was to detect and identify uncontrolled landfill sites. Remote sensing and GIS techniques were used to determine these uncontrolled landfill sites. The datasets included the IKONOS satellite images acquired in 2001 and a 2000 land cover map. Similar to the study of Silvestri and Omri (2008), the ML classification technique was applied to detect the locations and conditions of the landfills by classifying the study areas into stressed vegetation, authorized landfill sites, and industrial sites. Road networks for easy access roads and a low population density were further identified using GIS. The results showed that the integration of remote sensing techniques and GIS maps can be used efficiently to narrow down suspicious locations of uncontrolled landfill sites (Biotto et al., 2009).

Previously, Mirtorabi (2010) conducted a preliminary analysis on the Trail Road landfill site by using four Landsat images acquired in different years and different seasons. However, the work focused on the use of NDVI and LST to investigate the contamination process within the landfill site and the surrounding vegetation. In this study, an in-depth analysis was carried out in the Trail Road landfill by analyzing more remote sensing Landsat images and improving the quality of the derived LST using the atmospheric correction process.

2.3. A Review of Optical Remote Sensing Sensors

There are a number of optical remote sensing sensors that are commonly used for Earth observation and environmental monitoring. Optical remote sensing sensors acquire images of the Earth surface by recording the solar radiation reflected from targets on the ground. Commonly these optical remote sensing sensors acquire images in a visible spectrum (red, green, and blue), near infrared spectrum, and up to a shortwave infrared spectrum. Different materials have different characteristics of absorption and reflection of energy across these spectrum ranges; therefore, optical remote sensing images are of particular usefulness to distinguish different features and derive precise information that represents the nature of the Earth surface. Optical remote sensing sensors can be further categorized into panchromatic (PAN), multi-spectral (MS) and hyper-spectral imaging systems (Jensen, 2005).

High resolution remote sensing sensors, such as GeoEye, IKONOS, QuickBird, and WorldView, acquire images with a spatial resolution less than 1m. Such types of remote sensing images commonly provide three channels, namely, a visible spectrum, one PAN channel, and one channel in a near-infrared red (NIR) spectrum. Tables 2.2 and 2.3 show the technical specifications of IKONOS and QuickBird sensors. Due to their high spatial resolution, they are commonly used for

feature extraction, data fusion, topographic mapping, and digital elevation model (DEM) generation (Shaker et al., 2010). However, this type of remote sensing image is not suggested for multi-temporal analysis as 1) it does not have thermal bands, and 2) the acquisition cost is high.

Table 2.2. Technical Specifications of IKONOS

Band	Spectral Range (μm)	Pixel Size (m)	Quantization	Swath Width
1 (blue)	0.45 - 0.52	4	11 bit	11 km
2 (Green)	0.52 - 0.60	4	11 bit	11 km
3 (Red)	0.63 - 0.69	4	11 bit	11 km
4 (NIR)	0.76 - 0.90	4	11 bit	11 km
5 (PAN)	0.45 - 0.90	1	11 bit	11 km

Table 2.3. Technical Specifications of QuickBird

Band	Spectral Range (μm)	Pixel Size (m)	Quantization	Swath Width
1 (blue)	0.45 - 0.52	2.44	11 bit	20-40 km
2 (Green)	0.52 - 0.60	2.44	11 bit	20-40 km
3 (Red)	0.63 - 0.69	2.44	11 bit	20-40 km
4 (NIR)	0.76 - 0.90	2.44	11 bit	20-40 km
5 (PAN)	0.45 - 0.90	0.61	11 bit	20-40 km

Mid-resolution remote sensors, such as the Système Probatoire d'Observation de la Terre (SPOT) and the Indian Remote Sensing (IRS) sensors have lower spatial resolution than the aforementioned sensors. Their spatial resolution can vary from 10 m to 20 m (see Tables 2.4 and 2.5). However, these kinds of sensors usually acquire more than one channel in the NIR spectrum and even shortwave infrared red (SWIR). Therefore, they are particularly useful for determining bio-physical parameters, such as the Normalized Difference Vegetation Index (NDVI), Leaf Area Index (LAI), or biomass estimation. With such fruitful spectrum information, these sensors are

commonly used for land cover classifications and land cover mapping because the high dimension data (multi-spectral bands as well as the derived biophysical parameters) can provide high separabilities for the different land cover materials.

Table 2.4. Technical Specifications of IRS-1C and 1D

Band	Spectral Range (μm)	Pixel Size (m)	Quantization	Swath Width
2 (Green)	0.52 - 0.59	23.5	8 bit	141 km
3 (Red)	0.62 - 0.68	23.5	8 bit	141 km
4 (NIR)	0.77 - 0.86	23.5	8 bit	141 km
5 (MIR)	1.55 - 1.70	70.5	8 bit	148 km
6 (PAN)	0.50 - 0.75	5.2	8 bit	70 km
7 (WiFS1)	0.62 - 0.68	188	8 bit	692 km
8 (WiFS2)	0.77 - 0.86	188	8 bit	692 km

Table 2.5. Technical Specifications of SPOT IV

Band	Spectral Range (μm)	Pixel Size (m)	Quantization	Swath Width
1 (Green)	0.50 - 0.59	20	8 bit	60 km
2 (Red)	0.60 - 0.68	20	8 bit	60 km
3 (NIR)	0.79 - 0.89	20	8 bit	60 km
4 (PAN)	0.48 - 0.71	10	8 bit	60 km
5 (SWIR)	1.58 - 1.75	20	8 bit	60 km

In this study, the remote sensing images acquired by the Landsat satellites are utilized to monitor the landfill. The Landsat satellite has both a Thematic Mapper (TM) and an Enhanced Thermatic Mapper plus (ETM^{+}) sensors (See Tables 2.6 and 2.7). An archive of these data was released free to the public by the United States Geological Survey (USGS) in 2008. Therefore, there is no need to consider actual data acquisition costs. In addition, the Landsat sensors have a thermal infrared (TIR) channel not available on all the afore-mentioned sensors. Although the spatial resolution of

the Landsat images are in 30m for the MS channels and 60 m in the TIR channel, they are still useful for monitoring landfill sites and their surrounding areas. The high repeating cycle also offers an high- dimension data archive for the same study which is then helpful in the multi-temporal analysis.

Table 2.6. Technical Specifications of Landsat TM

Band	Spectral Range (μm)	Pixel Size (m)	Quantization	Swath Width
1 (Blue)	0.45 - 0.52	30	8 bit	185 km
2 (Green)	0.52 - 0.60	30	8 bit	185 km
3 (Red)	0.63 - 0.69	30	8 bit	185 km
4 (NIR)	0.76 - 0.90	30	8 bit	185 km
5 (MIR)	1.55 - 1.75	30	8 bit	185 km
6 (TIR)	10.40 - 12.5	60	8 bit	185 km
7 (MIR)	2.08 - 2.35	30	8 bit	185 km

Table 2.7. Technical Specifications of Landsat ETM^{+}

Band	Spectral Range (μm)	Pixel Size (m)	Quantization	Swath Width
1 (Blue)	0.45 - 0.52	30	8 bit	185 km
2 (Green)	0.52 - 0.60	30	8 bit	185 km
3 (Red)	0.63 - 0.69	30	8 bit	185 km
4 (NIR)	0.76 - 0.90	30	8 bit	185 km
5 (MIR)	1.55 - 1.75	30	8 bit	185 km
6 (TIR)	10.40 - 12.5	60	8 bit	185 km
7 (MIR)	2.08 - 2.35	30	8 bit	185 km
8 (PAN)	0.52 - 0.90	15	8 bit	185 km

3. METHODOLOGY

3.1. Overall Workflow

Figure 3.1 shows the overall workflow for the two case studies (Trail Road landfill and Al-Jleeb landfill) which can be summarized in the following steps. First, the multi-temporal Landsat images were downloaded from the USGS Earth Explorer where the images have been released to the public since year 2008. Landsat TM and Landsat ETM$^+$ images were both acquired for the experimental work because Landsat TM images have a huge archive of data since 1984. Although the multi-spectral bands of Landsat images can be used for classification and feature extraction, only the thermal band (Band 6 of Landsat TM and Band 61 of Landsat ETM$^+$) are used to determine land surface temperature (LST) in this study.

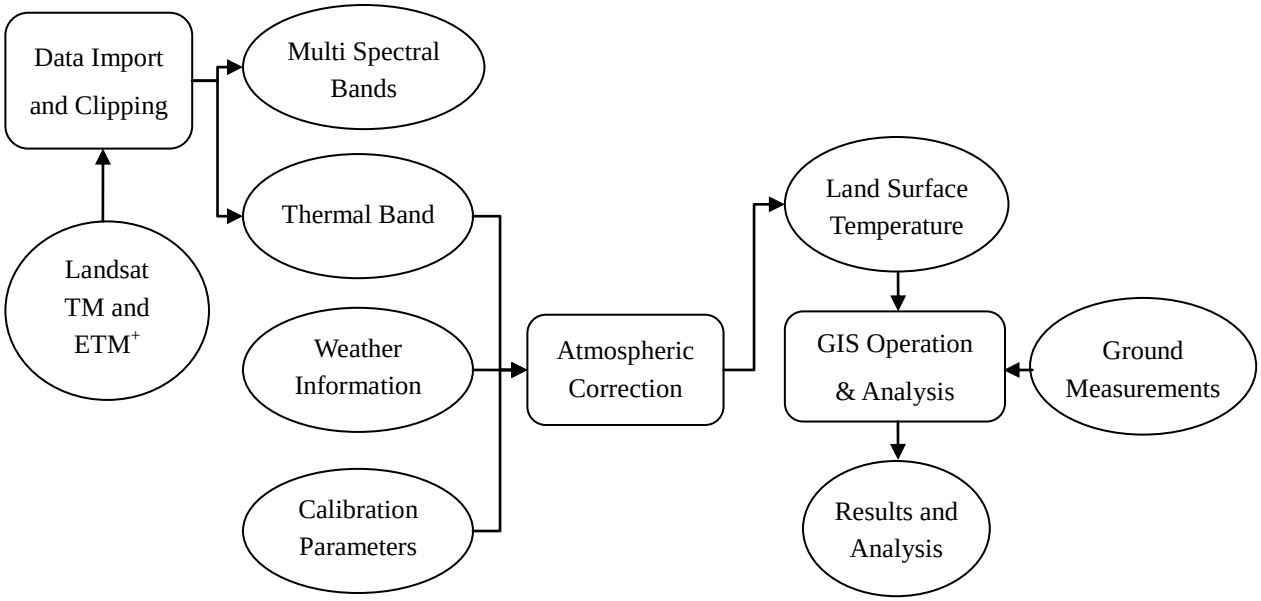

Figure 3.1. Experimental Workflow

In the case study of the Trail Road landfill, 30 Landsat TM images are downloaded from years 2001 to 2009. The reason to acquire the data within this period is mainly due to the set- up of

ground monitoring stations in the Trail Road landfill site in 2001. In the case study on the Al-Jleeb landfill, 11 Landsat TM and ETM^+ images were acquired from years 1985 to 2001. As the acquired Landsat images cover the area of 185 x 185 km^2, the images were clipped to the landfill sites to improve the performance of data processing. Finally, all the subsets of the images were projected into the UTM coordinate system.

Before computing the LST, atmospheric corrections were conducted for all the multi-temporal Landsat images. The atmospheric correction model (ATCOR2) developed by Richter (1998) was utilized to calculate the transmission and the up and down radiance. Details of the atmospheric correction will be discussed in Section 3.2. To run the ATCOR2 model, weather information (e.g. air temperature, visibility, etc.) were obtained from the Government's national climate and weather data archive. The calibration parameters for Landsat TM and ETM^+ sensor (biases and gains) were also required for an atmospheric correction. Table 3.1 shows the newly calibration parameters for Landsat TM used in this study, as revised by the USGS on the 2nd of April, 2007 (Chander, 2007). After conducting the atmospheric correction, the LST was derived from the thermal band of the Landsat images, the details of which can be found in Section 3.3.

Table 3.1. Revised Landsat TM Calibration Parameters (Chander, 2007)

	Mar. 1, 1984 to Dec., 31, 1991		**Jan. 1, 1992 to Present**	
Band	**Biases (W/m^2 sr µm)/DN**	**Gains (W/m^2 sr µm)**	**Biases (W/m^2 sr µm)/DN**	**Gains (W/m^2 sr µm)**
1	0.668706	-1.52	0.762824	-1.52
2	1.317020	-2.84	1.442510	-2.84
3	1.039880	-1.17	1.039880	-1.17
4	0.872588	-1.51	0.872588	-1.51
5	0.119882	-0.37	0.119882	-0.37

6	0.055158	1.2378	0.055158	1.2378
7	0.065294	-0.15	0.065294	-0.15

After the atmospheric correction, the final step conducted an analysis of the multi-temporal LST images for both case studies. In the case of the Trail Road landfill, the LST for the landfill site was compared to the LST of the surrounding areas as well as the air temperature for each of the Landsat images (from 2001 to 2009). This comparison was achieved by using the GIS zonal analysis, together with the boundary of the landfill site. The LST for the closed stages was also compared with the LST of the active stage as well as the recently closed stage. A preliminary analysis was carried out to investigate the correlation between the LST and the amount of landfill gas. The measurements of methane (CH_4) from the two monitoring wells (GM-2 and GM-17) were obtained within years 2008 and 2009, and a regression analysis was conducted to derive the relation between these two factors.

In the Al-Jleeb landfill, the multi-temporal LST images (from 1985 to 2001) were imported in the GIS environment for further analysis. Temperature contours (polylines) were generated for each of the LST images by using the raster to vector conversion tool. As the goal for the Al-Jleeb landfill case study aimed at determining the suspicious location of the waste dumping area, the highest temperature of the contours was extracted from the polylines for each of the LST images. The extracted temperature contours were then overlaid in the GIS environment and the location with high dense overlapping areas was regarded as the possible location for the waste dumping areas in the Al-Jleeb landfill site. Finally, a topographic map was produced by overlaying all the temperature contours to the boundary of Al-Jleeb landfill site.

3.2. Atmospheric Correction

Atmospheric correction is a significant step in many remote sensing applications (Mausel et al., 2002). The atmospheric correction usually removes atmosphere attenuation, which is caused by scattering and absorption in the atmosphere (Jensen, 2005). Other definitions specified that the atmospheric correction is used to remove the effects that change the spectral characteristics of the land features (Paolini et al., 2006). Jensen (2005) addressed the importance of the atmospheric correction if bio-physical parameters are extracted from the satellite images. The atmospheric correction is of particular importance for multi-temporal data studies. If the data extracted from the image are compared to the same data from a different image obtained at different dates, it is generally important that the remote sensor data are atmospherically corrected to minimize seasonal effects (Jensen, 2005).

Although there are a few previous studies that have adopted multi-temporal Landsat images to monitor the landfills, atmospheric corrections were not considered in these studies (Kwarteng and Al-Enezi, 2004; Yang et al., 2008). The importance of atmospheric correction has been addressed in many remote sensing studies for calculation of vegetation indices and land surface temperature (Ou et al., 2002; Hadjimitsis et al., 2010). To obtain the most optimal results of the LST, atmospheric correction for all the Landsat images were conducted in both of our case studies. The absolute atmospheric correction model, ATCOR2 (Atmospheric Correction and Haze Reduction) built-in PCI Geomatics software was used (Richter, 1998). After applying the ATCOR2 model, the LST of each image was computed. To atmospherically correct the Landsat images, numerous environmental and system data were obtained, such as sensor information (sensor type, acquisition date, and pixel size); the atmospheric conditions (reference to weather information from the Government weather office); calibration parameters for the Landsat TM and ETM^{+} images as

mentioned in Section 3.1; and the correction parameters (solar zenith and azimuth, visibility, and adjacency). The output of the ATCOR2 model includes the corrected original Landsat image and an option to calculate the LST and other value-added products from the corrected images. The equation for the atmospheric correction model is as follows:

$$\rho_i(x,y) = \frac{\pi\left(d^2[c_0 + c_1 DN(x,y)] - L_p(z)\right)}{T_v(z)[bE_s T_s(z)\cos\beta(x,y) + E_d*(x,y,z) + E_g(z)\overline{\rho}_{terrain}^{(i)} V_{terrain(x,y)} / \pi]} \quad (3.1)$$

where (x, y) are the horizontal coordinates corresponding to the geo-referenced pixel positions; z is the vertical coordinate containing the elevation information from the digital elevation model (DEM); $DN(x, y)$ refers to the digital number (DN) of the geo-referenced pixel; $L_p(z)$ is the elevation dependent path radiance; $T_v(z)$ is ground-to-sensor view angle transmittance with direct plus diffuse components; and $T_s(z)$ is the sun-to-ground beam (direct) transmittance. The term, $E_s T_s(z)\cos\beta(x, y)$, represents the beam irradiance. It is preceded by a binary factor b, where b = 1 if direct radiation illuminates the pixel (x, y).The factor b = 0 if $\cos\beta(x, y) < 0$ which means that the pixel is completely under the shadow and does not receive direct solar radiation. $\beta(x, y)$ is the angle between the solar ray and the surface normal (illumination angle). The term E_s is the extraterrestrial solar irradiance; $E_{d*}(x, y, z)$ is the diffuse solar flux; $E_{g*}(z)$ is the global flux which refers to the direct plus diffuse solar flux on a horizontal surface at elevation z; $\bar{\rho}_{terrain}^{(0)}$ is the initial value (constant for each band) of average terrain reflectance, $\bar{\rho}_{terrain}^{(i)}(x, y)$ is the locally varying average terrain reflectance calculated iteratively (i = 1, 2, 3) by low pass filtering of the image with a box of 1 km by 1 km; $V_{terrain}(x, y)$ is the terrain view factor (0 to 1 range) calculated from the local slope or a horizon analysis. Figure 3.2 illustrates the entire radiation components that were taken into account in the atmospheric correction model developed by Richter (1998).

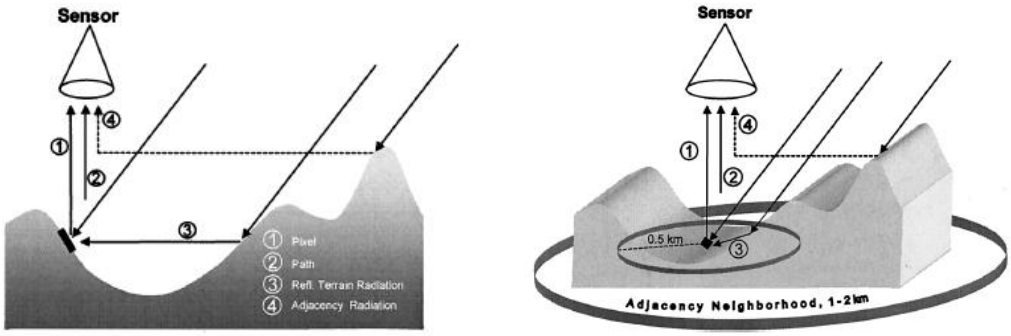

Figure 3.1. Radiation components for the ATCOR model (Richter, 1998)

3.3. Land Surface Temperature (LST)

The LST is an essential parameter in a variety of disciplines used to study the biosphere process (Wang et al., 2009), the urban climate (Norman et al, 1995; Czajkowski et al., 2004), urban environmental quality (Nichol and Wong, 2009), and urban heat islands (Weng et al., 2004). LST is the result of a land-surface process that combines the results of all surface-atmosphere interactions and energy fluxes between the atmosphere and the ground. Mapping the LST from thermal remote sensing sensors can be a useful tool for large scale environmental and urban studies. Currently, there are number of satellite-borne sensors that acquire thermal infrared spectrum information, such as the Advanced Very High Resolution Radiometer (AVHRR) from National Oceanic and Atmospheric Administration (NOAA), the Moderate-Resolution Imaging Spectroradiometer (MODIS) from the National Aeronautics and Space Administration (NASA), and the Advanced Spaceborne Thermal Emission and Reflection Radiometer (ASTER) from NASA. However, most of these sensors are used to monitor the Earth's surface on regional or global scales where the spatial resolution of the remote sensing data can vary from one hundred to a thousand meters. In this study, the Landsat TM and ETM^{+} data are used to derive the LST because 1) it offers free-to-public data (since 1984) through the web; 2) the spatial resolution of the thermal band is 60 m; and 3) Landsat has a high repeat cycle (16 days) which produces

voluminous data archive for multi-temporal studies.

The computation of LST mainly involves two steps. The first step is to convert the pixel value of the thermal band into radiance using the following equation (3.2):

$$L = \left[\frac{L_{\max} - L_{\min}}{Q_{cal.\max} - Q_{cal.\min}} \right] \left(Q_{cal} - Q_{cal.\min} \right) + L_{\min} \tag{3.2}$$

where L is the radiance; L_{max} is the spectral radiance that is scaled to $Q_{cal.max}$; L_{min} is the spectral radiance to $Q_{cal.min}$; Q_{cal} is the quantized calibrated pixel value in a digital number; and $Q_{cal.max}$ is the maximum quantized calibrated pixel value corresponding to L_{max}. For Landsat TM Band 6, the values for L_{max}, L_{min}, and $Q_{cal.max}$ are 15.3032 $Wm^{-2}sr^{-1}\mu m^{-1}$, 1.2378 $Wm^{-2}sr^{-1}\mu m^{-1}$, and 255, respectively. The second step is to convert the calibrated radiance into an at-sensor brightness temperature using the following equation (3.3):-

$$T_{BBT} = \frac{K_2}{\ln\left(\frac{K_1}{L} + 1 \right)} \tag{3.3}$$

where T_{BBT} is the blackbody temperature in Kelvin (K), K_1 is the calibration Constant 1 in $Wm^{-2}sr^{-1}\mu m^{-1}$, and K_2 is the calibration Constant 2 in Kelvin (K). For Landsat TM, K_1, and K_2 are 607.76 $Wm^{-2}sr^{-1}\mu m^{-1}$ and 1260.56 K, respectively (Chander et al., 2009). The computed T_{BBT} is regarded as the LST derived from the Landsat image.

4. EXPERIMENTAL WORK

4.1. The Study Areas

4.1.1. The Trail Road Landfill, Ottawa, Canada

Canadians produce over 35 million tons of waste every year. Among these wastes, 22 million tons of waste comes from non-residential sources, such as industrial, commercial, and institutional sectors, and the remaining 13 million tons of waste are produced from residential disposals. To handle all these wastes, about 77% of the wastes are sent to the landfills or incinerators while the rest of the 23% are recycled from the disposal. One-third of the total waste disposal in the landfills is from residential sources, while the rest are from industrial, commercial, and institutional waste (Federation of Canadian Municipalities, 2006). The City of Ottawa, the capital city of Canada, is the second largest city in the Province of Ontario and the fourth largest city in the country with a total population of about 812,129 (Statistics Canada, 2008). With respect to municipal solid waste, the City of Ottawa collects about 975,000 tons of solid waste every year. Among these wastes, 195,000 tons are diverted from landfills disposal to recycling programs, which leaves about 780,000 tons of solid waste that needs to be disposed of in the local landfills (Federation of Canadian Municipalities, 2006).

The Trail Road landfill site is located in Ottawa City, Ontario, Canada (45°14’ N, 75°45’ W) as shown in Figure 4.1. The Trail Road landfill was constructed in December 1978. The completed operation of the adjacent Nepean landfill was the reason behind the establishment of the Trail Road landfill site. The new area acquired on the North side of the Nepean landfill site in March 1975 was designated to be the new landfill site. The Trail Road landfill site started to accept solid waste in 1980 to the present. Trail Road landfill contains four stages developed sequentially

beginning at Stage 1 (farthest to the East) and moving Westward to Stage 4 (see Figures 4.1 and 4.2). The total area of the Trail Road landfill site is approximately 2.02 (km^2) surrounded by farmlands, Highway 416 and some light industry. The Trail Road landfill is considered the primary disposal site for municipal solid waste for the City of Ottawa. The Trail Road landfill site is a municipal non-hazardous landfill that only accepts residential garbage, construction, commercial, institutional, and light industrial waste (Dillon Consulting Limited, 2008).

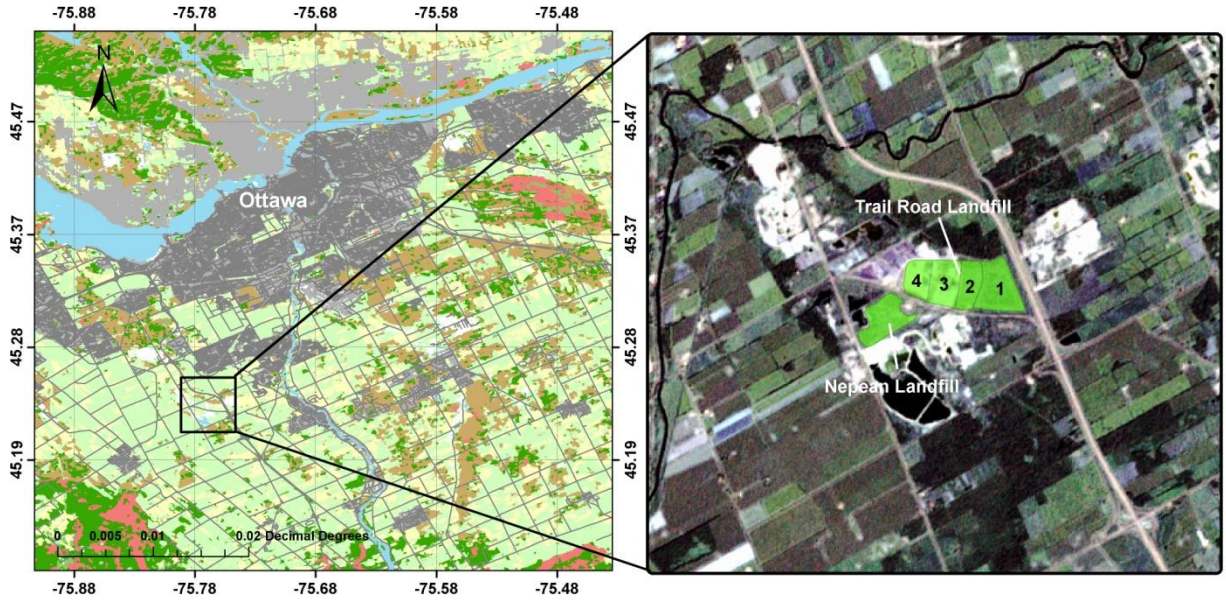

Figure 4.1. The Trail Road Landfill in the City of Ottawa, Canada

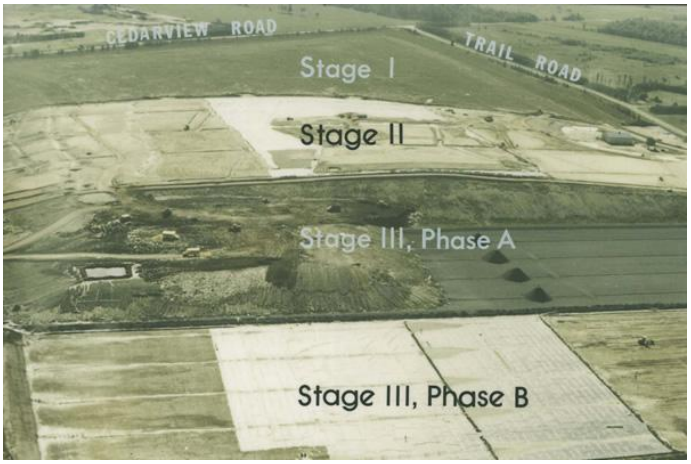

Figure 4.2. Oblique Aerial Photo of the Trail Road Landfill (J.L. Richards & Associates, 2011)

4.1.2. The Al-Jleeb Landfill, Al-Farwanyah, Kuwait

The Al-Jleeb landfill site is considered the largest existing landfill in the City of Al-Farwanyah with a total area 5.5 km² (Schrapp & Mutairi, 2010). The Al-Jleeb landfill site is located in the City of Al-Farwanyah, Kuwait as shown in Figure 4.3. The site accepts industrial, commercial, and municipal solid waste. However, construction, demolition, and sludge waste are all located in the southeastern half of the landfill. The Al-Jleeb landfill site is owned by the Government of Kuwait. The landfill site was licensed by Kuwait Municipality to dispose municipal solid waste in 1980, and the landfill has received about 58% of the total domestic waste in Kuwait (Al-Mutairi, 2004). Since 1992, complaints regarding the hazardous effects of the landfill site have been reported due to bad odors emanating (Schrapp & Mutairi, 2010). Therefore, prevention of further improper disposal operations in the landfill should be ensured.

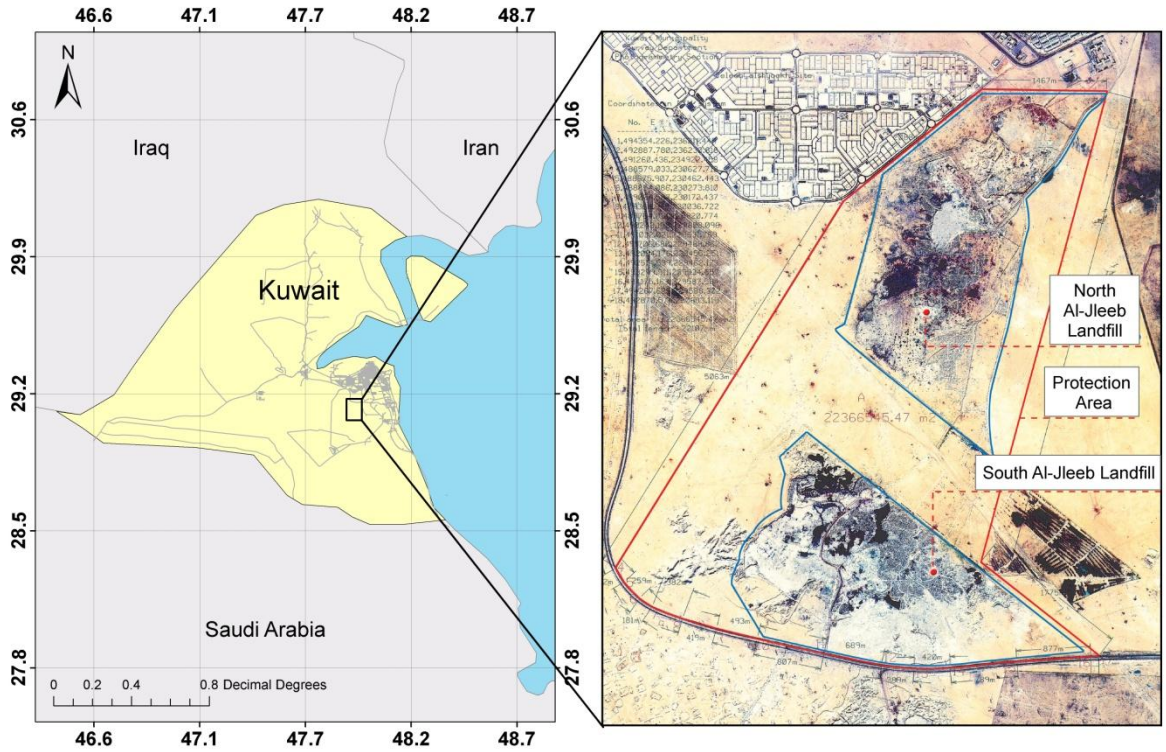

Figure 4.3. The Al-Jleeb Landfill in the city of Al-Farwanyah, Kuwait

4.2. Multi-Temporal Remote Sensing Data

4.2.1. The Trail Road Landfill, Ottawa, Canada

The case study of the Trail Road landfill involves two categories of data: 1) multi-temporal Landsat satellite images; and 2) landfill gas measurement acquired from ground monitoring wells. Regarding the remote sensing data, over 30 Landsat TM images were downloaded from the USGS Earth Explorer for years 2001 to 2009 as shown in Table 4.1. The spatial resolution for the Landsat image is 30 m for the multi -spectral bands and 60 m for the thermal bands. All these images were imported into PCI Geomatics V10.1, clipped, and then projected into the UTM Zone 18 coordinate system. The atmospheric correction was conducted to retrieve optimal results for the LST, using sensor parameters data, (sensor type, acquisition date, sun elevation, sun zenith and pixel size) and weather conditions (air temperature and visibility). Figure 4.4 shows the graphical user interface for ATCOR2 in PCI Geomatica. The weather information was obtained from historical records at the Ottawa Macdonald-Cartier International Airport, which is approximately 10 km away from the Trail Road landfill site. Sensor parameters, such as sensor type, acquisition date, sun elevation, sun azmuith, and image resolution, were obtained from metadata for the Landsat images. In this thesis, multi-temporal Landsat images from 2001 to 2009 were used to derive the land surface temperature in the Trial Road landfill site. Moreover, the Landsat images from years 2007 and 2008 and taken at different acquisition dates (April to October) were used to verify the relationship between the satellite-based and ground-based measurements. The acquisition dates from November to March were neglected due to the weather conditions which could affect data results. The difference in temperature measurements were used to correlate with the emitting landfill gas Methane (CH4) measurements acquired at two monitoring stations, GM-2 and GM-17, located near Stages 1 and 3 of the Trail Road landfill. The location of the ground monitoring stations is shown in Figure 4.1.

Table 4.1. Landsat TM Images for the Trail Road Landfill Case Study

Acquisition Date	GMT Time	Sun Azimuth	Sun Elevation	Air Temperature	Visibility
May 13, 2001	15:31:11	136°30'53"	57°40'32"	12.4°C	40.2 km
Aug., 1 2001	15:31:21	133°24'58"	55°52'44"	30.2°C	32.2 km
Aug. 20, 2002	15:25:32	137°13'01"	50°46'53"	23.3°C	32.2 km
May 19, 2003	15:25:57	135°36'33"	57°20'53"	25.0°C	32.2 km
Jul. 6, 2003	15:27:18	127°25'29"	59°30'43"	27.4°C	24.1 km
Jul. 15, 2003	15:21:14	128°24'45"	58°26'11"	27.1°C	24.1 km
Jun. 15, 2004	15:26:17	130°08'47"	61°21'03"	23.9°C	32.2 km
Jul. 24, 2004	15:33:34	132°26'41"	57°42'57"	20.2°C	32.2 km
Jun. 2, 2005	15:32:18	134°46'38"	61°33'31"	26.5°C	24.1 km
Aug. 21, 2005	15:32:55	142°21'20"	52°00'53"	25.5°C	28.5 km
Aug. 8, 2006	15:38:12	140°13'46"	56°00'58"	22.2°C	24.1 km
Aug. 31, 2006	15:44:38	147°38'07"	49°47'59"	19.2°C	24.1 km
May 7, 2007	15:39:26	143°26'04"	57°46'10"	19.2°C	24.1 km
May 23, 2007	15:39:15	139°51'36"	61°04'15"	23.0°C	24.1 km
Jun. 15, 2007	15:45:05	135°13'09"	62°56'24"	26.6°C	24.1 km
Jul. 17, 2007	15:44:41	135°11'55"	60°24'47"	24.0°C	24.1 km
Aug. 2, 2007	15:44:31	138°32'23"	57°26'05"	31.3°C	19.3 km
Aug. 27, 2007	15:38:04	146°06'56"	51°02'11"	21.4°C	32.2 km
Sept. 19, 2007	15:43:41	154°23'04"	42°32'57"	23.2°C	24.1 km
Oct. 5, 2007	15:43:56	157°20'47"	38°08'41"	23.8°C	24.1 km
Apr. 14, 2008	15:40:21	145°21'34"	50°26'12"	6.9°C	32.2 km
May 25, 2008	15:33:06	136°43'17"	60°45'52"	20.9°C	24.1 km
Jul. 12, 2008	15:31:46	131°54'54"	60°06'60"	23.7°C	24.1 km
Aug. 20, 2008	15:36:24	142°57'47"	51°00'51"	19.9°C	24.1 km
Sept. 5, 2008	15:35:58	147°50'43"	46°13'37"	29.0°C	21.2 km
Oct. 7, 2008	15:35:00	156°12'43"	35°21'37"	11.2°C	24.1 km
Oct. 23, 2008	15:34:27	158°53'26"	29°53'26"	5.5°C	24.1 km
Jul. 15, 2009	15:33:18	133°05'04"	60°01'05"	23.7°C	24.1 km

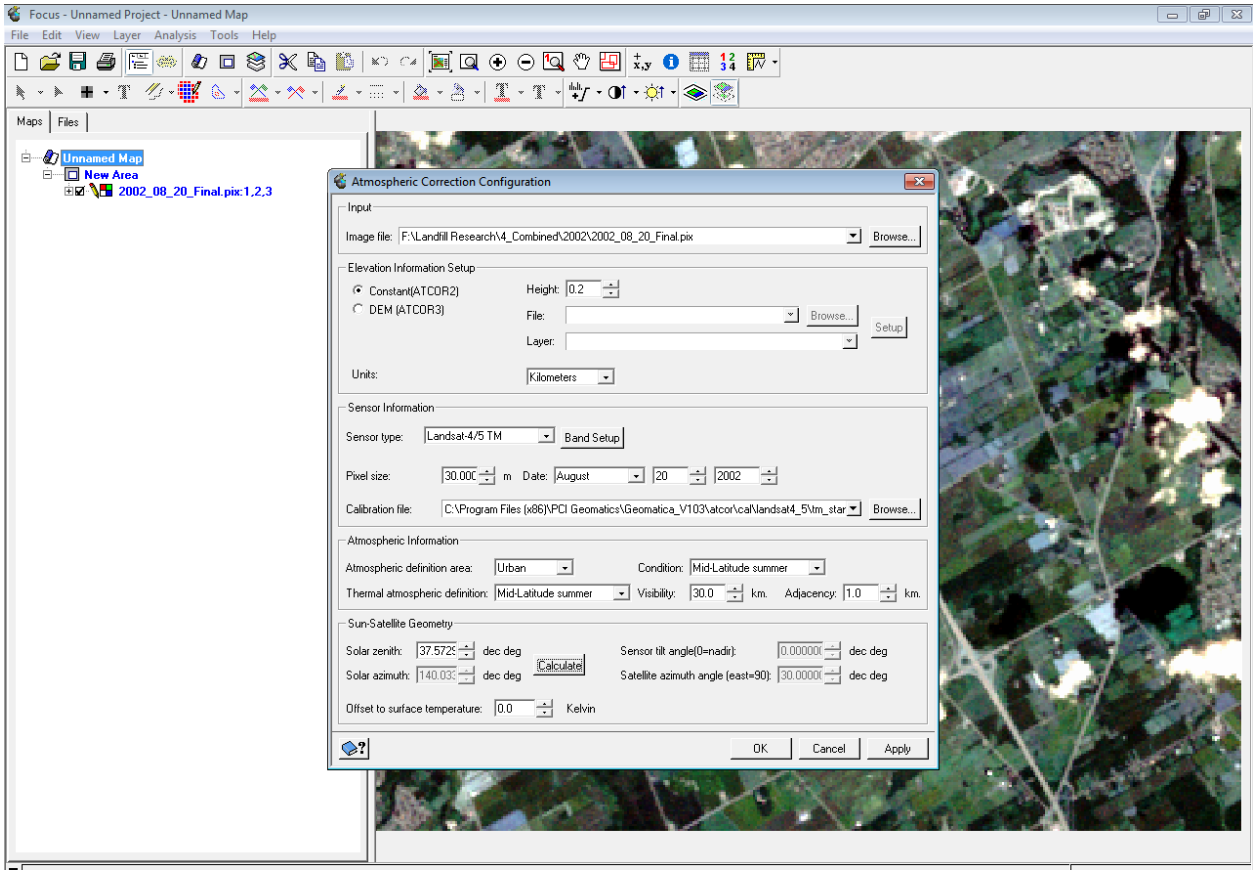

Figure 4.4. The Graphical User Interface forATCOR2 in PCI Geomatica

4.2.2. The Al-Jleeb Landfill, Al-Farwanyah, Kuwait

In this case study, multi-temporal Landsat TM and ETM^{+} images covering the City of Kuwait were downloaded for the last 25 years. However, not all the images were used due to the problem of radiometric quality, i.e., scan line corrector problem. Consequently, only 11 Landsat images were used from 1985 to 2001. All the images were imported into PCI Geomatics V10.1, clipped, and then projected into the UTM Zone 39 coordinate system. Similar to the case study on the Trial Road landfill, the sensor parameters and the weather information (see Table 4.2) were used for atmospheric correction and computation of LST. The weather information was obtained from the Environmental Public Authority of Kuwait, but some of that data was found to be missing due to

the Gulf War in 1991. In this case study, the multi -temporal Landsat images are used to predict suspicious dumping areas within the landfill site.

Table 0.2. Landsat TM and ETM$^+$ Images for the Al-Jleeb Landfill Case Study

Acquisition Date	Sensor	GMT Time	Sun Azimuth	Sun Elevation	Air Temperature	Visibility
Jan. 13, 1985	TM	6:46:36	144°54'45"	30°57'47"	18.30°C	6 km
Dec. 29, 1987	TM	6:39:08	145°54'19"	29°23'51"	8.50°C	10 km
Jun. 12, 1990	TM	6:38:06	95°08'38"	62°41'27"	38.00°C	10 km
Sept. 27, 1991	TM	6:40:12	132°16'19"	48°45'03"	32.50°C	5 km
Oct. 29, 1991	TM	6:40:25	144°12'20"	40°15'31"	28.67°C	5 km
Feb. 28, 1993	TM	6:29:44	129°59'36"	38°38'26"	21.45°C	10 km
Apr. 7, 1998	TM	6:53:09	123°350'4"	55°02'08"	22.00°C	10 km
May 30, 2000	TM	6:52:17	99°18'45"	63°59'46"	36.45°C	4 km
Sept., 3, 2000	TM	6:54:19	123°59'23"	56°12'38"	32.70°C	3 km
May 25, 2001	ETM$^+$	7:06:12	104°16'18"	66°41'56"	33.80°C	4 km
Oct. 16, 2001	ETM$^+$	7:04:31	147°40'38"	46°44'44"	27.00°C	5 km

4.3. Data Processing and GIS Analysis

4.3.1. The Trail Road Landfill, Ottawa, Canada

After atmospheric correction for all the Landsat images, the LST images were exported into a GIS environment for further data processing and analysis. The boundary of the landfill site and the location of the ground monitoring wells were acquired from the prepared Trail Road Landfill Annual Report (Dillon Consulting Limited, 2008). Figure 4.5 shows the LST image with the landfill site boundary in an ArcGIS ArcMap. As the boundary of the landfill site included four development stages, the LST for each development stage was acquired using “Zonal Statistics” in the ArcToolBox. Finally, the average LST for each development stage as well as the entire Trail

Road landfill were computed using this tool. The process was repeated to acquire the LST for the two ground- monitoring wells, so that the correlation between the LST and the amount of emitted methane (CH_4) could be conducted later.

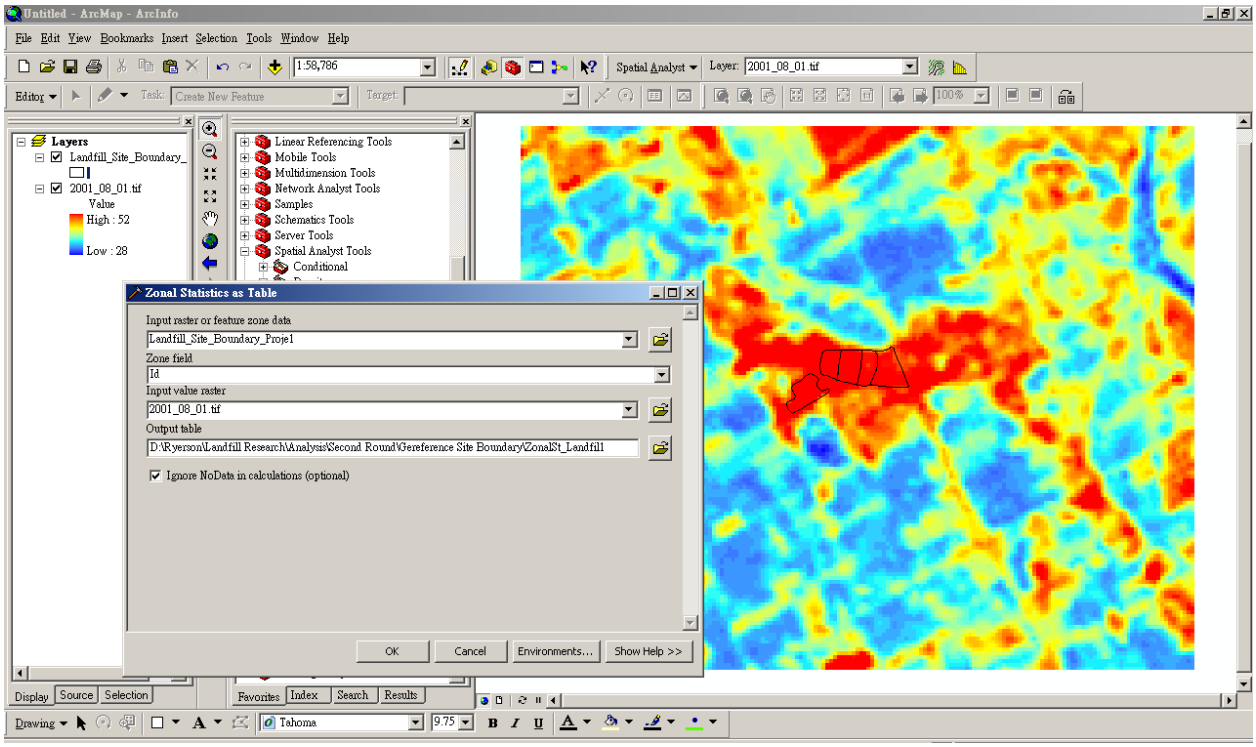

Figure 4.5. Computed LST image in the ArcGIS Environment for Zonal Statistics

In terms of the measurements acquired from the ground monitoring stations, the City of Ottawa since 2001 conducted an annual environmental monitoring program to document and monitor the groundwater, surface water, and the gas emissions in the Trail Road landfill site. Therefore, the annual reports for 2007 and 2008 were obtained from the City of Ottawa to acquire ground measurement data. Figure 4.6 shows the distribution of landfill gas monitoring wells in the Trail Road landfill.

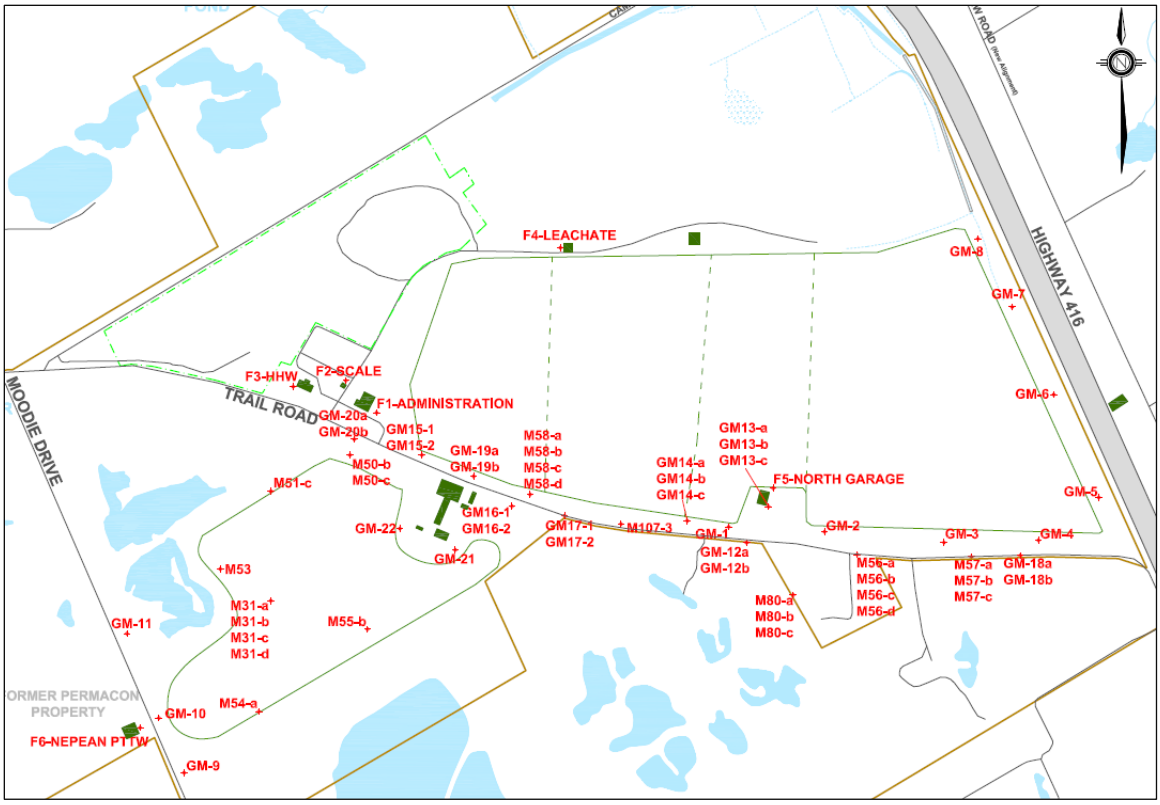

Figure 4.6. Distribution of the Landfill Gas Monitoring Wells in the Trail Road Landfill (Dillon Consulting Limited, 2008)

The main reason for the landfill gas monitoring stations aimed at identifying the distribution of soil gas pressure and concentration. For each of the landfill gas monitoring stations, there are different levels of measurements, including shallow, mid, and deep. A preliminary analysis was conducted to establish the relationship between the amount of emitting methane (CH_4) and the LST acquired from the Landsat images for 2007 and 2008. This process was performed using the regression analysis in Microsoft Excel. Two ground monitoring stations were selected for the analysis because 1) they are well distributed to different stages (South of Stages 1 and 3) of the landfill site and 2) they produced enough records to establish this regression analysis. Table 11 shows the amount of emitting CH_4 recorded from the two ground monitoring wells (GM-2 and GM-17).

Table 0 . Amount of Methane (CH_4) Recorded from Two Ground Monitoring Wells

Date	GM-2	GM-17
Apr. 21, 2007	13.32%	16.00%
May 7, 2007	9.10%	19.60%
May 23, 2007	1.70%	5.10%
Jun. 15, 2007	10.45%	13.57%
Jul. 17, 2007	1.70%	2.37%
Aug. 2, 2007	12.03%	14.32%
Aug. 27, 2007	15.56%	0.10%
Sept. 19, 2007	13.50%	2.70%
Oct. 5, 2007	10.40%	3.50%
Apr. 14, 2008	15.00%	1.02%
May 25, 2008	35.35%	2.80%
Jul. 12, 2008	21.32%	0.56%
Sept. 5, 2008	28.50%	0.35%
Oct. 7, 2008	21.53%	1.08%
Oct. 23, 2008	0.080%	0.01%

4.3.2. The Al-Jleeb Landfill, Al-Farwanyah, Kuwait

Similar to the case study on the Trail Road landfill, eleven LST images were generated and exported to the GIS environment after conducting an atmospheric correction. As this case study aims to detect the suspicious location of dumping areas within the landfill site, temperature contours were generated for each of the LST images. This goal was achieved by using the "Raster to Polyline" conversion tool (see Figure 4.7). Due to the bulky contour data for each of the LST images, contours with the highest temperature were selected and extracted. Finally, the contour lines for each of the datasets were overlaid on the ArcMap to determine the suspicious locations of dumping areas.

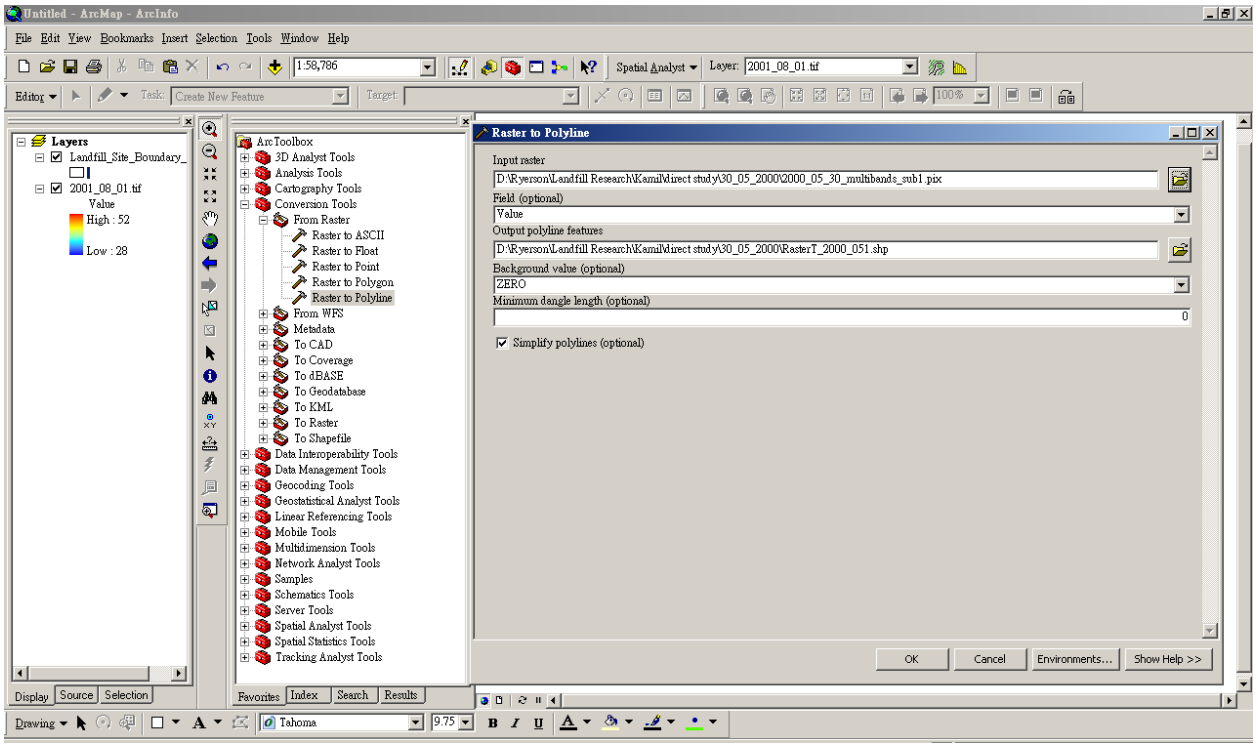

Figure 4.7. Generation of Temperature Contours Using the “Raster to Polyline” Tool

5. RESULTS AND ANALYSIS

5.1. The Trail Road Landfill, Ottawa, Canada

The 30 multi-temporal Landsat TM images are displayed with their band combinations Red (Band 3), Green (Band 2), and Blue (Band 1) in the Appendix. The derived LST images are also listed in the same Appendix. The pixel values represent the LST in Degree Celsius (°C). To analyze the results for the Trail Road landfill, the LST derived from the Landsat images were compared with the air temperature are presented in Section 5.1.1. The differences in LST between the closed stages in the Trail Road landfill were compared with the LST for the active stage and presented in Section 5.1.2. Finally, the correlation between the ground measurement data (methane CH_4) and the LST derived from the Landsat images is presented in Section 5.1.3.

5.1.1. LST vs. Air Temperature

Figure 5.1 illustrates the LST derived from the multi-temporal Landsat images and the corresponding air temperature acquired from the historical record at the Ottawa Macdonald-Cartier International Airport. It is approximately 10 km away from the landfill site. As it is impossible to acquire the Landsat image on the same date for each year, the LST images derived in summer (July or August) were used for the comparison, thus minimizing the effects due to seasonal variation. Generally, the LST for the Trail Road landfill was always higher than the air temperature across the years from 2001 to 2009. The difference in temperature varies from 5°C and 20°C. This difference can be explained by 1) the emission of landfill gas leading to the release of thermal energy from the landfill site; and 2) bare ground without vegetation cover absorbs the solar heat within the landfill site.

With a close examination of the data, the air temperature is 25°C on average across all the years, and the LST of the landfill site is close to or even higher than 35°C in most of the years (except 2008). The LST climbed up to 42°C in both 2001 and 2009. The significant difference between LST and the air temperature occurred in 2009. This behavior can be explained due to the recent approval of the City of Ottawa to vertically expansion the Trail Road landfill by the creation of a Stage 5 (Dillon Consulting Limited, 2008). Construction activities can be found near Stages 3 and 4 in the landfill site (see Landsat image for 2009 shown in the Appendix section).

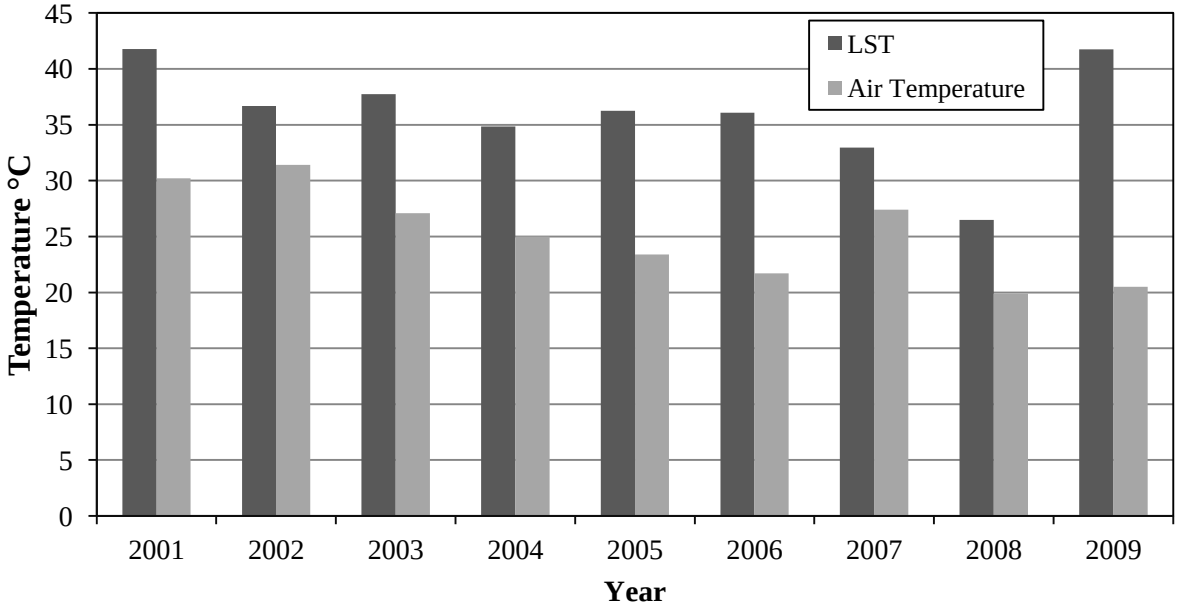

Figure 5.1. Comparison of the LST and Air Temperature for the Trail Road Landfill for 2001 to 2009 during Summer (July / August)

Figures 5.2 and 5.3 show the comparison between the LST and the air temperature for specific dates in 2007 and 2008. In 2007, the LST for the Trail Road landfill in April and June is always higher than the air temperature by 10°C. A drop in the temperature difference is found in July and August, mainly due to relative low sky visibility on July 17th and August 2nd and haze effects on

the remote sensing images. This result may affect the derived LST even when the atmospheric correction is applied. The LST for the landfill site is constantly higher than the air temperature by 6°C during September and October.

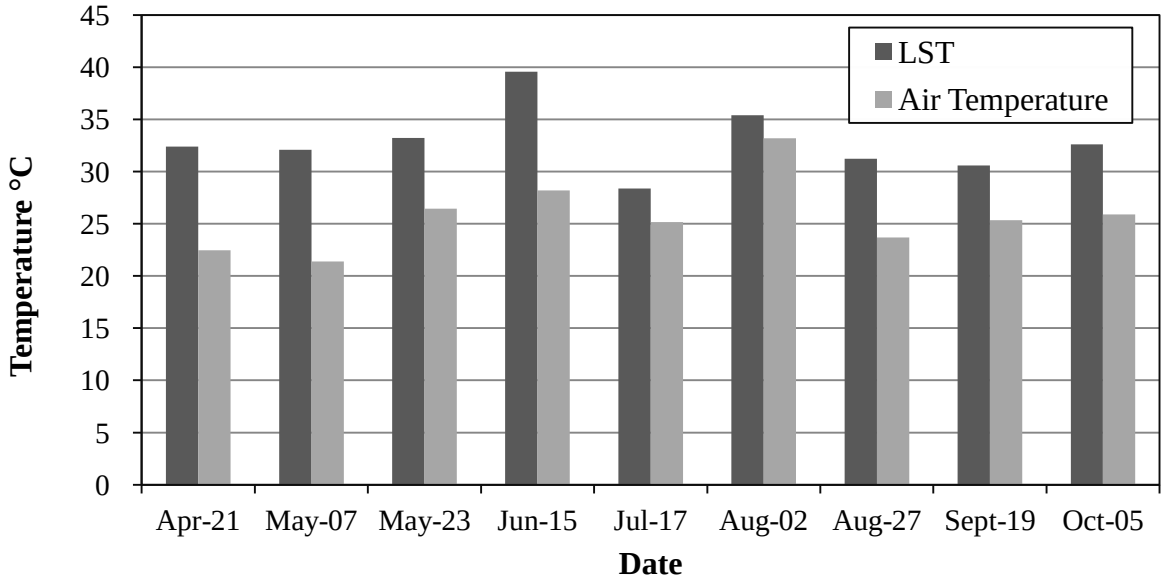

Figure 5.2. Comparison of LST and the Air Temperature for the Trail Road Landfill in 2007

In 2008, the difference between the LST and the air temperature varied due to seasonal changes. On April 14, the LST was 7°C higher than the air temperature and the difference in the temperature was more than 10°C during May to August. The high difference in temperature can also be explained due to the absorption of solar energy during the summer season. The temperature difference drops below 7°C after September except for the result in October 7th. Based on the results from 2001 to 2009 as well as the results for 2007 and 2008, one can conclude that the LST for the landfill site is always higher than the air temperature.

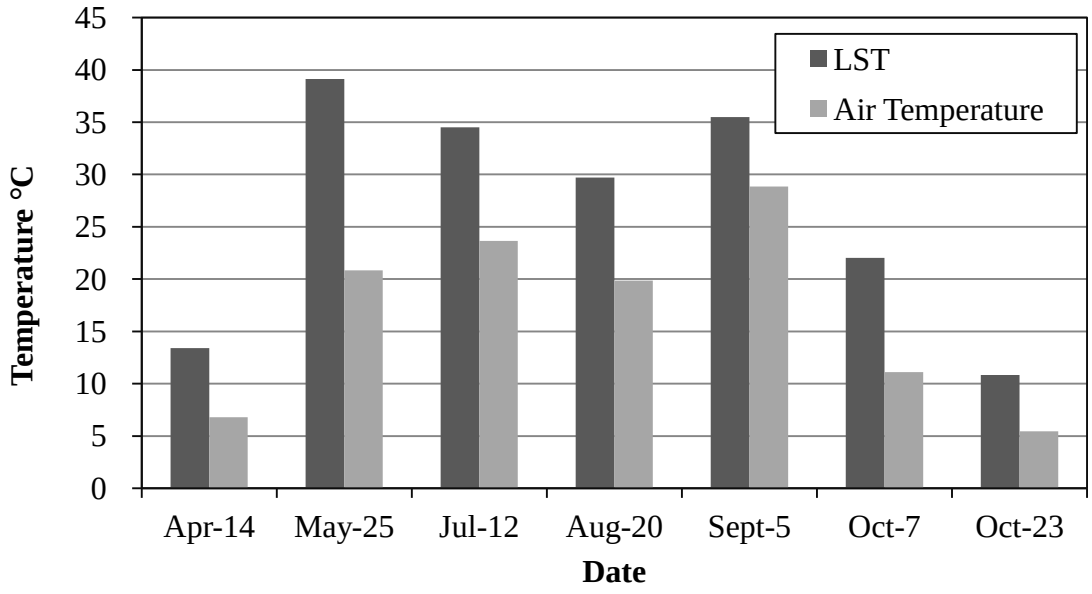

Figure 5.3. Comparison of LST and the Air Temperature for the Trail Road Landfill for Year 2008

5.1.2. LST of the Closed Stages vs. LST of the Active Stage

An in-depth analysis was conducted to investigate the LST for the closed stages and the active stage. When a landfill reaches its full capacity, the development stage is capped and closed. For the Trail Road landfill, Stage 1 was closed in 1988, and Stage 2 was closed in 1991. Then Stage 3 closed and completed its dumping activities in early 2003 leaving Stage 4 as the active stage. Figure 5.4 shows a picture of the interim capping in the Trail Road landfill (J.L. Richards & Associates, 2011). Regardless of the development stages, one should also note that LST for a landfill site is always higher than its surroundings. This observation can be justified by a visual inspection and review of all the LST images listed in the Appendix.

Figure 5.4. Interim Capping of the Trail Road Landfill (J.L. Richards & Associates, 2011)

Figure 5.5 shows the LST calculated for the Trail Road landfill's division into closed stage (Stages 1 and 2), the recently closed stage (Stage 3), and the current active stage (Stage 4). Generally, the LST for the active stage is higher than the LST for the closed phases by 2°C to 10°C. This result can be explained as Stages 1 and 2 were closed and capped before 2001; there were no further activities found in the ground level of these stages. Moreover, these two stages are now capped and planted with vegetation cover which can significantly reduce the LST (refer to the Landsat images in Appendix I). One should note that the difference between the LST for the recently closed stage (Stage 3) and the closed stages reduced after 2003; however, the difference rose significantly after year 2008. This finding also applies to Stage 4 in year 2009. Again, these can be explained by the recently approved expansion to increase site capacity. This landfill expansion may require further construction activities that can increase the LST within the landfill site (Dillon Consulting Ltd., 2008).

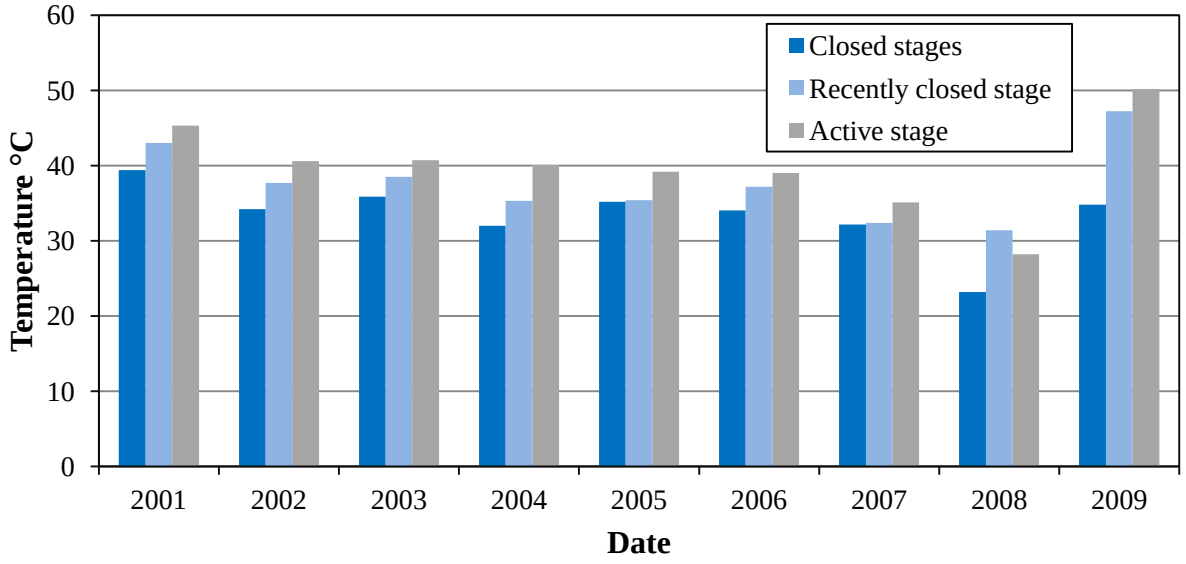

Figure 5.5. Comparison of the LST for the Close Stages (Stages 1 and 2), the recently Closed Stage (Stage 3) and the Active Stage (Stage 4)

5.1.3. Correlation between the Methane (CH_4) and the LST

The Trail Road landfill site is monitored by a comprehensive ground monitoring system, which measures and records the amount of landfill gas, the quality of surface and groundwater, and soil contamination. A preliminary analysis was conducted to determine the correlation between the measurements from these monitoring wells and the LST derived from the remote sensing images. Such an analysis has not been performed for the previous literature (Kwarteng and Al-Enezi 2004; Yang et al., 2008) which adopted Landsat images for landfill monitoring. The measurements of two landfill gas monitoring stations (GM-2 and GM-17) are utilized for this preliminary analysis. The reasons to select these two stations from the total of 28 stations are mainly the availability of the measurements recorded in the annual reports and the well distribution of these stations among Stages 1 to 4 (see Figure 4.1). These monitoring wells measure the percentage of emitting methane (CH_4) and the pressure; the records of CH_4 are taken to perform a correlation, as CH4 is the main

element of landfill gas. Also, the measurements from the shallow level of the monitoring wells are taken as it is close to the ground level that will be close to the land surface for the calculation of LST. Due to inconsistency between the date of ground measurement and the date of the remote sensing image acquisition, the ground data were linearly interpolated so as to align the dates to the remote sensing image. Correlation analysis is conducted for both 2007 and 2008 by using the regression analysis available in Microsoft Excel. To calculate the linear regression the following equation was applied:

$$(y) = a + bx \tag{5.1}$$

Where x and y are the variables.

b = the slope of the regression line

a = the intercept point of the regression line and the y axis.

Finally, the coefficient of correlation (R^2) is computed where 0 indicates no correlation between the two datasets, and 1 represents a linear relationship between the two datasets.

Figures 5.6 and 5.7 show the relationship between the percentages of emitting methane recorded in station GM-2 (located at the south of Stage 1) and the LST in 2007 and 2008, respectively. Figures 5.8 and 5.9 show the relationship between the percentages of emitting methane recorded in station GM-17 (located at the south of Stage 3) and the LST in 2007 and 2008, respectively. To remove seasonal effects in the derived LST data, the LST value is subtracted from the air temperature, so all the measurements are reduced to the same base. Preliminary analysis revealed that a mid-correlation was observed for both of the ground- monitoring wells in 2008 where R^2 is 0.573

in GM-2 and R^2 is 0.914 in GM-17. However, both stations had low correlation coefficient for both stations recorded in 2007 where R^2 ws 0.066 in GM-2 and R^2 was 0.332 in GM-17). In spite of these results, all the fitted regression lines show that the amount of emitting methane has a somewhat direct proportional relationship to temperature.

The results for GM-2 can be explained due to its location at the southbound area of Stage 1 in the landfill site. Stage 1 was closed in year 1988 and was originally designed as natural attenuation landfill area. Therefore, the City of Ottawa neglected to build engineered bottom liners in Stage 1. All the wastes are dumped directly into former sand and gravel pit in the ground (Dillon Consulting Limited, 2008). In general, landfill gas was not detected at most of the landfill gas stations located in the south and east areas of Stage 1. The average of emitting methane concentration at GM-2 was 12% and measured in 2007. The monitoring station GM-17 is close to the Stage 3 which was closed in 2003. Stage 3 contains clay and a geomembrane bottom liner and a leachate collection system (Dillon Consulting Ltd., 2008). Higher values for emitting methane (CH_4) were observed at GM-17, as the average emitting methane concentration at this location in 2007 was 25% (Dillon Consulting Ltd., 2007), and achieved up to 68% in 2008. The methane concentration at this monitoring station also relates to landfill gas migration from the Trail Road landfill in Stage 3 (Dillon Consulting Limited, 2008).

Although atmospheric corrections were conducted to improve the quality of the derived products, the LST that is derived may not be as accurate as LST measured from the ground. Therefore, a calibration of the LST derived from the remote sensing images should be carried out with respect to the ground measurement. In addition, the data used in building the regression tests was not enough to draw a significant conclusion about whether the increase of methane leads to an increase

of LST. Therefore, more analysis should be done to the preceding years as well as the remaining ground monitor stations.

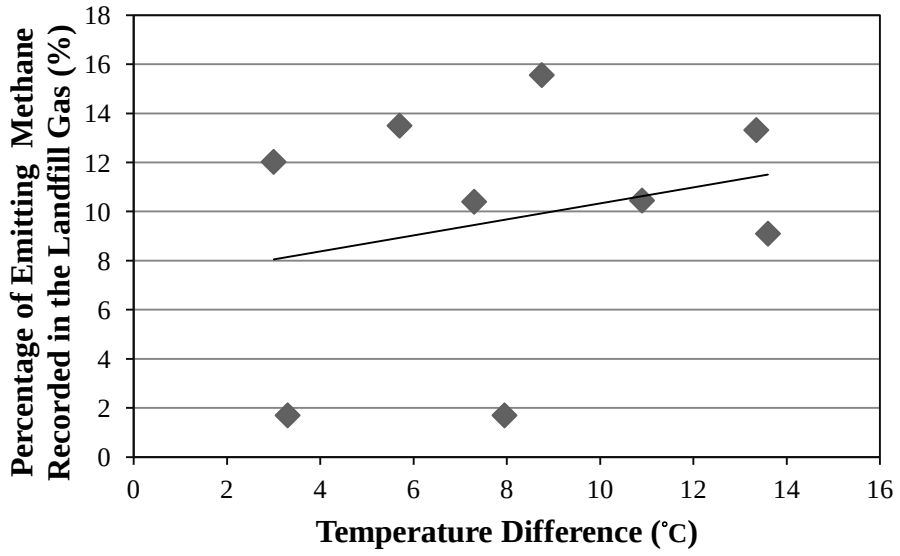

Figure 5.6. Relationship between the Percentage of Emitting Methane Recorded in GM-2 and the Temperature in 2007 (R^2 = 0.066)

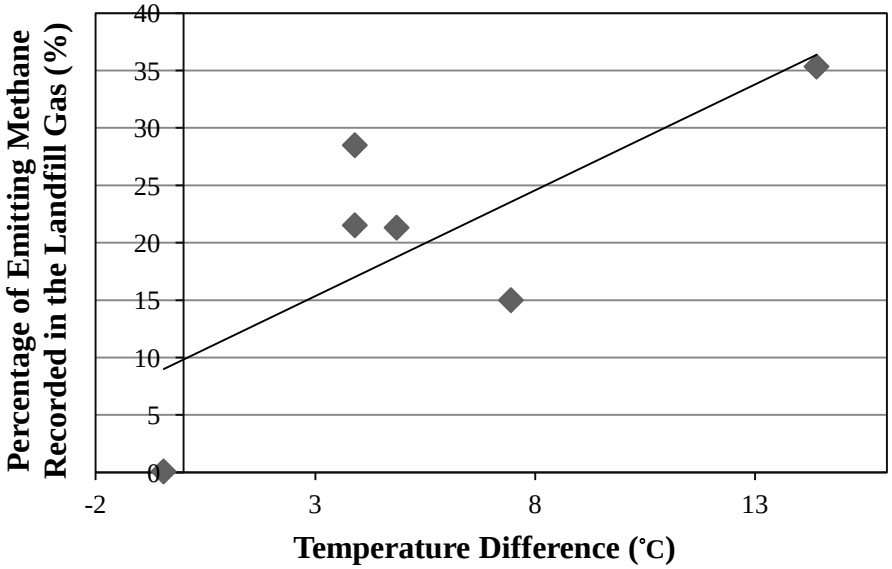

Figure 5.7. Relationship between the Percentage of Emitting Methane Recorded in GM-2 and the Temperature in 2008 (R^2 = 0.573)

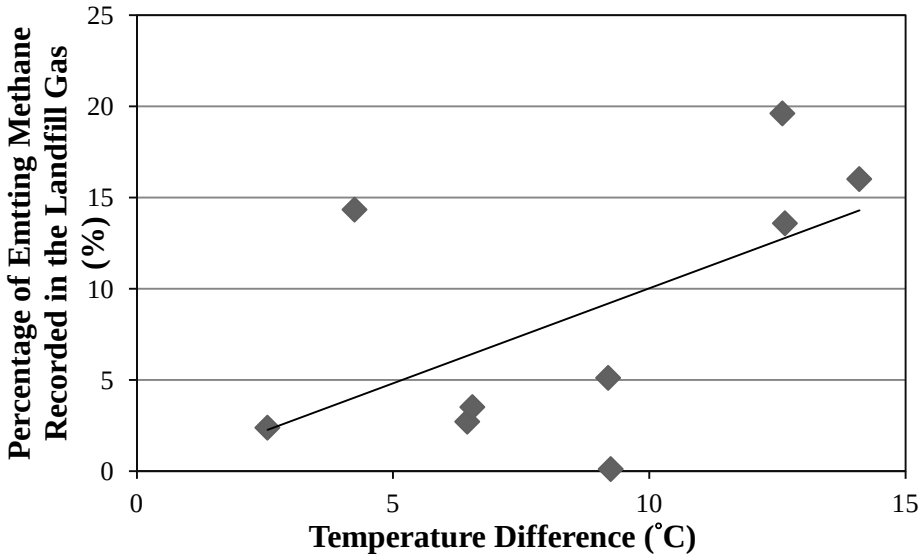

Figure 5.8. Relationship between the Percentage of Emitting Methane Recorded in GM-17 and the Temperature in 2007 (R^2 = 0.332)

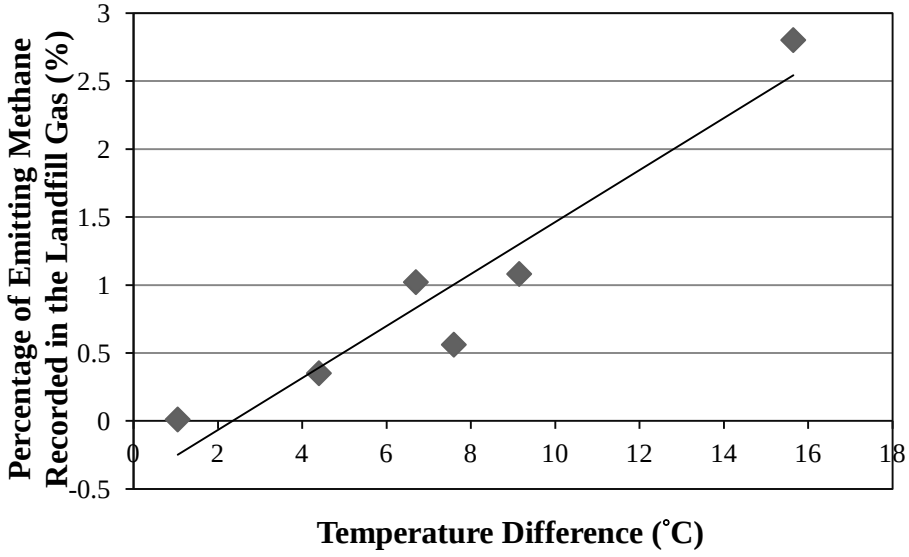

Figure 5.9. Relationship between the Percentage of Emitting Methane Recorded in GM-17 and the Temperature in 2008 (R^2 = 0.914)

5.2. The Al-Jleeb Landfill, Al-Farwanyah, Kuwait

With the findings for the Trail Road landfill case study, it is observed that 1) the LST of the landfill site is significantly higher than the air temperature as well as the LST of the surroundings; and 2) the LST of the active landfill is always higher than the closed landfill. Based on these two observations, we utilize the LST derived from the remote sensing images to detect suspicious dumping areas in the Al-Jleeb landfill. Although the boundary of the Al-Jleeb landfill is known from historical records, the specific dumping areas are unknown. It is hard to locate these areas by field investigation, as most of the dumping sites are capped, and the area of the Al-Jleeb is 5.5 km^2.

5.2.1. LST vs. Air Temperature

Figure 5.10 plots the LST derived from the multi-temporal Landsat images and the corresponding air temperature in the Al-Jleeb landfill. Unlike the Trail Road landfill, it was observed that some of the LST derived from the remote sensing images are lower than the air temperature. It is worth mentioning that most of these cases occur when images are acquired in the winter (Jan. 13, 1985; Dec. 29 1987; Oct. 29, 1993; and Feb. 28, 1993) and water (waste water) was found in these areas. In the rest of the data, the LST is always higher than the air temperature by 9 °C to 16 °C, which aligns with the findings from the Trail Road landfill. However, it seems that the landfill site located in a desert area does not have such large temperature differences, compared to the landfill site located in a mid-latitude area where the highest temperature difference can be up to 20 °C, i.e, the Trail Road landfill.

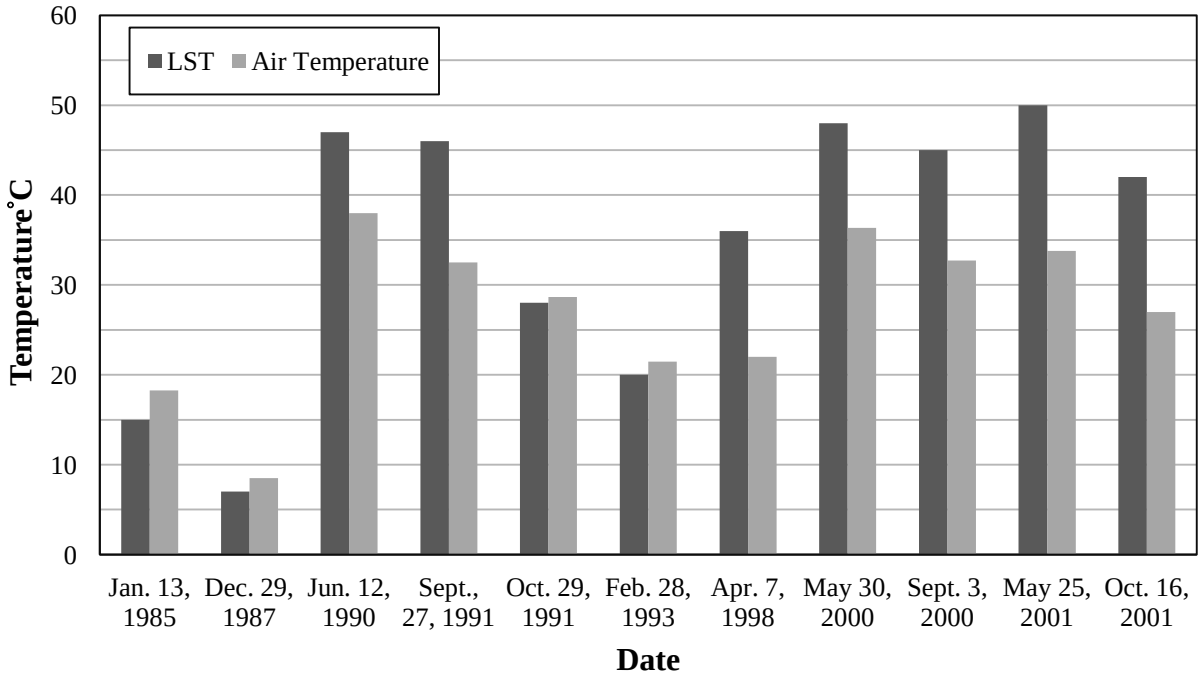

Figure 5.10. Comparison of the LST and the Air Temperature in the Al-Jleeb Landfill

5.2.2. Determination of Suspicious Dumping Areas

Figure 5.11 shows the Landsat image and the derived LST image acquired on the January 13th of 1985 and the air temperature of 16°C. The distribution of the LST within the Al-Jleeb landfill site varied from 5°C to 21°C. The result shows that the LST in the Al-Jleeb landfill is higher than in the surrounding areas by 2°C (see A and B in Figure 5.11). However, the LST was lower than the air temperature by 3°C. Contour lines were generated to display the LST that is more than the air temperature (>14°C). The purpose of generating the LST contour line is to investigate the local peak of LST within the landfill site. In this case, these areas can be regarded as being suspicious dumping areas in the landfill site.

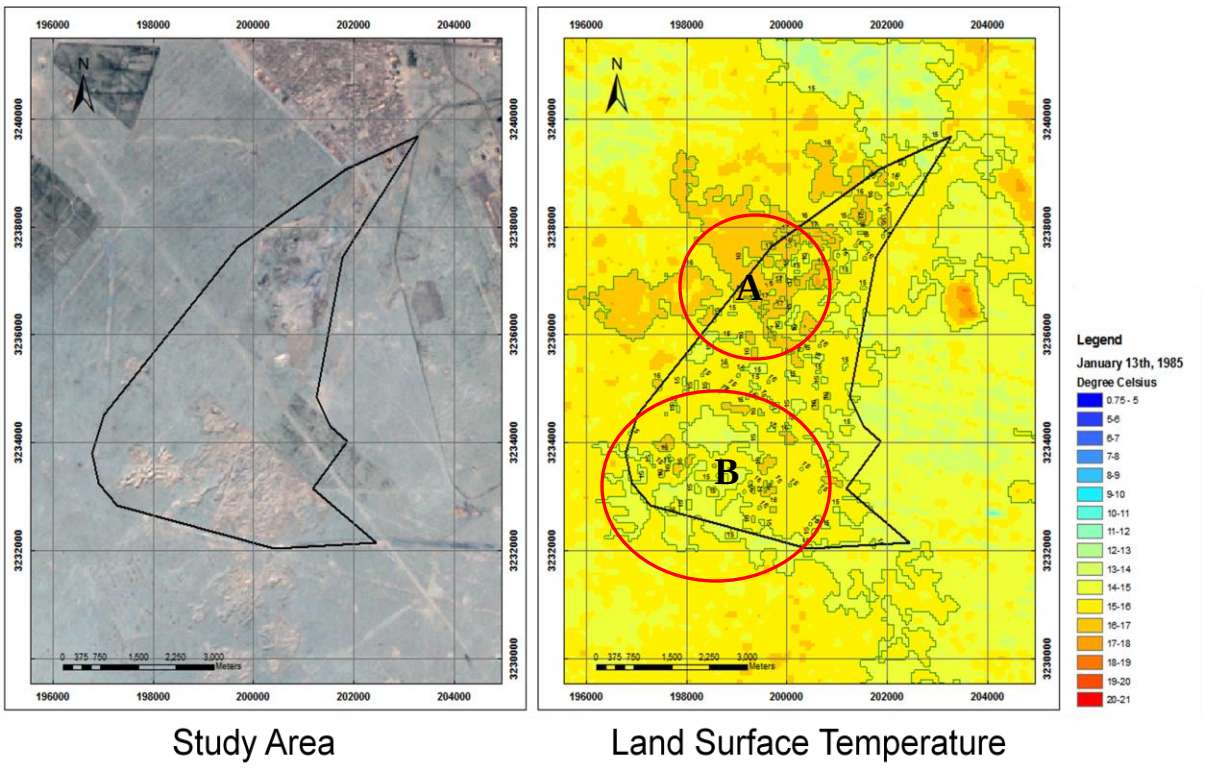

Figure 5.11. Original Landsat Image (Left) Acquired on Jan. 13, 1985, and the LST image (Right)

Figure 5.12 shows the Landsat image and the derived LST image that was acquired on the 29th of December 1987 and the air temperature being close to 10°C. The distribution of the LST within the Al-Jleeb landfill site varied from 4°C to 18°C. The result shows that the LST in the Al-Jleeb landfill is higher than in the surrounding areas by 3°C (see A in Figure 5.12). The contour lines illustrated areas where the LST is higher than the air temperature (≥9°C). This result indicates that the general LST in this image is higher than in the previous image (year 1985). The highest LST was indicated in the north part within the Al-Jleeb landfill at a range between 12 to 13°C (see A in Figure 5.12).

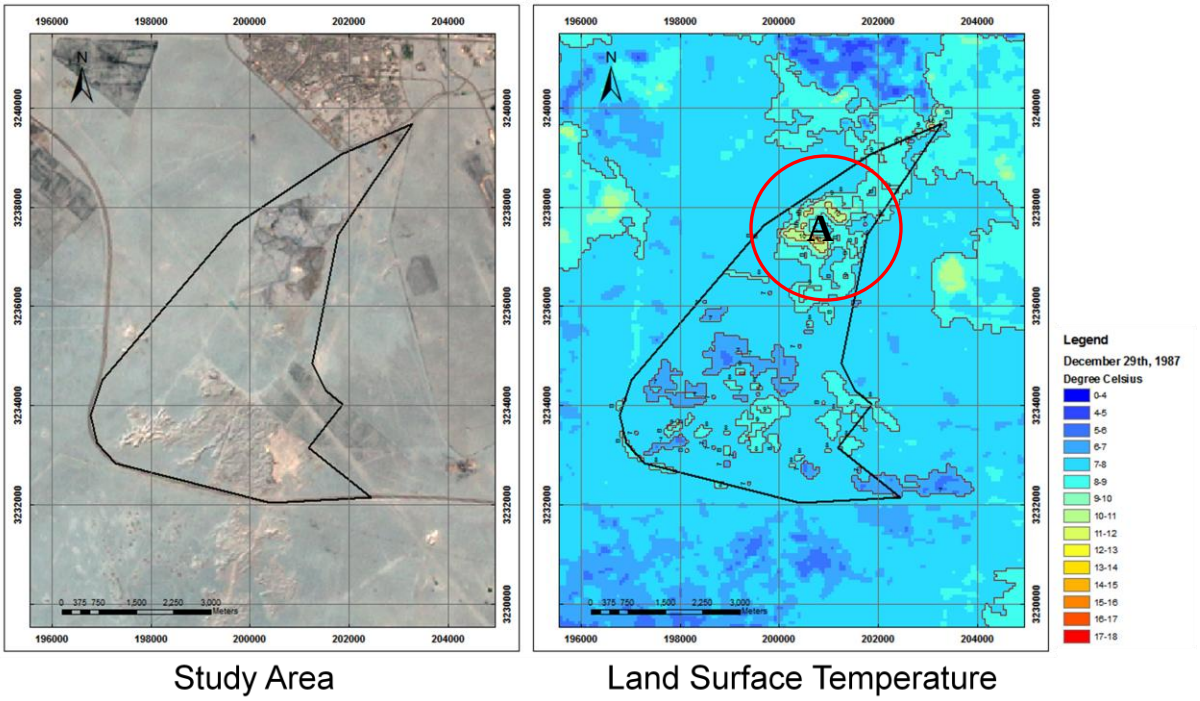

Figure 5.12. Original Landsat Image (Left) Acquired on Dec. 29, 1987, and the LST image (Right)

Figure 5.13 shows the original Landsat image and the LST image on the 12th of June 1990, where the air temperature was 38°C. The distribution of the LST within the Al-Jleeb landfill site varied from 23°C to 60°C. The result shows that the LST in the Al-Jleeb landfill is higher than the surrounding areas by 8 to 10°C (see A and B in Figure 5.13). Further the LST is higher than the air temperature by 1°C. The contour lines are generated to display the LST, which is more than the air temperature by 8°C (≥47°C) to identify the warmer areas within the landfill site. The result shows that the highest LST value was captured at the north and east sides within the landfill at a range between 57 to 58°C (see A and B in Figure 5.13).

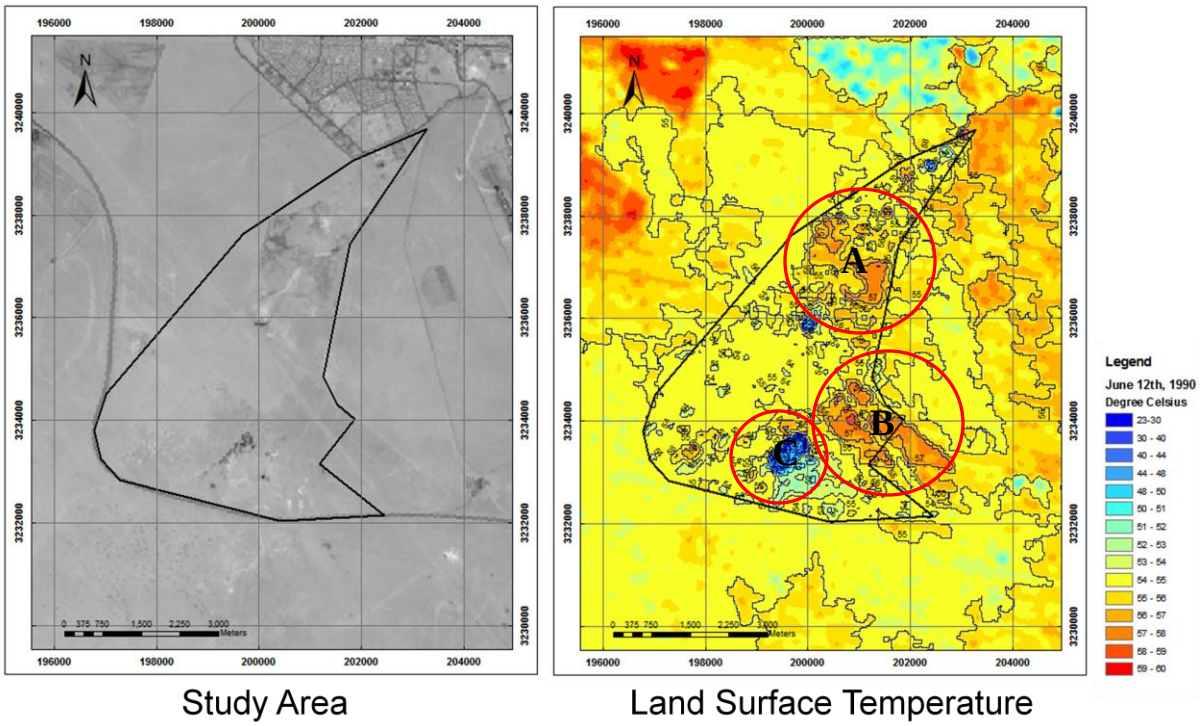

Figure 5.13. Original Landsat Image (Left) Acquired on Jun. 12, 1990, and the LST image (Right)

Figure 5.14 shows the original Landsat image and the LST image on the 27th of September 1991 when the air temperature was 32°C. The distribution of the LST within the Al-Jleeb landfill site varied from 23°C to 60°C. The result shows that the LST in the Al-Jleeb landfill is higher than the surrounding areas by 5°C and the LST is higher than the air temperature by 10°C. The contour lines are then generated to display the LST ≥44°C. The highest LST is found in the east side of the image with a value up to 49°C. That year marked the Gulf War where smoke released from the oil fires and the bombing areas were found to be close to the Al-Jleeb landfill site.

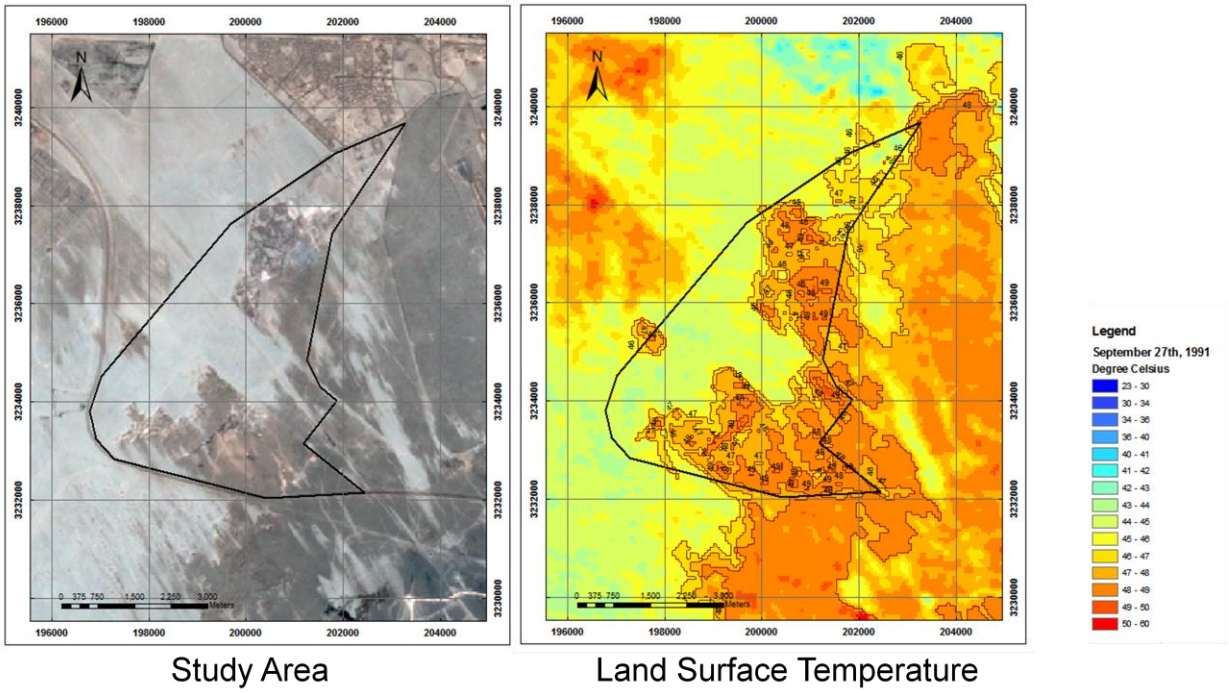

Figure 5.14. Original Landsat Image (Left) Acquired on Sept. 27, 1991, and the LST image (Right)

Figure 5.15 shows the original Landsat image and the LST image on 29th October 1991,where the air temperature was 29°C. The distribution of the LST within the Al-Jleeb landfill site varied from 18°C to 40°C. The result shows that the LST in the Al-Jleeb landfill is higher than in the surrounding areas by 4°C. However, the LST and the air temperature are roughly equal to 29°C. The temperature contour lines were generated to display the LST ≥ 29°C. The result shows the south part of the landfill site has a high LST with 34°C compared to the surrounding areas. The main reason for the high LST in the south part of the landfill is the oil field fires during the Gulf War.

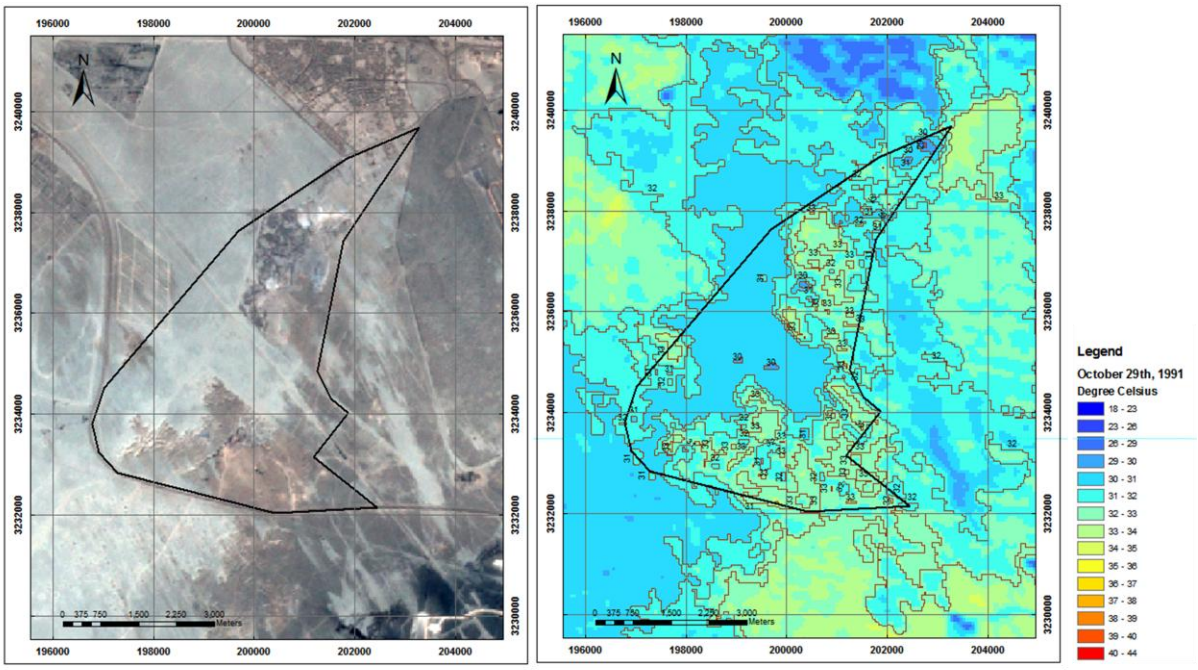

Figure 5.15. Original Landsat Image (Left) Acquired on Oct. 29, 1991, and the LST image (Right)

Figure 5.16 shows the original Landsat image and the LST image on the 28th of February 1993 where the air temperature was 21.5°C. The distribution of the LST within the Al-Jleeb landfill site varied from 12°C to 28°C. The result shows that the LST in the Al-Jleeb landfill is higher than in the surrounding areas by 3°C. The temperature contour lines were generated to display the LST ≥ 21°C. The result shows the southeast part and the north part of the Al-Jleeb landfill site has high surface temperatures compared to the surrounding areas by approximately 10°C (see A and B in Figure 5.16). Moreover, some locations in the surrounding area of the Al-Jleeb landfill (located in the southeast of the image) had high surface temperatures which again relates to the previous oil fires and bombing during the Gulf War.

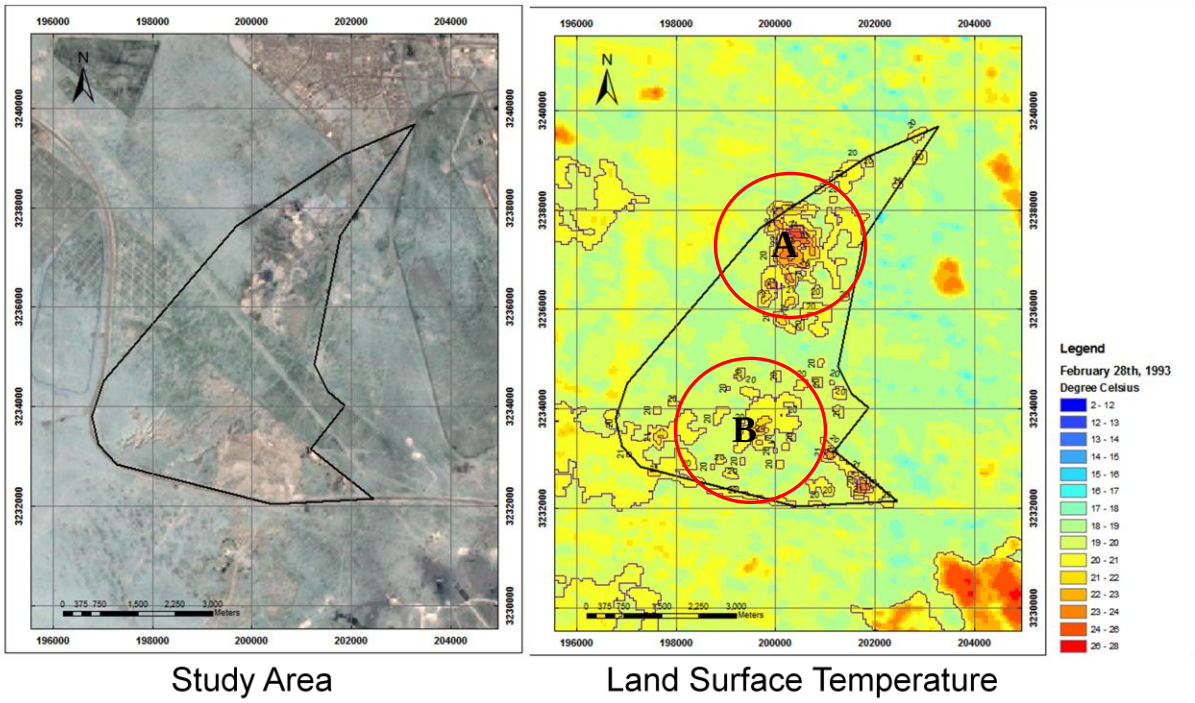

Figure 5.16. Original Landsat Image (Left) Acquired on Feb. 28, 1993, and the LST image (Right)

Figure 5.17 shows the original Landsat image and the LST image on the7th of April 1998 where the air temperature was 22°C. The distribution of the LST within the Al-Jleeb landfill site varied from 22°C to 50°C. The result shows that the LST in the Al-Jleeb landfill is higher than in the surrounding areas by 5°C. Moreover, the LST is higher than the air temperature by 14°C. The temperature contour lines were generated to display the LST ≥36°C. The result shows that the northwest part of the Al-Jleeb landfill site has a high LST compared with the surrounding areas by approximately 10 degrees Celsius (see A in Figure 5.17). The southwest part has the highest LST with a range of 43 to 44°C, which is higher than the surrounding area by 12°C (see B in Figure 5.17).

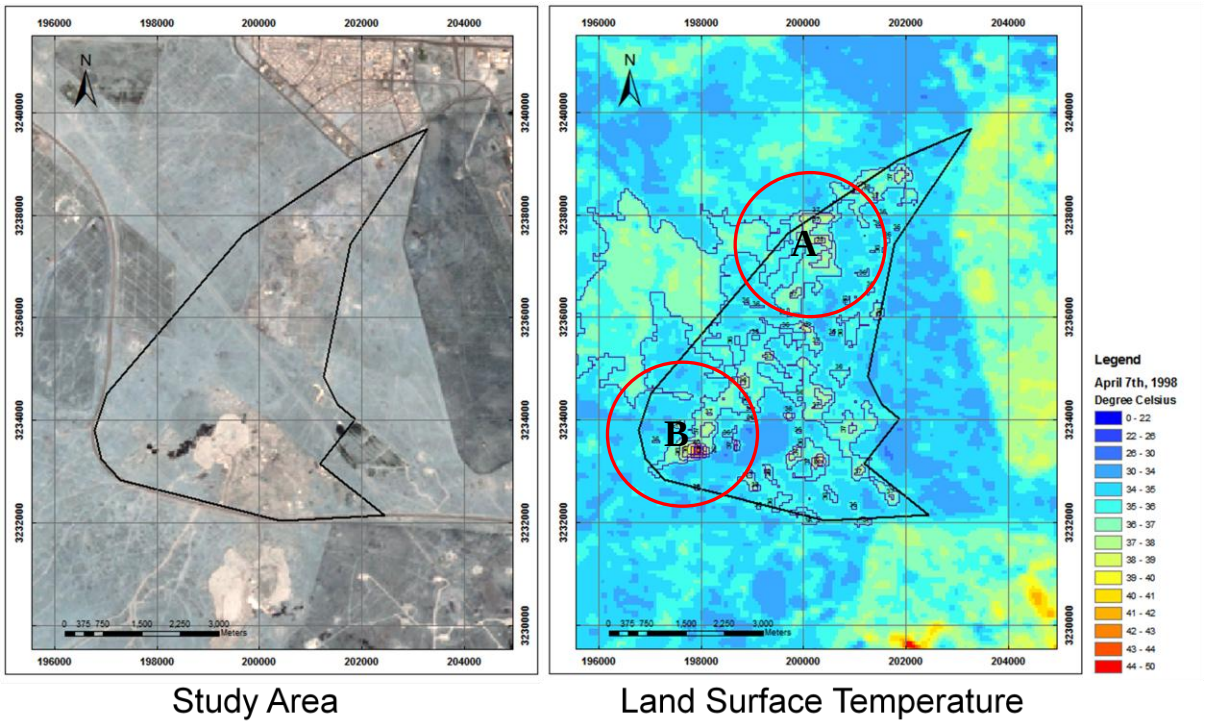

Figure 5.17. Original Landsat Image (Left) Acquired on Apr. 7, 1998, and the LST image (Right)

Figure 5.18 shows the original Landsat image and the LST image on the 30th of May 2000 where the air temperature was 36.5°C. The distribution of the LST within the Al-Jleeb landfill site varied from 30°C to 60°C. The result shows that the LST in the Al-Jleeb landfill is higher than the surrounding areas by 5°C. The LST is higher than the air temperature by 12°C. Therefore, the temperature contour lines were generated to display the LST ≥48°C. The highest LST captured at the north part of the landfill site was 5°C higher than the surrounding areas (see A in Figure 5.18). The lowest LST accrued in the south part of the landfill where water bodies are located (see B in Figure 5.18).

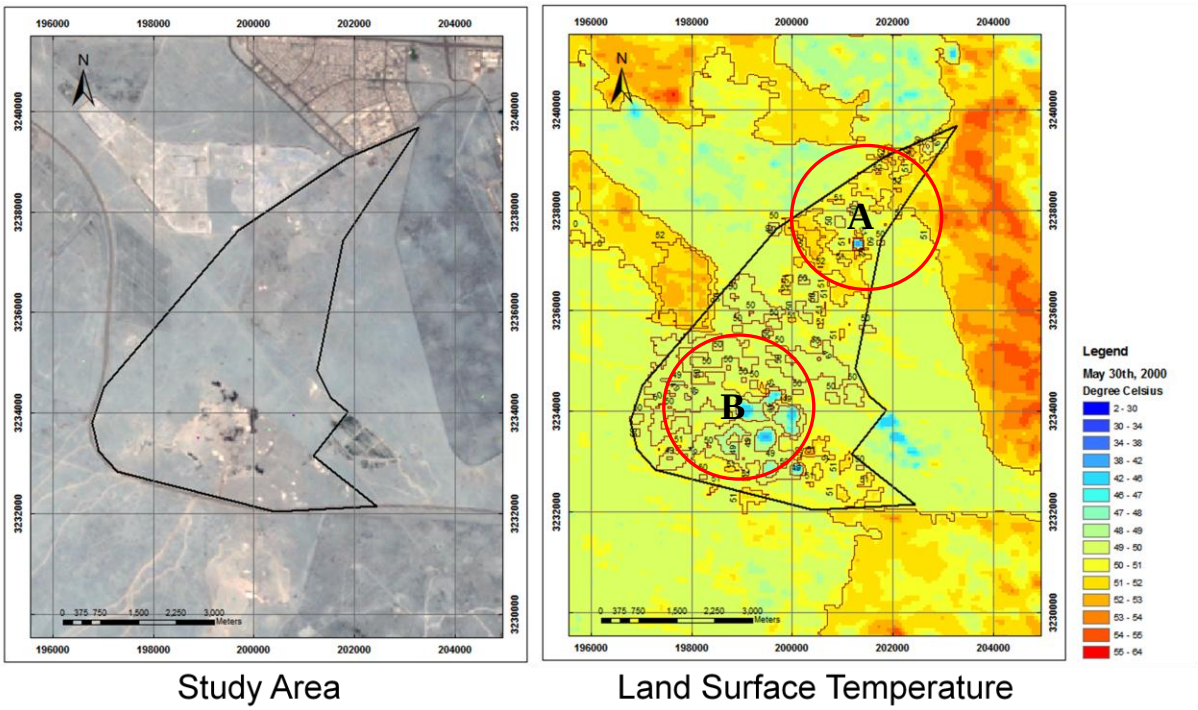

Figure 5.18. Original Landsat Image (Left) Acquired on May 30, 2000, and the LST image (Right)

Figure 5.19 shows the original Landsat image and the LST image on the 3rd of September 2000 where the air temperature was 33°C. The distribution of the LST within the Al-Jleeb landfill site varied from 30°C to 61°C. The result shows that the LST in the Al-Jleeb landfill is higher than the surrounding areas by 5°C, and the LST is higher than the air temperature by 13°C. Therefore, the temperature contour lines were generated to display the LST ≥ 48°C. The result shows that few locations in the Al-Jleeb landfill site had higher surface temperatures than the surrounding area by approximate 5°C (see A in Figure 5.19). Similar to the previous image (the 30th of May 2000), the lowest LST was found in the south part of the landfill where water bodies are located (see B in Figure 5.19).

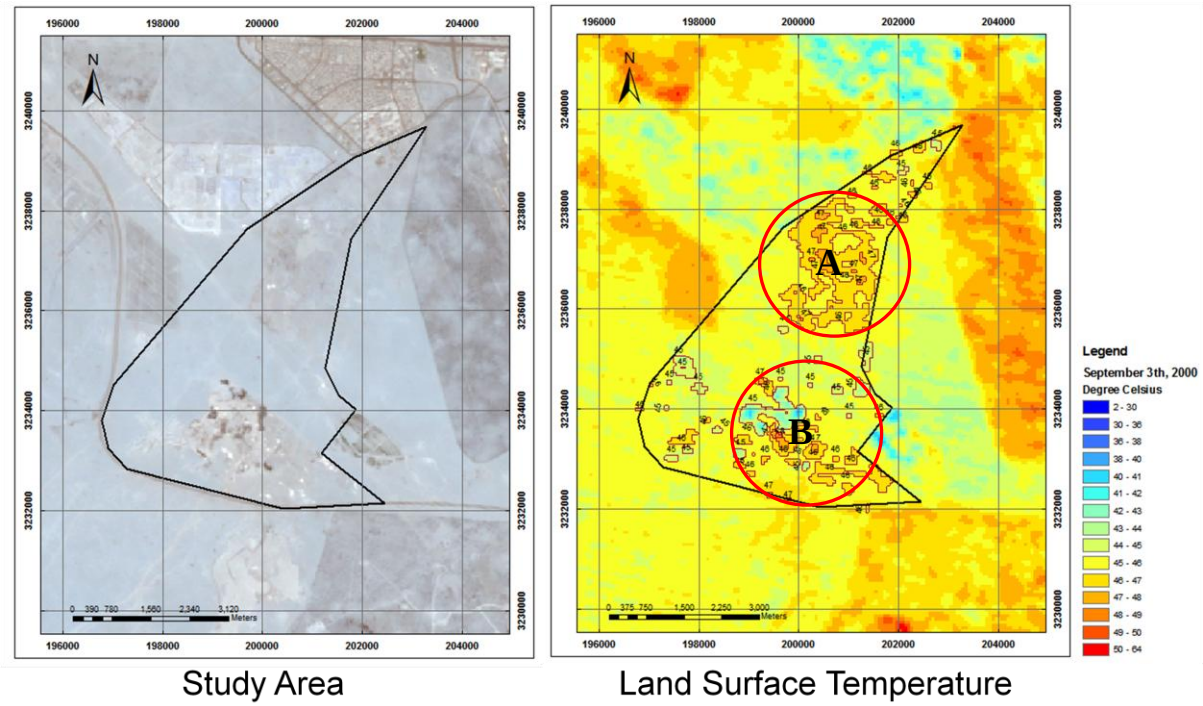

Figure 5.19. Original Landsat Image (Left) Acquired on Sept. 3, 2000, and the LST image (Right)

Figure 5.20 shows the original Landsat image and the LST image on the 25th of May 2001 where the air temperature was 34°C. The distribution of the LST within the Al-Jleeb landfill site varied from 30°C to 56°C. The result shows that the LST in the Al-Jleeb landfill is higher than the surrounding areas by 4°C. Moreover, the LST is higher than the air temperature by 12°C. The contour lines were generated to display the LST ≥ 50°C. The result shows that there are a few locations in Al-Jleeb landfill site with a high surface temperature than the surrounding area by approximate 10°C (see A in Figure 5.20). Moreover, the same as for the previous image (the 3th of September 2000) the lowest LST accrued in the south part of the landfill where water bodies are located (see B in Figure 5.20). This water could lead to sludge or other waste water (Schrapp & Al-Mutairi, 2010).

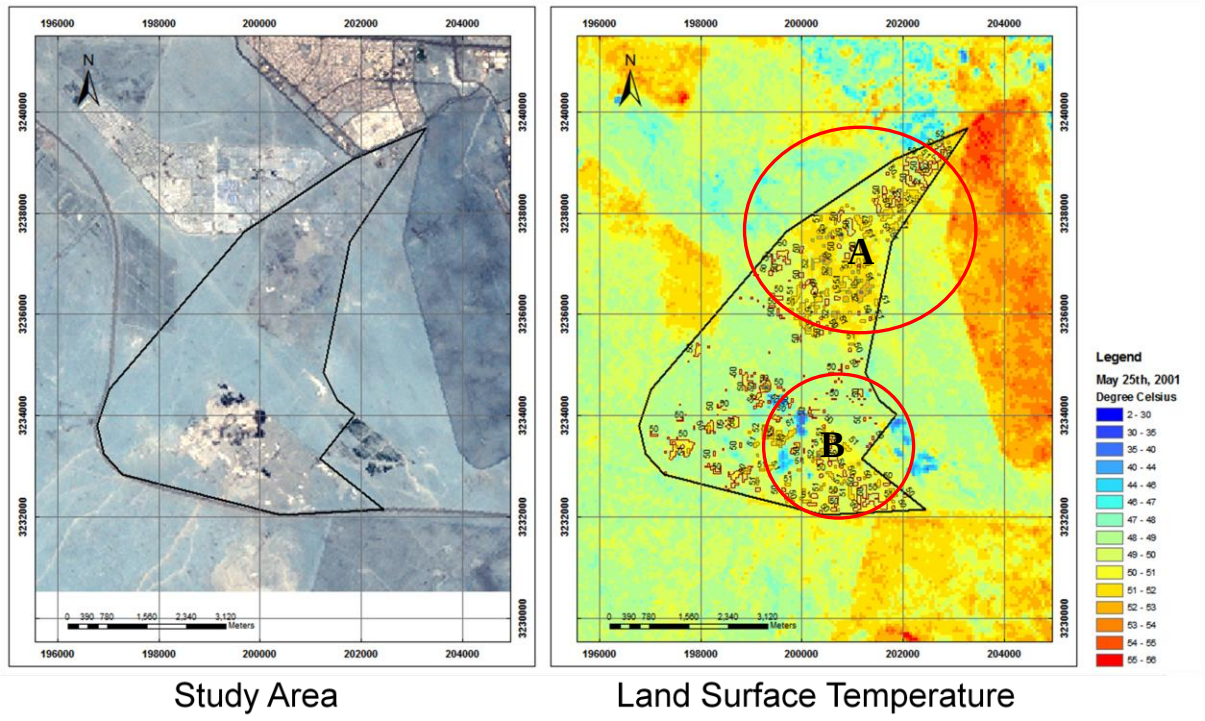

Figure 5.20. Original Landsat Image (Left) Acquired on May 25, 2001, and the LST image (Right)

Finally, Figure 5.21 shows the original Landsat image and the LST image on the 16th of October 2001 where the weather temperature was 27°C. The distribution of the LST within the Al-Jleeb landfill site varied from 25°C to 50°C. The result shows that the LST in the Al-Jleeb landfill is higher than in the surrounding areas by 6°C. The LST is higher than the air temperature by 13°C. The contour lines were then generated to display the LST ≥ 48°C. The result shows that the north and south parts of the landfill have a high LST at about 5°C and higher than the surrounding areas (see A and B Figure 5.21).

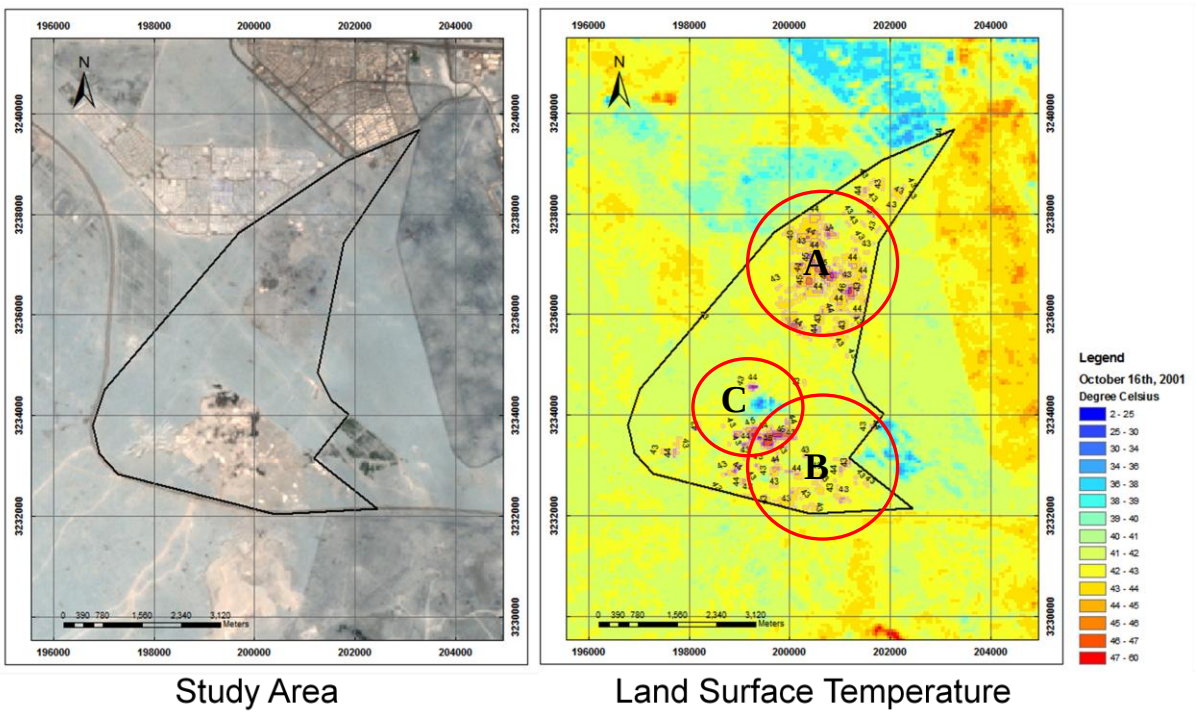

Figure 5.21. Original Landsat Image (Left) Acquired on Oct. 16, 2001, and the LST image (Right)

The final result shows that there is an increase in the size of the areas of those high LST reading from year 1985 to year 1990. Further investigation shows large dumping activities during this period of time. It also records a decrease in the LST during the period from 1990 to 1991, mainly because of the Gulf War during which the dumping activities were significantly reduced. The LST for the landfill increases again after October 1991 when the dumping activities resumed again after the war. In 1993, new locations with high LST reading were recorded, which indicated the establishment of new dumping areas. This trend continued in the years afterwards due to the increase in urbanization and residential extensions in the surrounding areas to the landfill. By combining all the temperature contours in GIS, the locations that do have higher LST can be intersected and overlaid. Five locations with high LST readings during the last twenty five years (A, B, C, D and E) are shown in Figure 5.22, indicating the suspicious dumping areas.

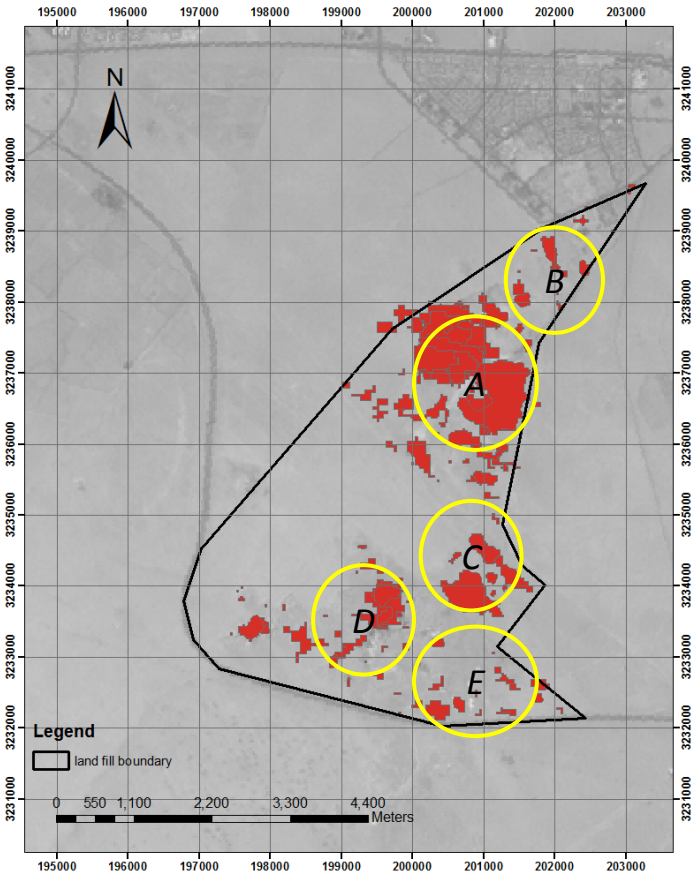

Figure 5.22. Suspicious Dumping Areas in the Al-Jleeb Landfill

6. CONCLUSIONS AND RECOMMENDATIONS

6.1. Conclusions

6.1.1. The Trail Road Landfill, Ottawa, Canada

In this study, 30 Landsat TM satellite images were downloaded from the free data archive of USGS Earth Explorer and processed for the Trail Road landfill sites from 2001 to 2009. Atmospheric corrections were applied to the Landsat images before retrieving the land surface temperatures from the thermal band of the Landsat images. From these 30 images, 16 Landsat images (9 images acquired in 2007 and 7 images acquired in 2008) were used to study the land surface temperatures of the Trail Road landfill site and correlate the data that was extracted to ground-based measurements. An analysis of the space-based measurements was conducted to investigate the relationship between the landfill gas (Methane CH_4) and the LST in 2007 and 2008, respectively. As the dates of ground measurements did not match the dates of the Landsat data in a number of ground monitoring stations (GM-2 and GM-17), a linear interpolation of the ground measurements was conducted to match the acquisition dates for the LST readings derived from the Landsat images.

The results show that the LST of the landfill site was always higher than the air temperature by 5 °C to 18 °C. The results for 2001 and 2009 show the highest LST in the Trail Road landfill site at about 15°C to 20°C when compared to the rest of the years. The LST for the closed stages (Stages 1 and 2) were lower than the other stages (Stages 3 and 4) by 2°C to 10°C. Moreover, the active stage (Stage 4) was higher than Stage 3 (closed recently) by 2°C to 5°C. The variation of these temperature differences depended on seasonal changes as well as the actual decomposition activities within the landfill site. Landfill gas measurements from two stations were correlated

with the LST for the Trail Road landfill site GM-2 and GM-17 with the LST derived from the Landsat images in 2007 and 2008. Landfill gas station GM-17 showed a high correlation between the amount of emitted methane and the land surface temperature. However, a poor relationship was found between the methane gas emitted at station GM-2 and the LST. It is worth mentioning that monitoring station GM-2 was located close to the area of Stages 1 and 2 which are closed few years ago while the monitoring station GM-17 was located close to Stages 3 and 4 which were recently closed or still active. To conclude, based on this study, the correlation between the amount of emitted methane in the landfill site and the increase in the LST needs further research to be confirmed fully.

6.1.2. The Al-Jleeb Landfill, Al-Farwanyah, Kuwait

- In this study, 11 Landsat TM and ETM^{+} images were used to detect suspicious solid waste dumping locations within Al-Jleeb site. Similar to the study of the Trail Road landfill site, the Landsat images were downloaded from the USGS EarthExplorer and were atmospherically corrected using the ATCOR2 model in PCI Geomatics. Finally, the LST for the study area was computed from the thermal band (Band 6 for Landsat TM and Band 61 for Landsat ETM^{+}). The LST images were imported into a GIS environment, and the temperature contour lines were derived from each of the images. Finally, the highest temperatures for the contour lines were overlaid for each of the images to define the locations for dumping waste. Five suspicious locations of these dumping areas were identified through the high dense overlap of the contour lines. Future ground verification is needed to confirm the finding using the LST.
-
- Based on these previous findings, the achievements of this research effort can be

summarized as follows:-

- The land surface temperature of the landfill sites was found to be always higher than the temperature of the immediate surroundings areas and the air temperature in the urban, agriculture, and desert areas.
- The difference in temperature between the LST of the landfill sites and the air temperature as well as for the immediate surrounding areas varied due to seasonal changes and the condition of the landfill (closed or active).
- The LST of the active stages in the landfill was higher than those stages which were closed and capped.
- The LST of the landfill sites sometimes correlate to emitted landfill gases, such as methane.
- As the set-up of ground monitoring stations are costly, integration of remote sensing and GIS are useful for providing supplementary information for landfill site monitoring in a large geographic region.
- Remote sensing archive data can be used effectively to trace back the development of the landfill site to its beginning and determine suspicious dumping areas that have not been recorded or registered as yet.
- Integration of space-based and ground-based monitoring methods can help further understand the decomposition process that takes place within landfill sites.

6.3. Recommendations

The results achieved and presented from this study demonstrate clearly that further research work needs to be done to confirm the correlation between the data extracted from satellite images and the data available from existing monitoring stations. More Landsat images should be acquired for the Trail Road landfill to further analyze the LST and the corresponding activities at different

stages. Records from more ground monitoring stations should be analyzed and additional records from the ground monitoring stations (such as H_2O in the landfill gas, ground and surface water samples) should also be investigated and analyzed. More fieldwork is thus required and recommended in order to verify the results achieved from using the satellite images.

In terms of image processing experiments, the atmospheric correction model ATCOR3 can be utilized along with the incorporation of the digital elevation model for both case studies. This effort can further improve the accuracy of the derived LST by considering topographic effects. In addition, the normalized difference vegetation index (NDVI) or soil-adjusted vegetation index (SAVI) derived from the Landsat images can be utilized to monitor the effects of the landfill sites on the surrounding areas. To monitor the landfill gas on a regional and global scale, the use of other satellite sensors, for instance, Atmospheric Infrared Sounder (AIRS), can also be incorporated to monitor the emission of methane gas from landfill sites.

APPENDIX

The multi-temporal Landsat and LST images for the Trail road landfill, Ottawa, Canada

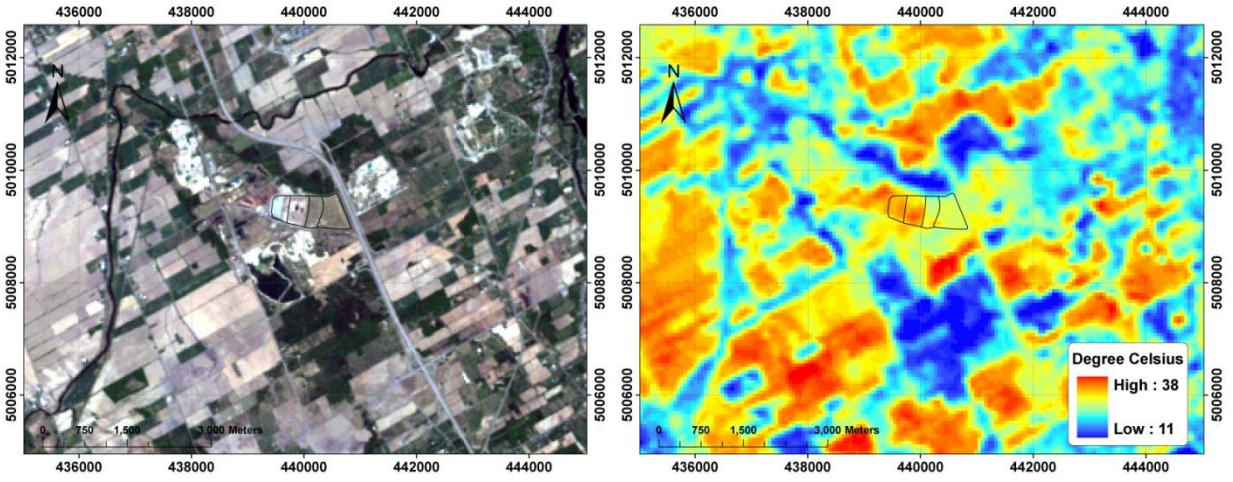

Original Landsat Image (Left) Acquired on May 13, 2001and the LST Image (Right)

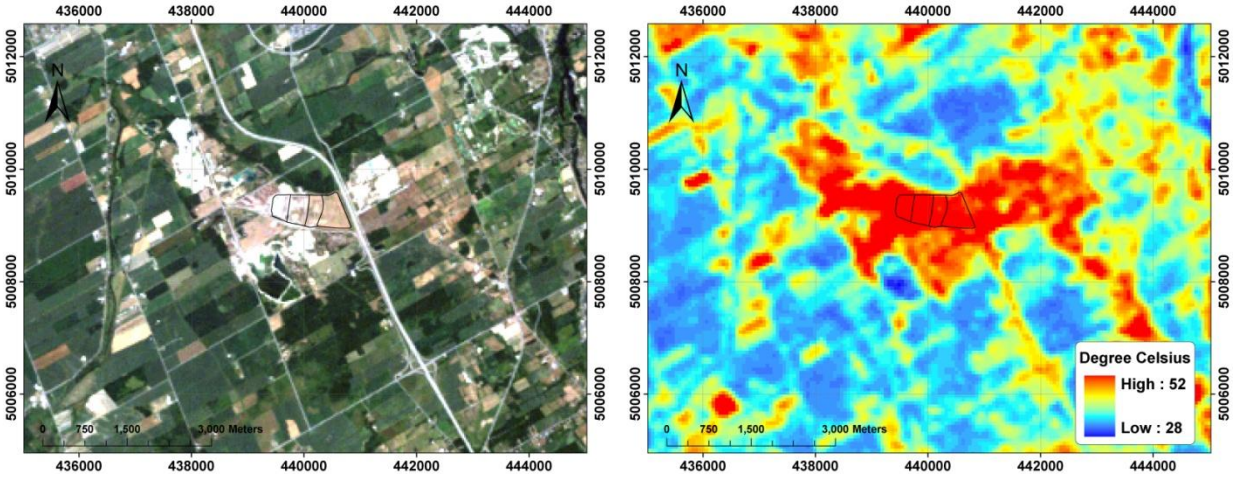

Original Landsat Image (Left) Acquired on Aug. 1, 2001 and the LST Image (Right)

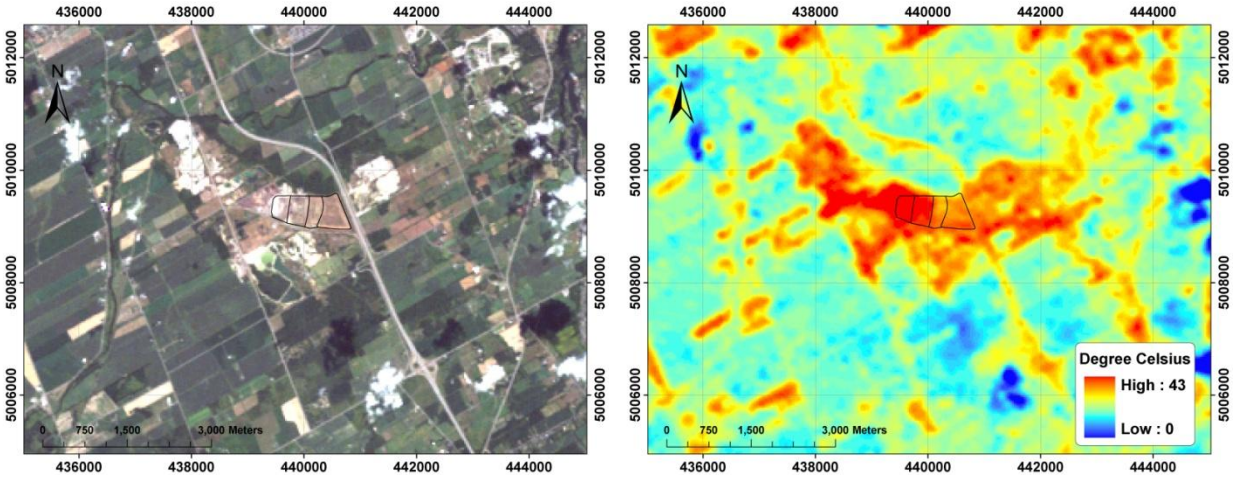

Original Landsat Image (Left) Acquired on Aug. 20, 2002 and the LST Image (Right)

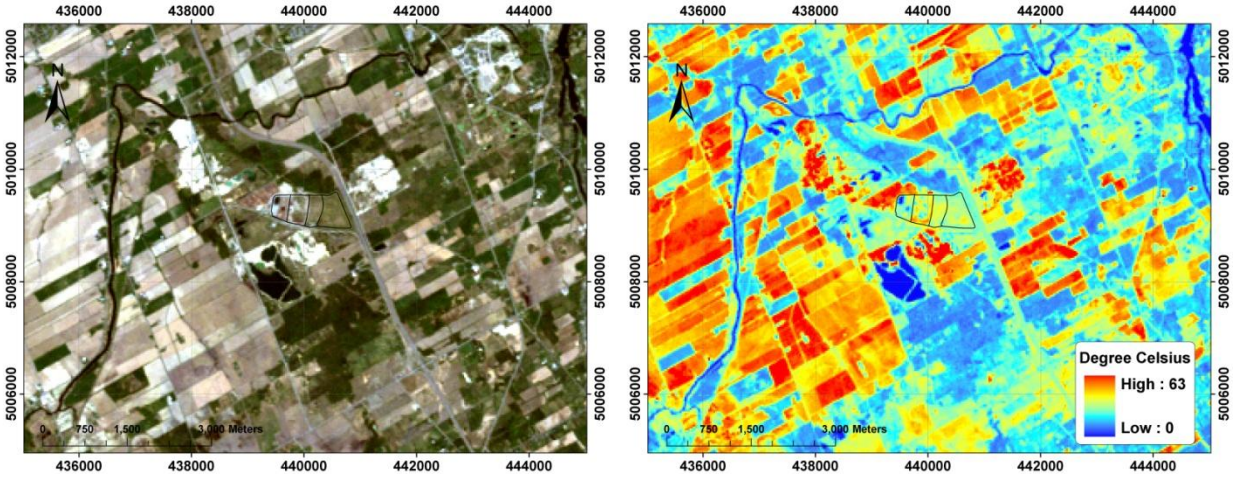

Original Landsat Image (Left) Acquired on May 19, 2003 and the LST Image (Right)

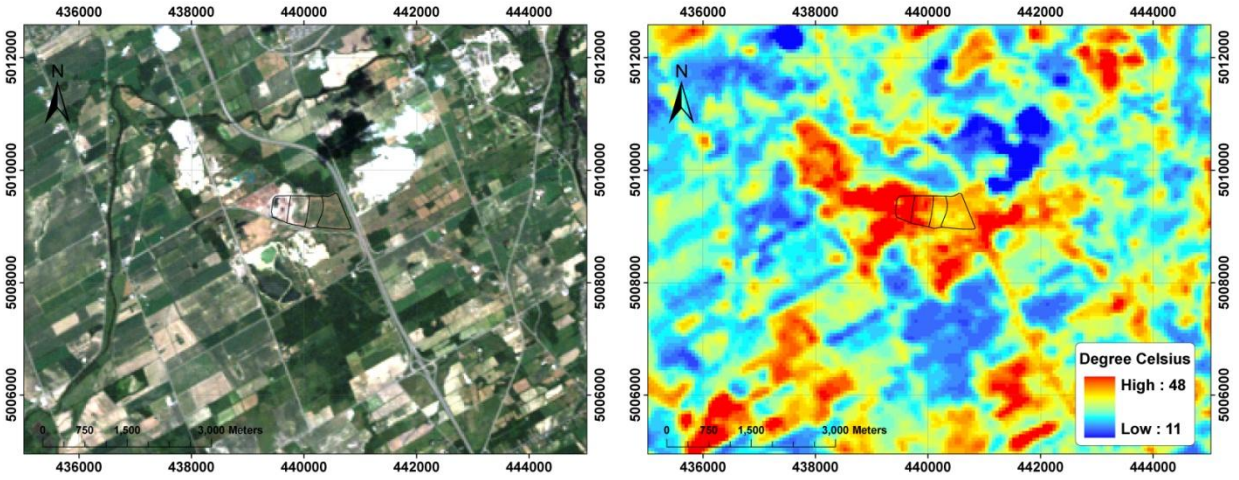

Original Landsat Image (Left) Acquired on Jul. 6, 2003 and the LST Image (Right)

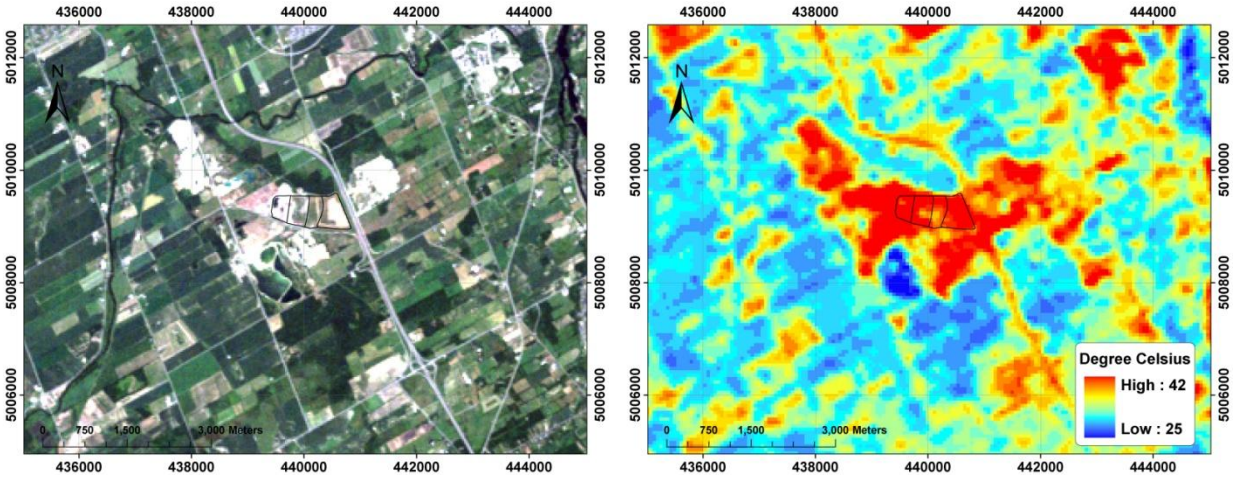

Original Landsat Image (Left) Acquired on Jul. 15, 2003 and the LST Image (Right)

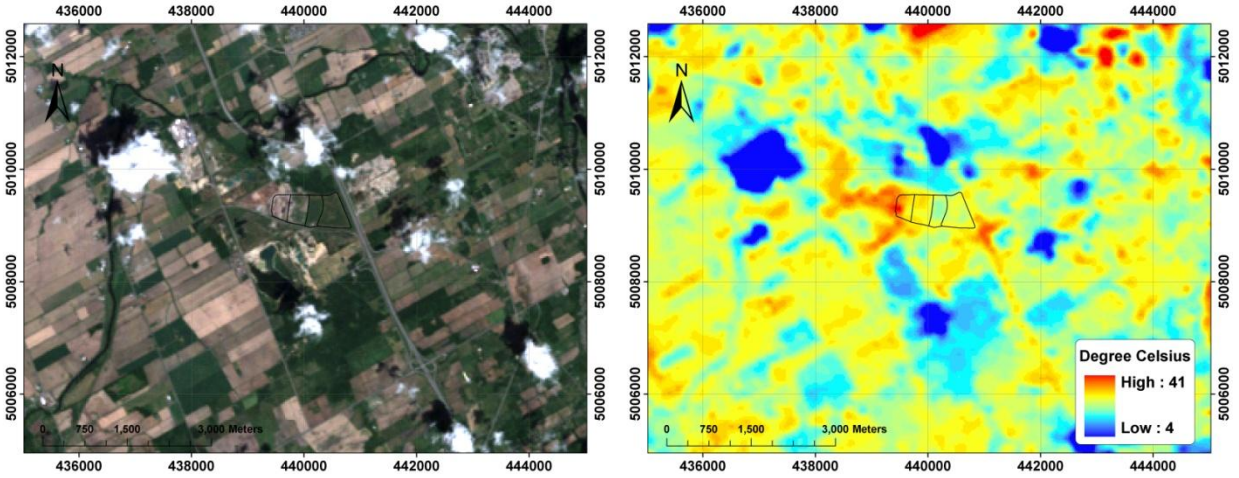

Original Landsat Image (Left) Acquired on Jun. 15, 2004 and the LST Image (Right)

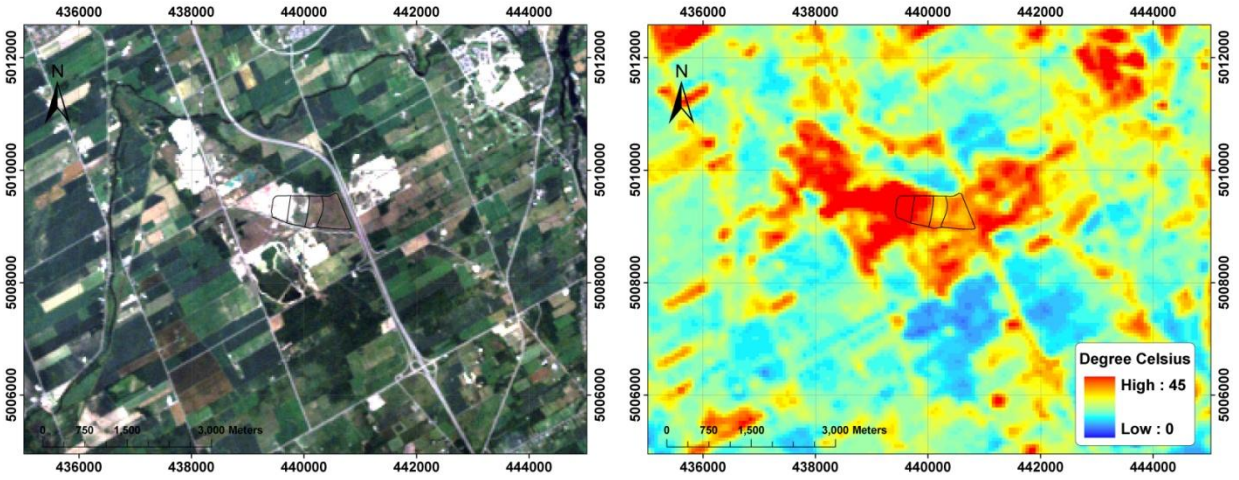

Original Landsat Image (Left) Acquired on Jul. 24, 2004 and the LST Image (Right)

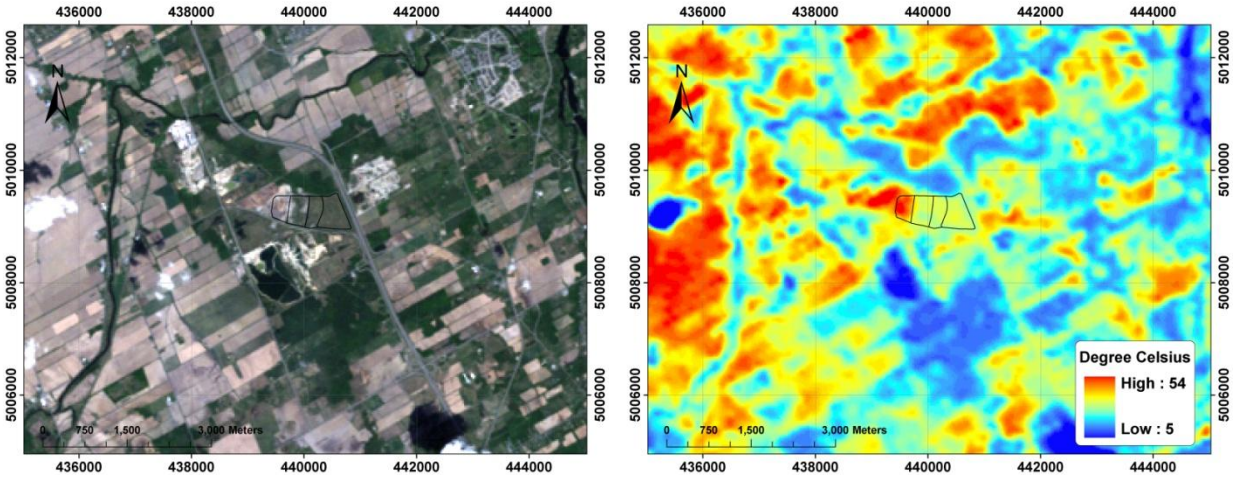

Original Landsat Image (Left) Acquired on Jun. 2, 2005 and the LST Image (Right)

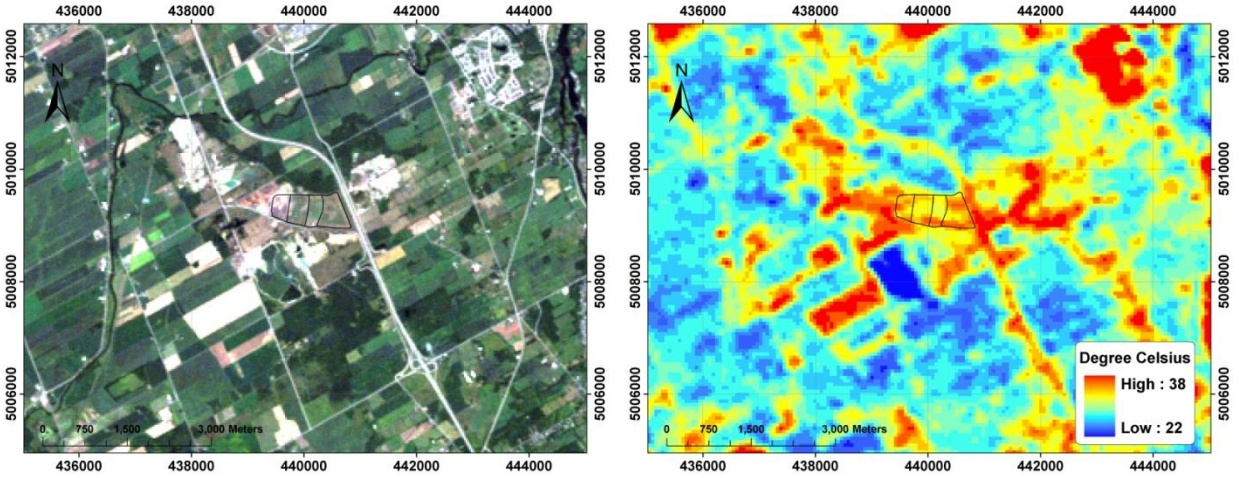

Original Landsat Image (Left) Acquired on Aug. 21, 2005 and the LST Image (Right)

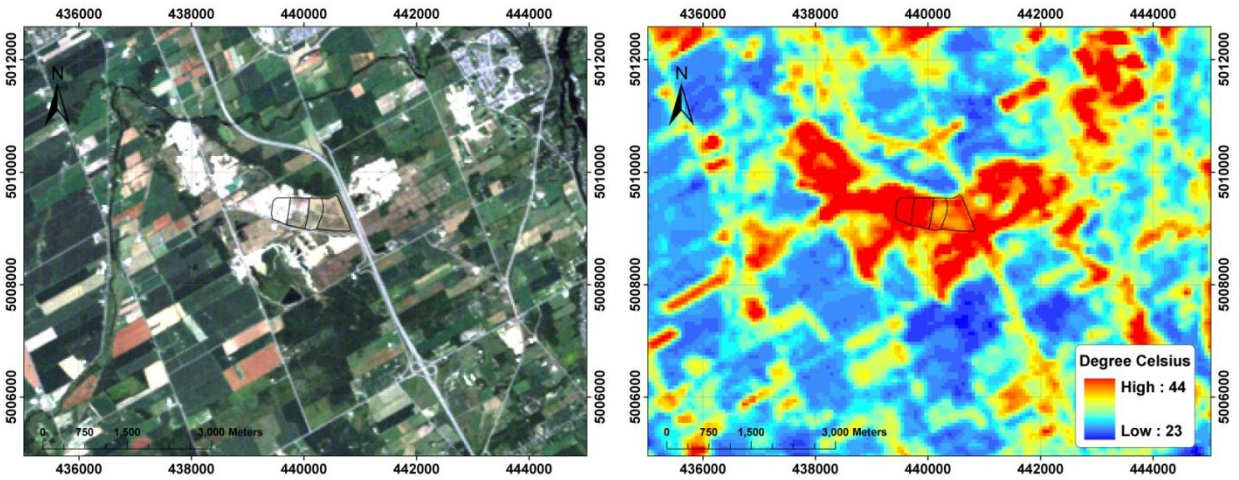

Original Landsat Image (Left) Acquired on Aug. 8, 2006 and the LST Image (Right)

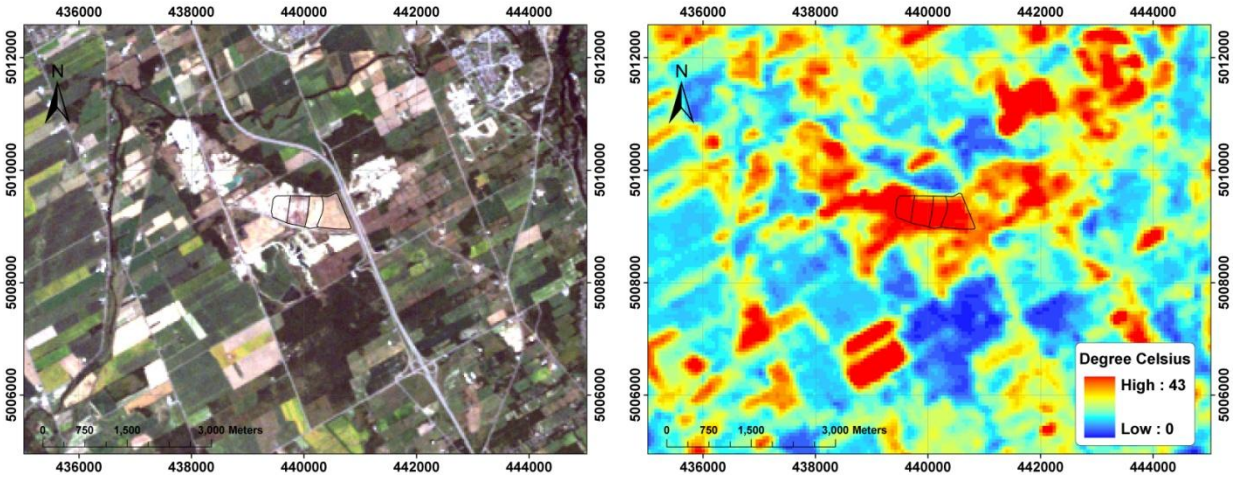

Original Landsat Image (Left) Acquired on Aug. 31, 2006 and the LST Image (Right)

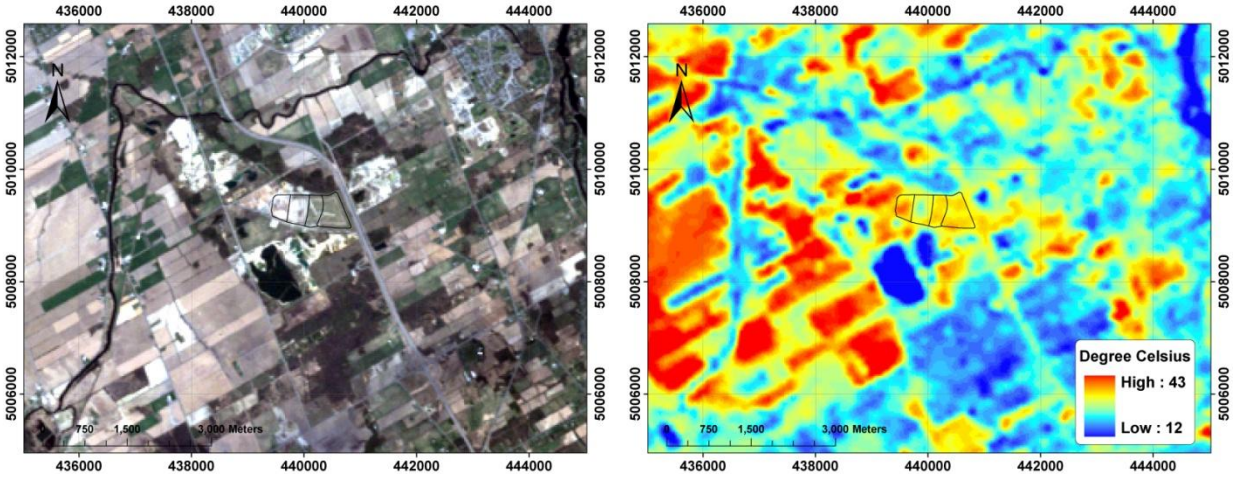

Original Landsat Image (Left) Acquired on May 7, 2007 and the LST Image (Right)

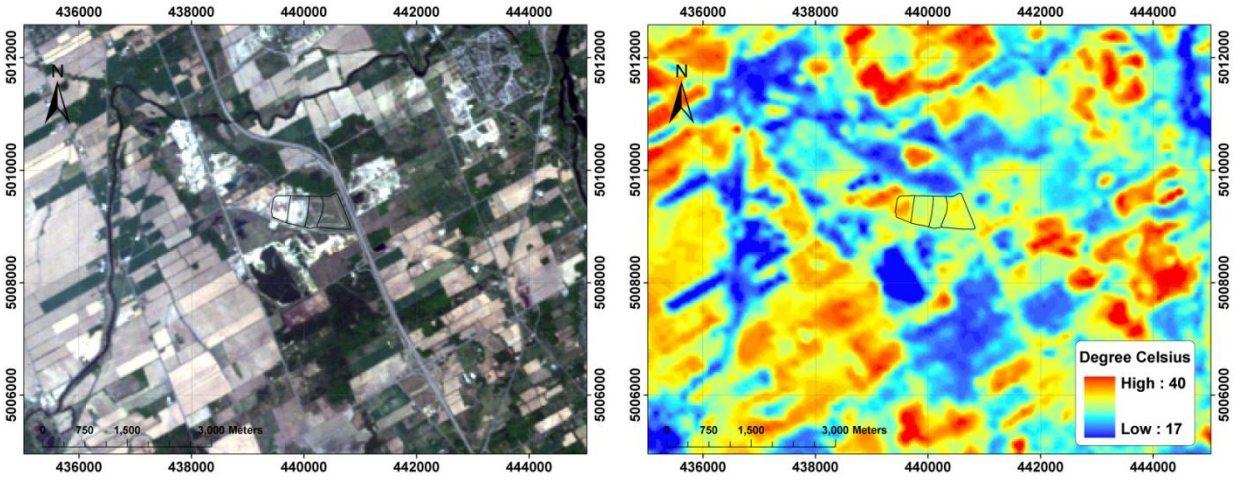

Original Landsat Image (Left) Acquired on May 23, 2007 and the LST Image (Right)

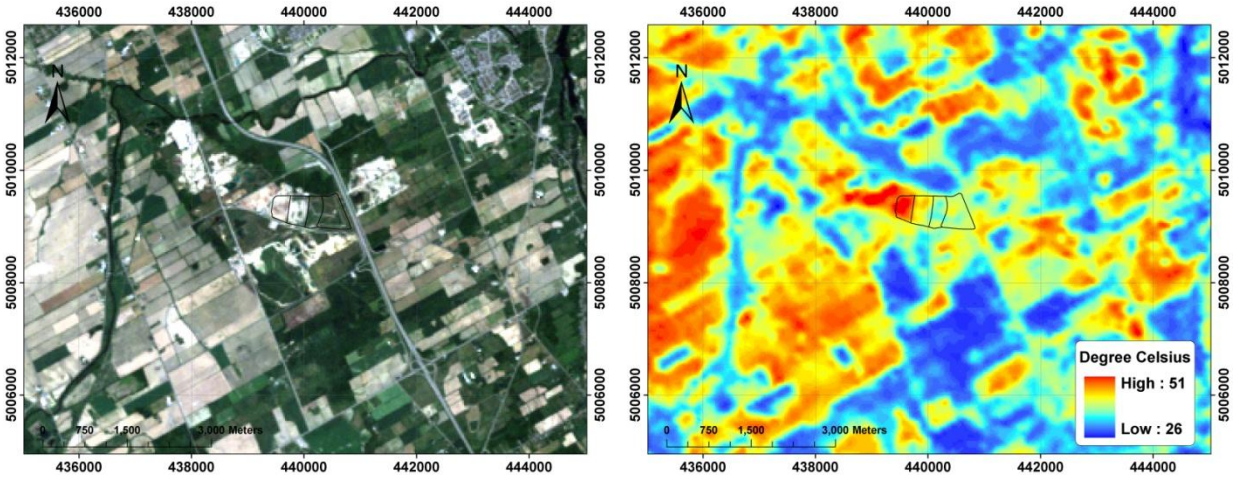

Original Landsat Image (Left) Acquired on Jun. 15, 2007 and the LST Image (Right)

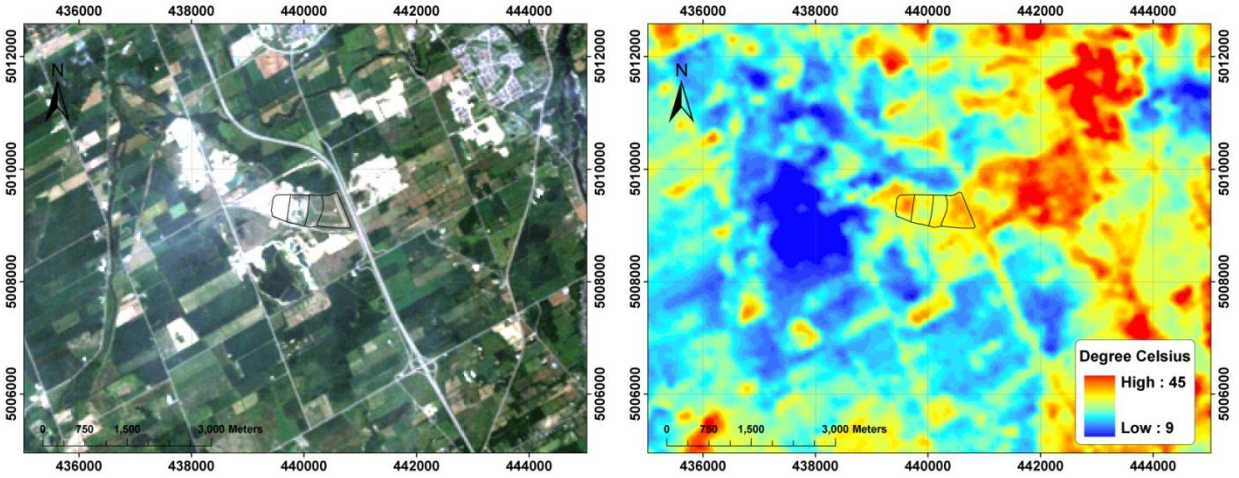

Original Landsat Image (Left) Acquired on Jul. 17, 2007 and the LST Image (Right)

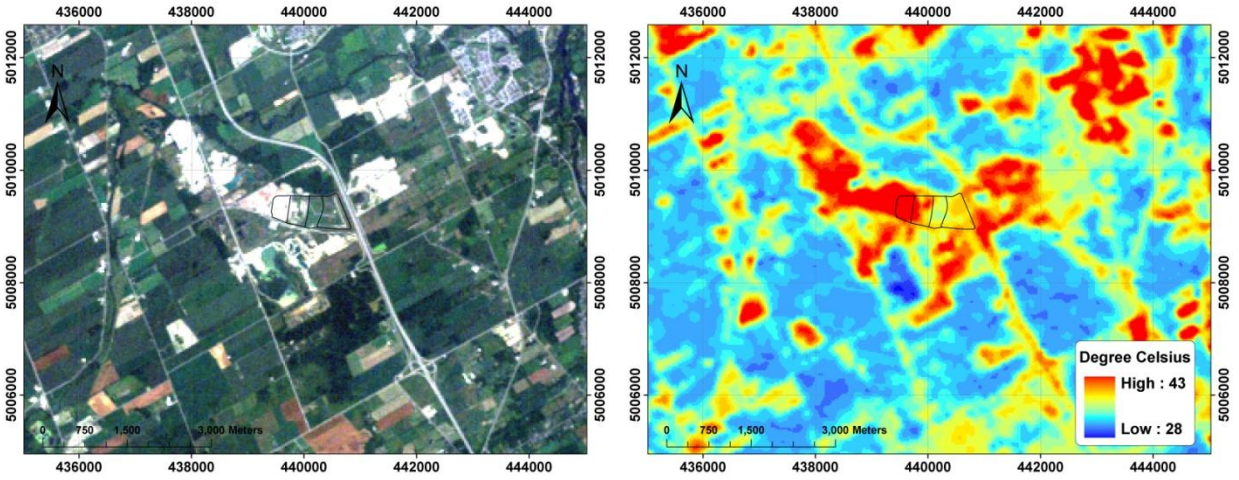

Original Landsat Image (Left) Acquired on Aug. 2, 2007 and the LST Image (Right)

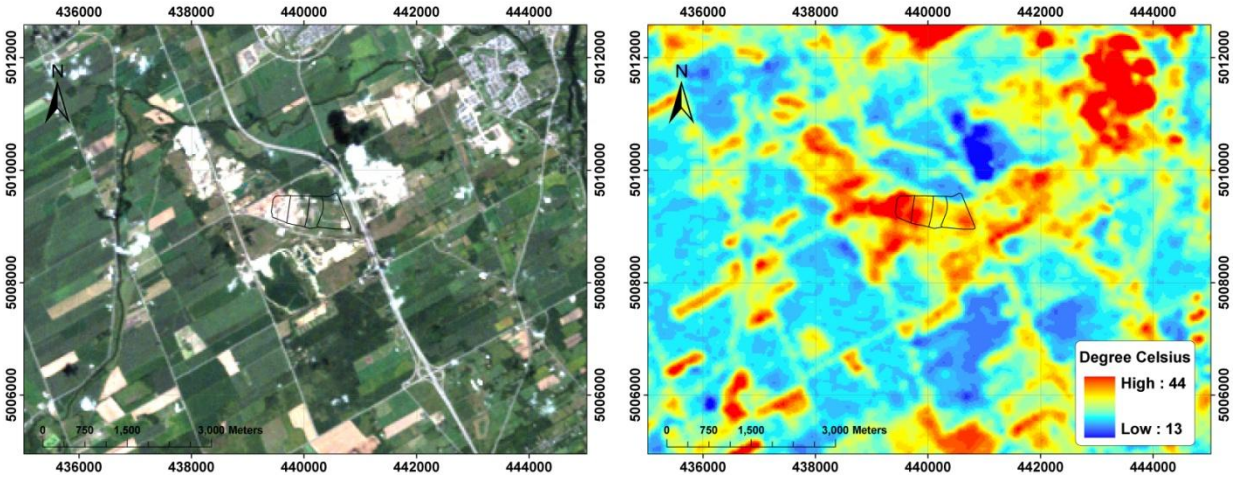

Original Landsat Image (Left) Acquired on Aug. 27, 2007 and the LST Image (Right)

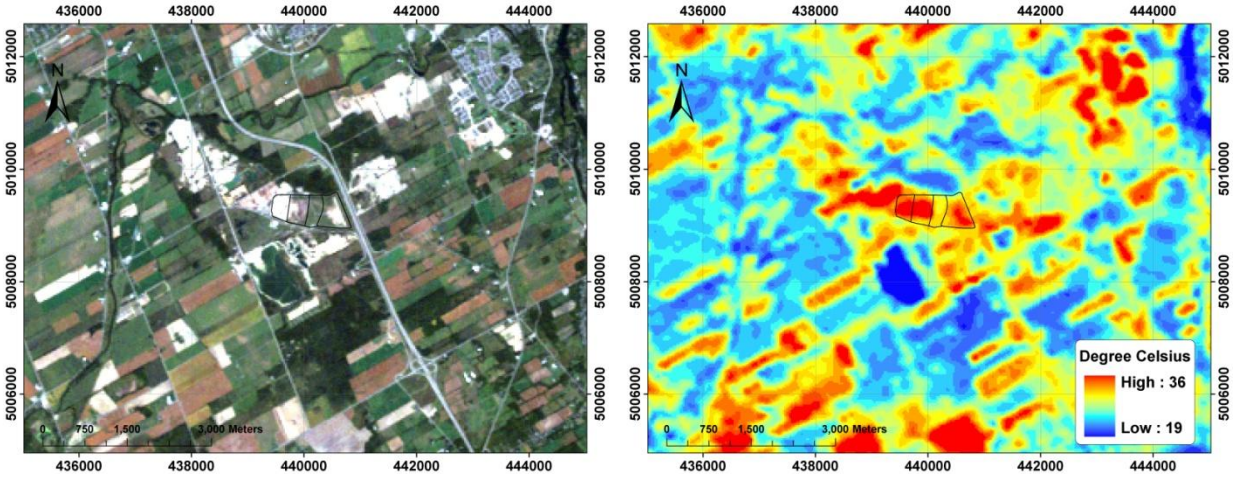

Original Landsat Image (Left) Acquired on Sept. 19, 2007 and the LST Image (Right)

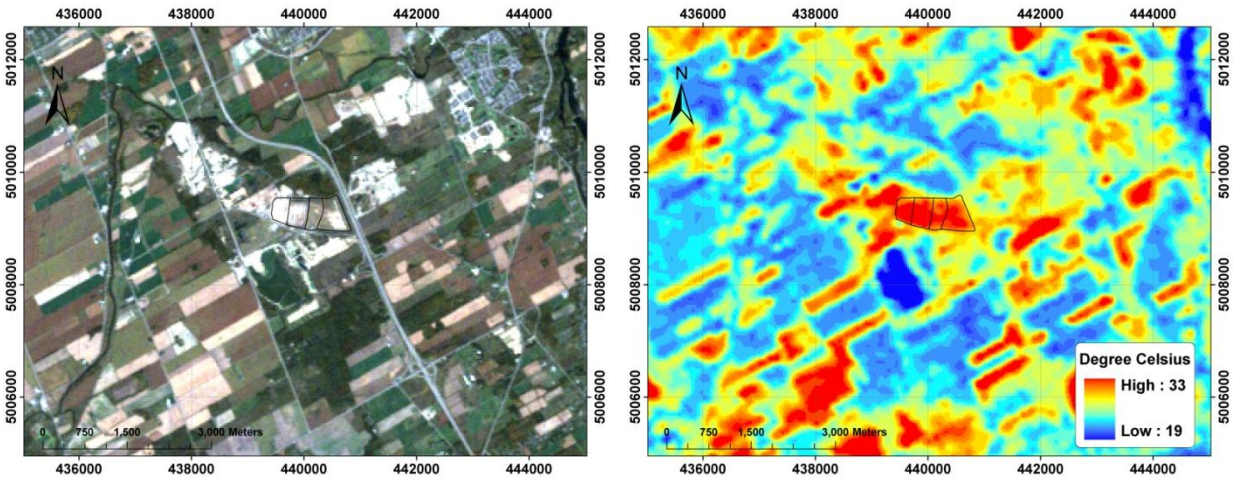

Original Landsat Image (Left) Acquired on Oct.5, 2007 and the LST Image (Right)

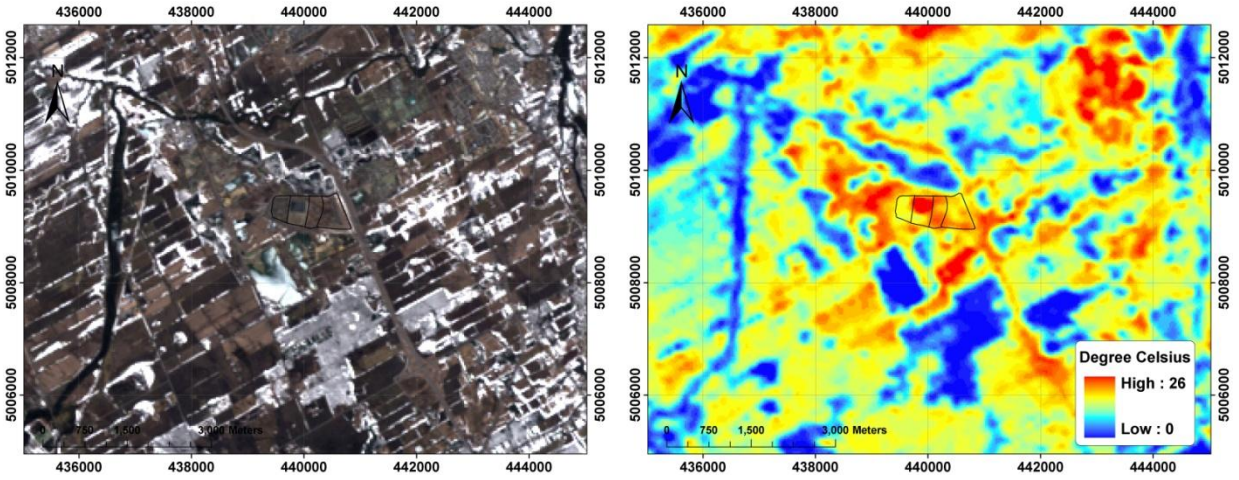

Original Landsat Image (Left) Acquired on Apr. 14, 2008 and the LST Image (Right)

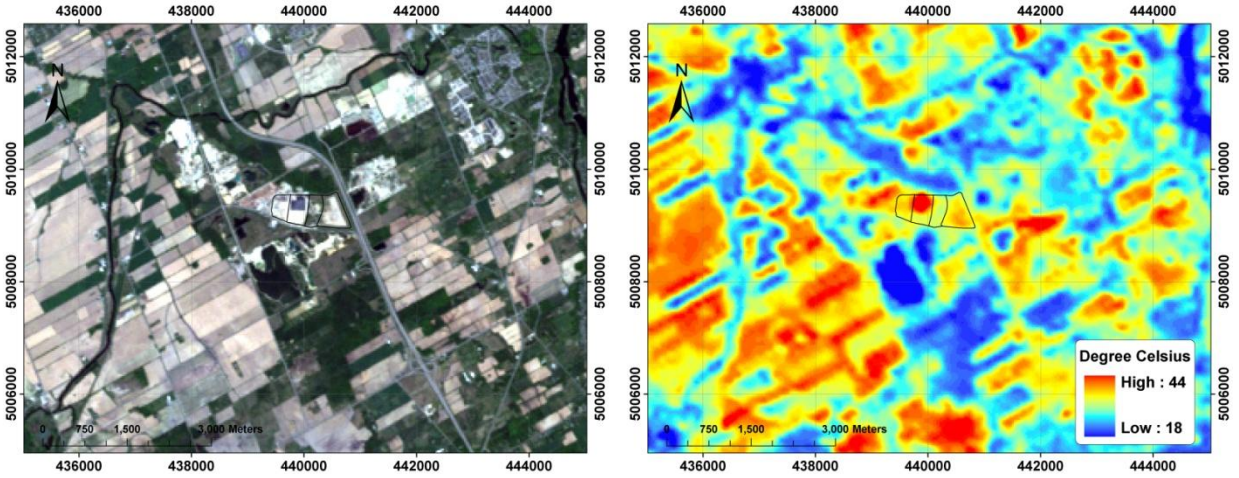

Original Landsat Image (Left) Acquired on May 25, 2008 and the LST Image (Right)

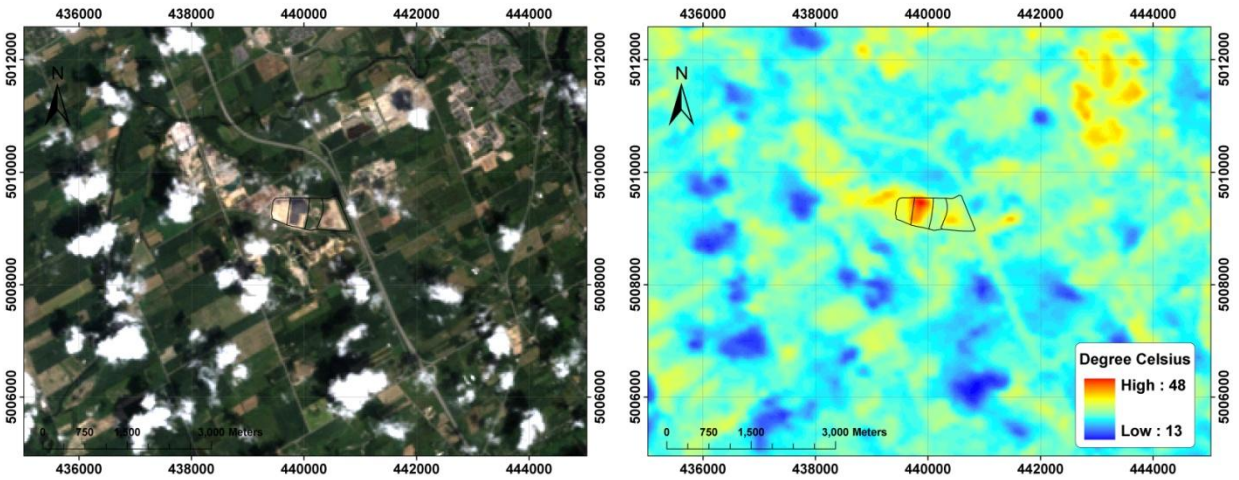

Original Landsat Image (Left) Acquired on Jul. 12, 2008 and the LST Image (Right)

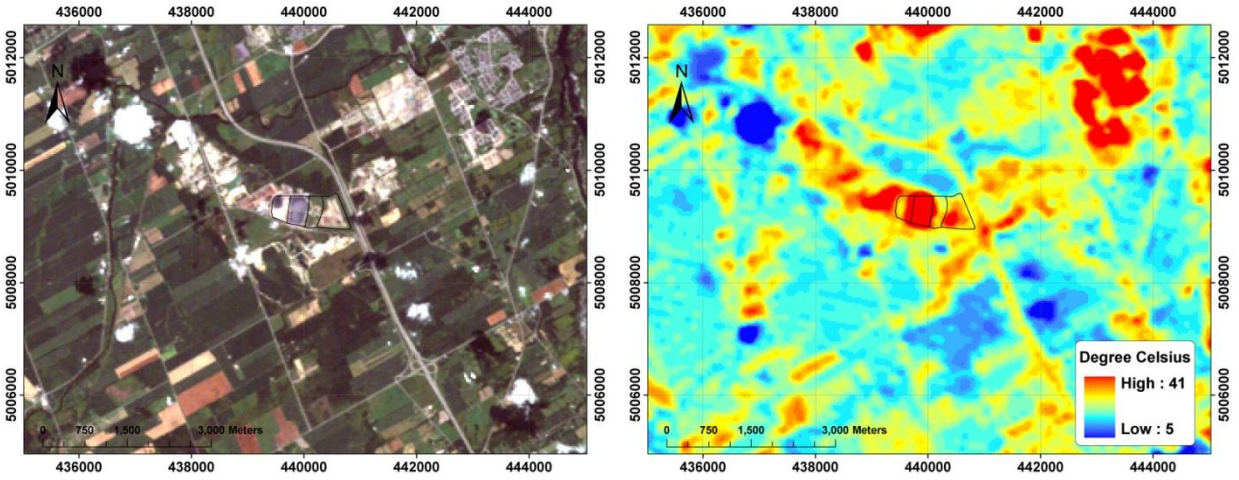

Original Landsat Image (Left) Acquired on Aug. 20, 2008 and the LST Image (Right)

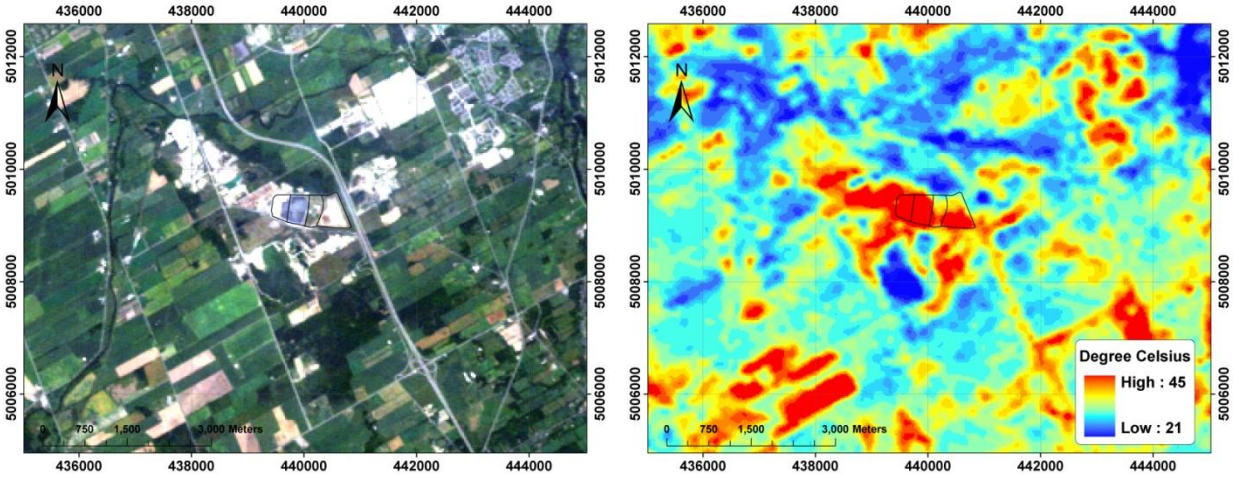

Original Landsat Image (Left) Acquired on Sept. 5, 2008 and the LST Image (Right)

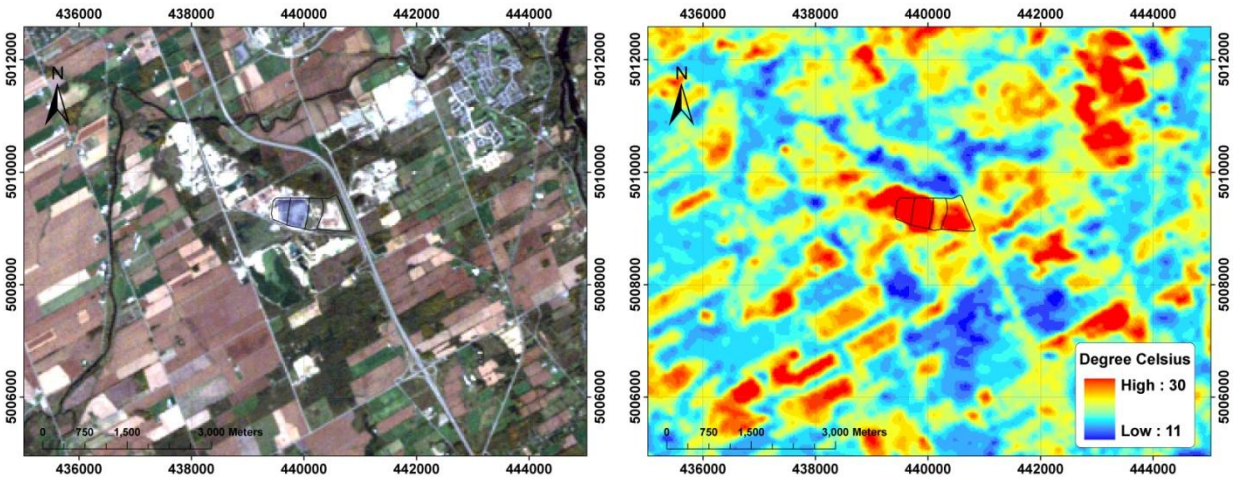

Original Landsat Image (Left) Acquired on Oct. 7, 2008 and the LST Image (Right)

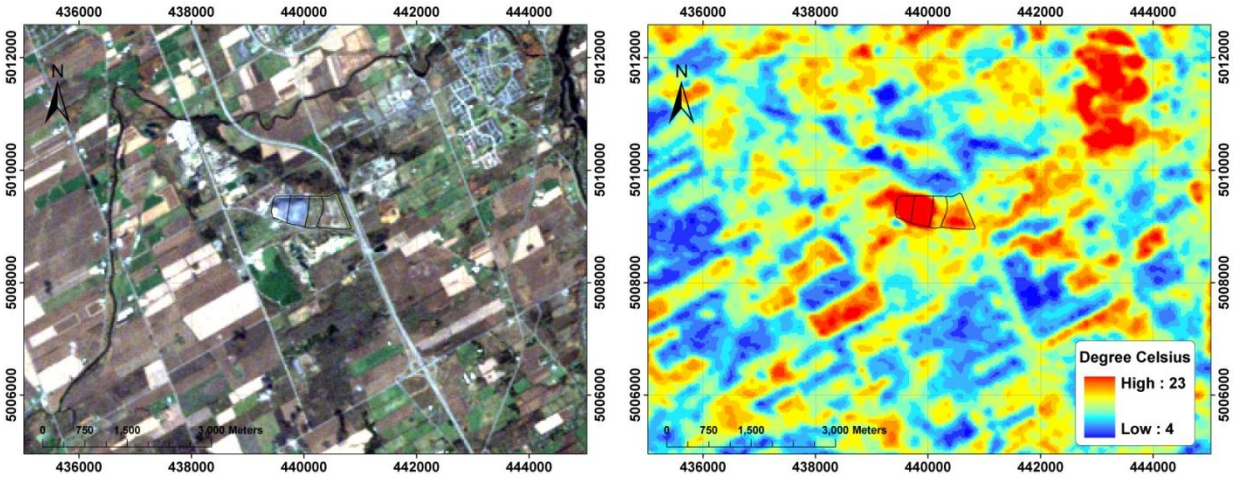

Original Landsat Image (Left) Acquired on Oct. 23, 2008 and the LST Image (Right)

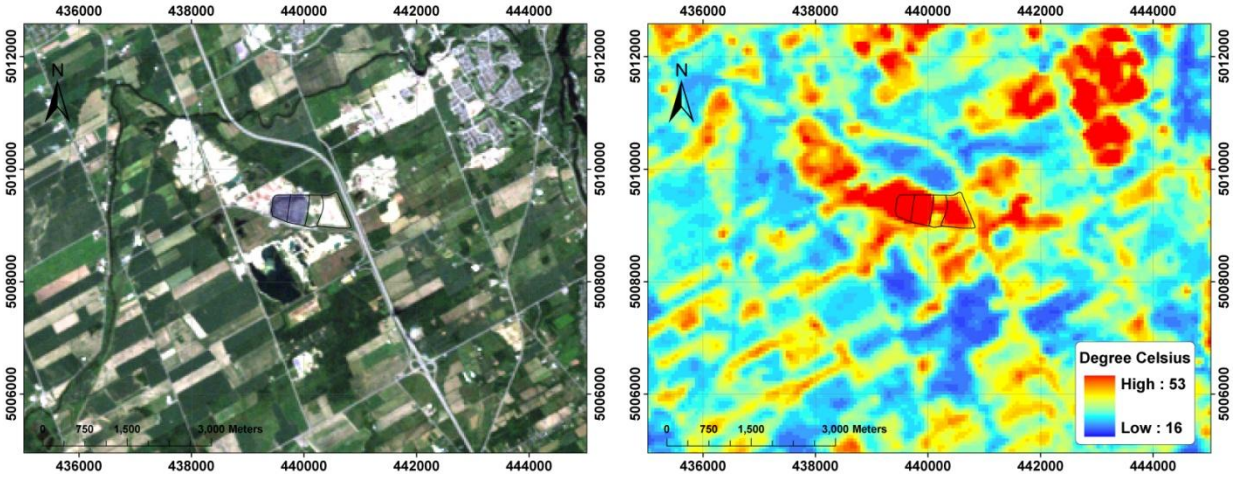

Original Landsat Image (Left) Acquired on Jul. 15, 2009 and the LST Image (Right)

REFERENCES

Al-Mutairi, N. (2004). Biological, chemical and physical assessment of Jeleeb Al-Shuyoukh landfill. Final Report to the Kuwait Environmental Protection Agency.

Al-Salem, S., and Al-Samhan, M. (2007). Plastic solid waste assessment in the state of Kuwait and proposed methods of recycling. *American Journal of Applied Sciences*, 4(6), 354–356.

Al-Salem, S. (2009). Life Cycle Assessment (LCA) of municipal solid waste management in the state of Kuwait. *European Journal of Scientific Research*, 34(3), 395–405.

Babalola, A., and Busu, I. (2011). Selection of landfill sites for solid waste treatment in Damaturu town using GIS Techniques. *Journal of Environmental Protection*, 2(1), 2152-2219.

Barsi, J. A., Barker, J. L., and Schott, J. R., (2003). An atmospheric correction parameter calculator for a single thermal band Earth-Sensing instrument. In: *Proceedings of the IEEE International Geosciences and Remote Sensing Symposium*, Toulouse, France, July 21-25, pp. 3014-3016.

Ball, J. M. (2005). Landfill site selection. In: *Proceedings of the Tenth International Waste Management and Landfill Symposium*. S. Margherita di Pula, Cagliari, Sardinia, Italy, October 3-7, 2005.

Biotto, G., Silvestri, S., Gobbo, L., Furlan, E., Valenti, S. and Rosselli R. (2009). GIS, multi-criteria and multi-factor spatial analysis for the probability assessment of the existence of illegal landfills. *International Journal of Geographical Information Science*, 23(10), 1233-1244.

Bogner, J., Ahmed, M., Diaz, C., Faaij, A., Gao, Q., Hashimoto, S., Mareckova, K., Pipatti, R., Zhang T. (2007) Waste management, In climate change: mitigation. contribution of working group III to the fourth assessment report of the intergovernmental panel on climate change [Metz, B., Davidson, O.R., Bosch, P.R. , Dave, R., Meyer L.A. (eds)], Cambridge University

Press, Cambridge, United Kingdom and New York, NY, USA.

Chander, C., and Markham, B. (2003). Revised Landsat-5 TM radiometric calibration procedures and postclibration dynamic ranges. *IEEE Transactions on Geoscience and Remote Sensing*, 41(11), 2674–2677.

Chander, G. (2007). Revised Landsat-5 thematic mapper radiometric calibration. *IEEE Geoscience and Remote Sensing Letters*, 4(3), 490–494.

Chander, G., Markham, B., and Helder, D. (2009). Summary of current radiometric calibration coefficients for Landsat MSS, TM, ETM+ and EO-1 ALI sensor. *Remote Sensing of Environment*, 113(5), 893–903.

Chen, J., Zhang, M., Wang, L., Shimazaki, H., and Tamura, M. (2005). A new index for mapping lichen-dominated biological soil crusts in desert areas. *Remote Sensing of Environment*, 96(2), 165 – 175.

Chen, N., and Price, J. C. (1992). Survey of radiometric calibration results and methods for visible and near infrared channels of NOAA-7, -9, and –11 AVHRRs. *Remote Sensing of Environment*, 41(1), 19–27.

Cobo, N., López, A., and Lobo, A. (2008). Biodegradation stability of organic solid waste characterized by physico-chemical parameters. *WIT Transactions on Ecology and the Environment*, 109(16), 153–162.

Czajkowski, K. P., Goward, S. N., Mulhern, T., Goetz, S. J., Walz, A., Shirey, D. and Dubayah, R. O. (2004). Estimating environmental variables using thermal remote sensing. In: *Thermal Remote Sensing in Land Surface Processes,* Edited by D.A. Quattrochi and J.C. Luvall. CRC Press, Washington D.C., pp. 11-32.

Dillon Consulting Limited (2007). *Trial Road landfill Site 2006 Monitoring and Operating Report*, City of Ottawa, Canada.

Dillon Consulting Limited (2008). *Trial Road landfill Site 2007 Monitoring and Operating Report*, City of Ottawa, Canada.

Environment Agency (2005). Guidance on monitoring MBT and other pretreatment processes for the landfill allowances schemes. UK (England and Wales).

Federal Emergency Management Agency (2002).Landfill fires. Available at: http://www.usfa.dhs.gov/downloads/pdf/publications/fa-225.pdf. [Accessed February 24, 2011].

Federation of Canadian Municipalities (2006). Solid waste as a resource. Available at: http://gmf.fcm .ca/capacity_building/waste/solid_waste_as_a_resource.asp. [Accessed February 24, 2011].

Francois, V., Feuillade, G., Skhiri, N., Lagier, T., and Matejka, G. (2006). Indicating the parameters of the state of degradation of municipal solid waste. *Journal of Hazardous Materials*, 137(2), 1008–1015.

Gu, Y., Hunt, E., Wardlow, B., Basara, J. B., Brown, J. F., and Verdin, J.P. (2008). Evaluation of MODIS NDVI and NDWI for vegetation drought monitoring using Oklahoma Mesonet soil moisture data. *Geophysical Research Letter*, 35(22), 1029-1034.

Ham, R. K., Norman, M. R., and Fritschel, P. R. (1993). Chemical characterization of fresh kills landfill refuse and extracts. *Journal of Environmental Engineering*, 119(6), 1176–1195.

Hadjimitsis, D. G., Papadavid, G., Agapiou, A., Themistocleous, K., Hadjimitsis, M. G., Retalis, A., Michaelides, S., Chrysoulakis, N., Toulios, L., and Clayton, C. R. I. (2010). Atmospheric correction for satellite remotely sensed data intended for agricultural applications: impact on vegetation indices. *Natural Hazards Earth System Science*, 10(1), 89-95.

Jensen, J. R. (2005). *Introductory Digital Image Processing*. (3rd Ed.). New Jersey: Pearson Prentice Hall, 544pp.

J.L. Richards and Associates (2011). Trail road landfill expansion, Ottawa, Canada. Available at: http://www.jlrichards.ca/services.php?p=14 [Accessed February 24, 2011].

Kelly, R. J., Shearer, B. D., Kim, J., Goldsmith, C. D. Hater, G. R., and Novak, J. T. (2006). Relationships between analytical methods utilized as tools in the evaluation of landfill waste stability. *Waste Management*, 26(12), 1349–1356.

Kwarteng, A. Y., and Al-Enezi, A. (2004). Assessment of Kuwait's Al-Qurain landfill using remotely-sensed data. *Journal of Environmental Science and Health, Part A*, 39(2), 351–364.

Kwarteng, A. Y., and Small, C. (2007). Remote sensing nnalysis of Kuwait city's thermal environment. In: *Proceedings of the Urban Remote Sensing Joint Event 2007*, Paris, France, April 11-13, pp.1-8.

Kwareng, A. Y. (2008). SAR-based land cover classification of Kuwait. *International Journal of Remote Sensing*, 29(23), 6739–6778.

Mahamid, I., and Thawaba, S. (2010). Multi criteria and landfill site selection using GIS: a case study from Palestine. *The Open Environmental Engineering Journal*, 3, 33-41.

Mausel, D., Brondizio, E., and Moran, E. (2002). Assessment of atmospheric correction methods for Landsat TM data applicable to Amazon basin LBA research. *International Journal Remote Sensing*, 23(13), 2651–2671.

Mehta, R., Barlaz, M. A., Yazdani, R., Augenstein, D., Bryars, M., and Sinderson, L. (2002). Refuse decomposition in the presence and absence of leachate recirculation. *Journal of Environmental Engineering*, 128(3), 228–236.

Mirtorabi, R. 2010. Comparison between satellite images and site data for monitoring at trail road landfill. Ryerson University, M.A.Sc. Thesis, 139 pp.

Nas, B., Cay, T., İşcan, F., and Berktay, A., (2010). Selection of MSW landfill site for Konya, Turkey using GIS and multi-criteria evaluation. *Environmental Monitoring and Assessment*,

160(1-4), 491-500.

Nichol, J. E., and Wong, M. S. (2009). Mapping urban environmental quality using multiple parameters, *Environment and Planning B: Planning and Design*, 36(1), 170-185.

Norman, J. M., Divakarla, M., and Goel, N. S. (1995). Algorithms for extracting information from remote thermal-IR observations of the earth's surface. *Remote Sensing of Environment*, 51(1), 157–168.

Ottavianelli, G. (2007). *Synthetic Aperture Radar Remote Sensing for Landfill Monitoring*. Ph.D. Dissertation, Cranfield University, United Kingdom, 298 pp.

Ou, S.C., Chen, Y., Liou, K.N., Cosh, M., and Brutsaert, W. (2002). Satellite remote sensing of land surface temperatures: application of the atmospheric correction method and split-window technique to data of ARM-SGP site. *International Journal of Remote Sensing*, 23(24), 5177-5192.

Paolini, L., Grings, F., Sobrino, J.A., Jimenez-Munoz, J.C., and Karszenbaum, H. (2006). Radiometric correction effects in Landsat multi data/multi sensor change detection studies. *International Journal of Remote Sensing*, 27(4), 685–704.

Plasynski, S., Beckert, H., and Newell, D. (2008). *Landfill gas sequestration in Kansas*. Fact Sheets of the National Energy Technology Laboratory, Office of Fossil Energy, U.S. Department of Energy.

Price, C., (1987). Calibration of satellite radiometers and the comparison of vegetation indices. *Remote Sensing of Environment*, 21(15), 15–27.

Richter, R. (1998). Correction of satellite imagery over mountainous terrain. Applied Optics, 37(18), 4004- 4015.

Schübeler,P.(1996). Conceptual framework for municipal aolid waste management in low -income countries. Available at: http://www.worldbank.org/urban/solid_wm/erm/CWG% 20folder

/conceptualframework.pdf. [Accessed February 24, 2011].

Schrapp, K. and Al-Mutairi, N. (2010). Associated health effects among residences near Jeleeb Al-Shuyoukh landfill. *American Journal of Environmental Sciences*, 6(2), 184–190.

Shaker, A., Yan, W. Y., and Easa, S. M. (2010). Using stereo satellite imagery for topographic and transportation applications: an accuracy assessment. *GIScience and Remote Sensing*, 47(3), 321-337.

Silvestri, S., and Omri, M. (2008). A method for the remote sensing identification of uncontrolled landfills: formulation and validation. *International Journal of Remote Sensing*, 29(4), 975-989.

Statistics Canada (2002). 2001 Community Profiles. Available at: http://www12.statcan.ca /english/Profil01/CP01/Index.cfm?Lang=E [Accessed February 24, 2011].

Statistics Canada (2008). Population and dwelling counts, for Canada and census subdivisions (municipalities), 2006 and 2001 censuses. Available at: http://www12.statcan.ca/english/ census06/data/popdwell/Table.cfm?T=301&S=3&O=D. [Accessed February 24, 2011].

The Public Authority for Civil Information. (2010). The Public Authority for Civil Information Available at: http://www.paci.gov.kw/ [Accessed February 24, 2011].

U.S. Environmental Protection Agency (1998). *MSW Landfill Criteria Technical Manual*. Washington, D.C.: U.S. Environmental Protection Agency. EPA530-R-93-017.

Voogt, J. A., and Oke, T. R. (2003). Thermal remote sensing of urban climates. *Remote Sensing of Environment*, 86(3), 370–384.

Wang, L., Koike, T., Yang, K., and Yeh, P.J.F. (2009). Assessment of a distributed biosphere hydrological model against streamflow and MODIS land surface temperature in the upper Tone River Basin. *Journal of Hydrology*, 377(1/2), 21-34.

Weng, Q., Lu, D., and Schubring, J. (2004). Estimation of land surface temperature-vegetation

abundance relationship for urban heat island studies. *Remote Sensing of Environment*, 89(4), 467-483.

Yahaya, O., Umoh, V. J. and Ameh, J. B. (2011). Public health implications of using water from wells located near municipal waste dump sites in parts of Zaria. *Medical Practice and Review*, 2(4), 44–49.

Yang, K., Zhou, X. N., Yan, W. A., Hang, D. R., and Steinmann, P. (2008). Landfills in Jiangsu province, China, and potential threats for public health: Leachate appraisal and spatial analysis using geographic information system and remote sensing. *Waste Management*, 2008(28), 2750-2757.